University of Alberta

CHARACTERISTIC-BASED CONTROL OF DISTRIBUTED PARAMETER SYSTEMS

by 

Huilan Shang

A thesis submitted to the Faculty of Graduate Studies and Research in partial fulfillment of the requirements for the degree of **Doctor of Philosophy**.

in

Process Control

Department of Chemical and Materials Engineering

Edmonton, Alberta

Spring 2003

Your file Votre référence
ISBN: 0-612-82164-1
Our file Notre référence
ISBN: 0-612-82164-1

University of Alberta

Library Release Form

Name of Author: Huilan Shang

Title of Thesis: Characteristic-based Control of Distributed Parameter Systems

Degree: Doctor of Philosophy

Year this Degree Granted: 2003

Huilan Shang

School of Engineering, Laurentian University

Sudbury, ON, Canada, P3E 2C6

Date: Dec. 3, 2002

University of Alberta

Faculty of Graduate Studies and Research

The undersigned certify that they have read, and recommend to the Faculty of Graduate Studies and Research for acceptance, a thesis entitled **Characteristic-based Control of Distributed Parameter Systems** submitted by Huilan Shang in partial fulfillment of the requirements for the degree of **Doctor of Philosophy** in *Process Control.*

. . . . . .

J. Fraser Forbes

. . . . . .

Martin Guay

. . . . . .

Horacio Marquez

. . . . . .

Biao Huang

. . . . . .

Hector Budman

Date: 3/12/2002

DEDICATION

This dissertation is dedicated, with respect, to Dr. J. Fraser Forbes and Dr. Martin Guay. Without their support and encouragement, my academic achievements in Canada would not have been possible. Their friendship enriched me. From them, I had the good fortune to learn how life can be rich and meaningful to oneself and to many others.

Abstract

Many processes are Distributed Parameter Systems (DPS) in which states vary in both time and space (*e.g.*, fixed-bed reactors, polymer extrusion, fibre spinlines, and sheet coating processes). Mathematical description of such systems, generally obtained by applying conservation laws, often takes the form of Partial Differential Equations (PDEs). The commonly used techniques of controlling DPS approximate the systems with a lumped parameter model and apply the available control techniques for Lumped Parameter Systems (LPS). It is generally recognized that such approximation approaches may lead to poor control performance. The research on the control methods that directly use the PDE models has been motivated with the expectation of improved performance, and a variety of feedback control laws have been proposed in the literature.

The objective of this thesis is to exploit the geometric properties of the PDEs used to model DPS and to develop geometric-based control methods to achieve high performance control with tractable computation. The thesis will focus mainly on hyperbolic models for DPS, and, as a result, extensive use will be made of the *Method of Characteristics*. The Method of Characteristics, a differential geometric approach of constructing integral

surfaces for hyperbolic PDEs, is used in the formulation of characteristics-based control methods for DPS in this thesis. A feedback control method is developed such that the hyperbolic systems are driven towards the desired behavior along the characteristic direction. The resulting controller possesses a simple form and provides significantly improved performance. However, studies have shown that, for PDE models, feedback control performance is limited by the time-horizon that is considered within the control calculations. Model Predictive Control (MPC), which takes the long-term process behavior into consideration, is a natural candidate for overcoming the "shortsightedness" of the standard feedback control methods. An extensive effort is made to develop a characteristics-based MPC for various PDE systems. Simulation studies are conducted to illustrate the strength and weakness of the proposed predictive controller, and extensions to parabolic systems are investigated. The research from this thesis shows that the characteristic-based control is a promising novel approach for DPS because of its efficient computation and high performance.

Acknowledgements

My most sincere thanks and appreciation are expressed to Dr. Forbes and Dr. Guay, my supervisors, who enthusiastically and unfailingly nurtured, encouraged, and guided me through all stages of my thesis. My discussion with them were a highlight of the research progress for me. Their interest in my work, careful reading and corrections, helpful suggestions as well as their supportive and caring attitude towards my work throughout my program were indispensable basis for the successful completion of this dissertation.

I would also like to express my gratitude to Dr. Biao Huang, Dr. Horacio J. Marquez, Dr. Krishnaswamy Nandakumar and Dr. Hector M. Budman, who kindly read through the whole dissertation and made valuable comments. I am grateful to the entire CPC group at U of A. Deep thanks go to to people at Laurentian University for welcoming me into their midst.

Contents

List of Tables

List of Figures

List of Abbreviations

DMC	Dynamic Matrix Control
DPS	Distributed Parameter Systems
GPC	Generalized Predictive Control
LPS	Lumped Parameter Systems
MPC	Model Predictive Control
ODE	Ordinary Differential Equation
PDE	Partial Differential Equation
PFR	Plug Flow Reactor
CSTR	Continuous Stirred Tank Reactor
LMPC	Linear Model Predictive Control
QDMC	Quadratic Dynamic Matrix Control
CBMPC	Characteristic Based Model Predictive Control
CMCFD	Combining the Method of Characteristics and the Finite Difference
NLMPC	Nonlinear Model Predictive Control

Chapter 1

Introduction

In the field of process control, processes are often classified into two categories: Lumped Parameter Systems (LPS) and Distributed Parameter Systems (DPS). Lumped parameter systems are processes in which any dependent variable can be assumed to be a function only of time and not of spatial position. When process variables are spatially uniform or only the spatial average of process variables is of interest, the processes can be considered to be LPS (*e.g.*, a Continuous Stirred Tank Reactor (CSTR)). The majority of control research has focused on LPS and numerous techniques are available for these systems. In distributed parameter systems, on the other hand, process variables vary in space as well as in time. Since the value of distributed state variables at each spatial point is a function of only time, and there are an infinite number of spatial positions, DPS can also be considered to consist of an infinite number of LPS and therefore are termed as infinite dimensional systems. A large number of processes in chemical, petroleum and metallurgical industries are distributed in nature (Butkowskii, 1969; Ray, 1978). These processes include heating and cooling problems associated with steel-making, fluid heat exchangers, some chemical reactors, polymer processing operations, plasmas (Sen, 1974), nuclear reactors and so forth. Many mechanical, resource recovery, environmental, physiological and sociological systems can also be characterized as distributed parameter

systems. Due to the wide existence of DPS, the study of DPS is important and high-performance control development for DPS has significant industrial and theoretical implications. In comparison to LPS, however, DPS usually have relatively complicated dynamics and the complexity of system dynamics has limited the research on these systems.

1.1 DPS Modelling Survey

A good understanding of the processes being controlled is advantageous, and sometimes even critical, for control design. The dynamics of DPS has distinct features from those of LPS, which will be discussed through examples in this section.

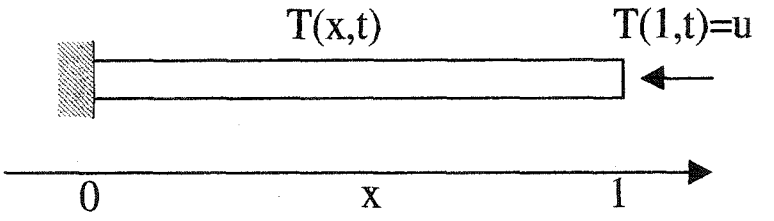

Figure 1.1: Heat transfer in a slab

One of the simplest DPS is heat transfer in a slab (see Figure 1.1). The temperature profile of the slab is controlled by the boundary temperature at $x = 1$. When the boundary temperature changes, the temperature profile (*i.e.*, the temperature at different locations), changes with time. For a temperature change at $x = 1$, the temperature response at $x = 0$ is relatively sluggish (*i.e.*, it takes some time for the effect of manipulated variable change at $x = 1$ to reach $x = 0$). The model of the process can be obtained using conservation laws and takes the form of the following Partial Differential Equation (PDE)

with boundary value problem (Laroche *et al.*, 1998):

$$\begin{aligned} &\frac{\partial T}{\partial t}(x,t) = \frac{\partial^2 T}{\partial x^2}(x,t), \qquad x \in [0,1], \\ &\frac{\partial T}{\partial x}(0,t) = 0, \\ &T(1,t) = u(t), \end{aligned} \tag{1.1}$$

where $T(x,t)$ is the temperature and $u(t)$ is the control input. The partial differential equation along with two other equations, called boundary conditions, constitutes the model of heat transfer in the slab. Note that in this process, the effect of the manipulated variable enters via one of the boundary conditions. Such control problems are called boundary control problems.

A common chemical engineering process is a tubular reactor. In contrast to a CSTR, the concentrations of chemical reactants and products in a tubular reactor vary along the reactor and possibly radially, as well. Very often the values of the distributed variables at a certain spatial position are the variables to be controlled (*e.g.*, outlet concentration), and the manipulated variables enter via the boundary conditions, such as inlet concentration or the variables related to the temperature control of the reactor. The behavior of tubular reactors is often discussed in terms of the relative importance of the diffusion, convection and reaction processes. When diffusion is unimportant and negligible, the reactors are idealized as Plug Flow Reactors (PFR). When diffusion dominates, the tubular reactor approaches the behavior of a CSTR. Consider the following chemical reaction in a tubular reactor:

$$C_1 \rightarrow bC_2, \tag{1.2}$$

where C_1 is the reactant, C_2 is the product and $b > 0$ is the stoichiometric coefficient of the reaction. The dynamics of a tubular reactor with axial dispersion can be represented as (Winkin *et al.*, 2000):

$$\frac{\partial c_1}{\partial t} = D_a \frac{\partial^2 c_1}{\partial x^2} - v\frac{\partial c_1}{\partial x} - r(c_1, c_2), \tag{1.3}$$

$$\frac{\partial c_2}{\partial t} = D_a \frac{\partial^2 c_2}{\partial x^2} - v\frac{\partial c_2}{\partial x} + br(c_1, c_2), \tag{1.4}$$

with the boundary conditions:

$$
\begin{aligned}
D_a \frac{\partial c_1}{\partial x}(0,t) - v c_1(0,t) &= -v c_{in}(t), \\
D_a \frac{\partial c_2}{\partial x}(0,t) - v c_2(0,t) &= 0, \\
D_a \frac{\partial c_1}{\partial x}(L,t) &= 0, \\
D_a \frac{\partial c_2}{\partial x}(L,t) &= 0,
\end{aligned}
\tag{1.5}
$$

where L, c_1, c_2, c_{in}, v, D_a and r are the reactor length, the concentrations of C_1 and C_2 (mol/l), the influent reactant concentration (mol/l), the fluid superficial velocity (m/s), the axial dispersion coefficient (m^2/s) and the reaction rate (mol/l s), respectively. When the dispersion coefficient D_a is zero, the plug-flow reactor model is derived.

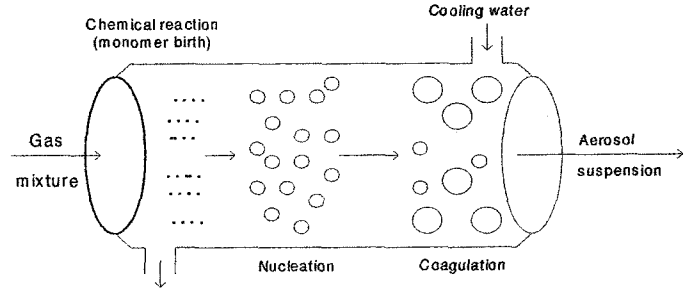

Figure 1.2: Aerosol flow reactor

Two other examples of DPS are aerosol processes and fibre spinning. Aerosol processes are widely used in industry for the production of fine particles (*e.g.*, pigments, carbon black, optical fibres, silicon and ceramic powers) and are characterized by coupled chemical reaction, nucleation, condensation and coagulation phenomenon. The distributed nature of this system becomes obvious by viewing the particle size along the aerosol flow reactor, as shown in Figure 1.2. A mathematical model describing the spatio-

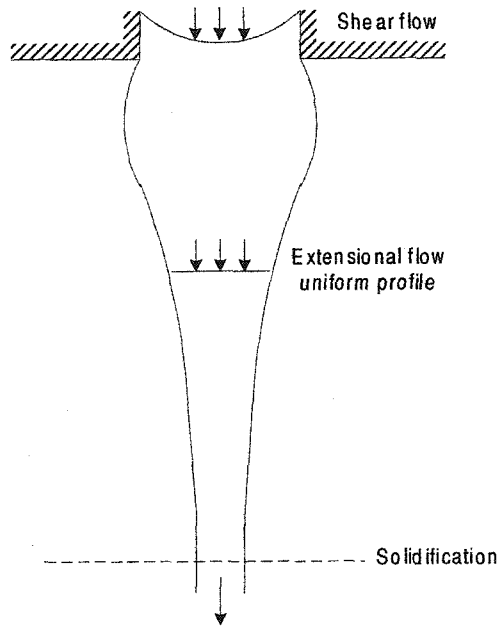

Figure 1.3: Melt spinning

temporal evolution of the particle size distribution can be obtained using a population balance:

$$\frac{\partial n}{\partial t} + v_x \frac{\partial n}{\partial x} + \frac{\partial (G(\bar{x}, v, x) n)}{\partial v} - I(v^*)\delta(v - v^*) = \frac{1}{2}\int_0^v \beta(v - \bar{v}, \bar{v}, \bar{x}) \\ n(v - \bar{v}, t) n(\bar{v}, t) d\bar{v} - n(v, t) \int_0^\infty \beta(v, \bar{v}, \bar{x}) n(\bar{v}, t) d\bar{v} \tag{1.6}$$

where $n(v, x, t)$ denotes the particle size distribution function, v is the particle volume, t is the time, $x \in [0, L]$ is the spatial variable, L is the length of the process, v_x is the velocity of the fluid, $G(\bar{x}, v, x), I(v^*), \beta(v - \bar{v}, \bar{v}, \bar{x})$ are nonlinear scalar functions and δ is the standard Dirac function. Fiber spinning is a process in which an extruded liquid filament, usually a polymeric liquid, is continuously drawn and solidifies simultaneously to form a continuous fiber (Denn, 1987). Figure 1.3 displays the change of filament radius with axial distance, which is a distributed state variable. Other distributed variables in this system include temperature and stress along the axial direction. The

final physical properties of the solid filament appear to correlate with these distributed state variables during spinning. The model of the process can be obtained using mass balance, momentum balance, heat transfer and stress constitutive equations:

$$\begin{aligned}
\frac{\partial}{\partial t}(R^2\rho) &= -\frac{\partial}{\partial x}(R^2\rho v), \\
R^2\rho^2\frac{\partial v}{\partial t} &= -R\rho v\frac{\partial v}{\partial x} + \frac{\partial}{\partial x}(R^2\tau_E) - \rho_a v^2 R C_D + R^2\rho g, \\
R^2\rho C_P\frac{\partial T}{\partial t} &= -R^2\rho v C_p\frac{\partial T}{\partial x} - 2\pi h R(T - T_a), \\
\tau_E + \frac{\eta}{G}\dot{\tau}_E &= 3\eta\frac{\partial v}{\partial x},
\end{aligned} \tag{1.7}$$

where $R(x)$ is the filament radius which changes slowly with axial distance x, τ_E is the tensile stress exerted on the control volume by the surrounding fluid, T is the temperature, v is the average velocity, ρ is the density, ρ_a is the air density of the air, C_D is the aerodynamic drag coefficient, g is the gravitational acceleration, η is the shear viscosity and G is the shear modulus.

From the above examples, several features of DPS can be enumerated. Models describing the dynamics of DPS are different from those for LPS and often take the form of partial differential equations, while LPS are usually modelled by Ordinary Differential Equations (ODE). The dynamics of DPS are such that the inputs of the process affect the infinite-dimensional state variables; however, it may take some time for the influence of the input to be observed in the process output at a specific spatial location, a situation analogous to the effect of time-delay in finite dimensional systems. Boundary conditions play an important role in DPS control since the manipulated variables and/or the control variables are usually located at a process boundary. Further, distributed state variables can only be measured at some set of spatial points, which may include the boundaries.

Since PDE models are most often used to represent DPS, they provide a reasonable basis for the development of control methods for these systems. Unfortunately, exact solutions for the PDEs, which describe even a moderately complex distributed process, are rarely available. As a result, distributed parameter systems are often approximated by linear low-order plus dead time models (Shirvani *et al.*, 1995), represented by simple transfer function models. Such simple approximations can then be used to design linear

model-based control strategies such as internal model control, model algorithmic control, Dynamic Matrix Control (DMC) and simplified model predictive control (Patwardhan *et al.*, 1992). Other simplification of DPS comes from the direct approximation of PDE models. Finite difference methods or finite element methods have been used to reduce the original DPS to one with finite dimensions, but the resulting approximate lumped parameter systems may require very high dimensionality to ensure accuracy. The use of such models for the purpose of control may lead to unacceptable computational requirements.

Modal analysis techniques reduce the PDE model to an infinite set of first-order Ordinary Differential Equations (ODEs) based on the ability to represent the spatially varying input and output of the system as the sum of infinite series of the system's spatial eigenfunctions (eigenmodes) with time-dependent coefficients (Ray, 1981). The dynamic behavior of each coefficient is then obtained as the solution to one of the independent ODEs. Modal analysis has been employed extensively to provide both approximate solutions and theoretical results regarding the control of DPS described by linear parabolic PDEs. The successful application of this technique relies on both the existence and knowledge of the eigenvalues and the eigenfunctions for the linear operators that describe the distributed system. The determination of the eigenfunctions for a practical physical system is not a simple task (Brown, 2001). If the system is non-self-adjoint or the coefficients of the PDE have a strong spatial dependence, analytic determination of the eigenfunctions may be intractable. Karhunen-Loève decomposition is a technique of obtaining empirical eigenfunctions from experimental or numerical data of a system and enables a stochastic field to be represented with a minimum number of empirical eigenfunctions (Park and Cho, 1996). This technique can treat a nonlinear DPS defined on irregular domains to yield lumped parameter systems with small dimensionality. However, the use of such eigenfunctions as basis functions for the systems can sacrifice the accuracy of representation.

An alternative approach uses singular values and singular functions as the basis of a truncated series expansion model in place of the conventional representation using

eigenvalues and eigenfunctions (Gay and Ray, 1995). According to singular value theory (Cochran, 1972), these functions exist for all linear operators, which can be expressed in terms of a Fredholm integral equation of the first kind with a generally unsymmetric square integrable kernel. A general structure for an input/output model of linear DPS can be expressed in terms of an integral equation with a $\mathcal{L}^2$ kernel $k(x, \xi, t-\tau)$ as:

$$y(x,t) = \int_0^t \int_0^1 k(x,\xi,t-\tau)u(\xi,\tau)d\xi d\tau. \tag{1.8}$$

The kernel $k(x, \xi, t-\tau)$ of Equation (1.8) defines a linear time-invariant compact operator $\mathcal{K}$, which maps a distributed input function $u(x,t)$ to a distributed output function $y(x,t)$ where both $u(x,t)$ and $y(x,t)$ are $\mathcal{L}^2$ (square integrable) functions defined on the region $\{x,t : 0 \leq x \leq 1, t \geq 0\}$. Equation (1.8) can be more compactly expressed as $y = \mathcal{K}u$. In the case that the system equations, eigenfunctions, boundary conditions and parameters are unknown, such an integral equation representation provides a more useful and general model structure for the purpose of identification and control of DPS. The singular functions can be determined with a high accuracy if a representation for the kernel is known, or in the more practical case, can be identified approximately from data obtained through input/output testing. The identification of singular functions for unknown DPS can be explored by suitable design of dynamic experiments (Chakravarti and Ray, 1999).

1.2 Status of Control for DPS

Given that DPS are industrially important, research has become increasingly active on the control of these systems and the control techniques have been developed based on specific types of process models. For some DPS, a complete understanding of the underlying physical phenomenon is lacking, and it is impossible to generate a highly accurate first principle model. An important group of such DPS is sheet and film processes, which include polymer film extrusion, paper making and coating, metal rolling, *etc.* Usually they are approximated with high-dimensional dynamics, a large time delay

and a periodic measurement matrix. Process models, obtained mostly using data-based system identification techniques, are typically empirical in nature. Control strategies, such as model predictive control, have been developed using such empirical models and have incorporated techniques to deal with model plant mismatch, actuator limitation and obtain uniform profiles for desired product properties (Braatz *et al.*, 1992; Campbell and Rawlings, 1998; VanAntwerp and Braatz, 2000).

For DPS with weak spatial variation, simplifying assumptions (*e.g.*, perfect mixing in a stirred tank) can often be validated to justify the use of lumped parameter approximations and ordinary differential equation models to represent the dynamics of these processes. However, there are a significant number of industrial processes that display strong dependence on spatial position. Since such systems cannot be approximated by lumped parameter models, controller design requires the use of integral equation or partial differential equation models to capture the spatially varying properties of the DPS. The complexity of DPS has forced control engineers to resort to approximation methods. The most commonly used methods are lumping approaches.

Most conventional approaches for control of the distributed parameter systems use lumping techniques to discretize the underlying PDE model into a finite number of ordinary differential equations (ODE). This technique allows one to design controllers using the rich theory available for Lumped Parameter Systems (LPS). These approaches can be classified into two categories (Ray, 1981). The most straightforward approach is termed *early lumping*. In this approach, a distributed parameter model is discretized into an approximate model consisting of a set of ordinary differential equations in time. The design methods for lumped parameter systems are then applied directly to design controllers without recourse to distributed parameter system theories. The alternative approach, *late lumping*, takes full advantage of the available distributed parameter control theories and analyzes the PDE model for controllability, stabilizability, controller structure design, *etc.* It is only at the last stages, after the controllers have been designed, that the controller equations are lumped to ease implementation.

The widely used discretization techniques, such as finite difference, finite element

and finite volume methods, discretize a PDE model into a set of ODEs or multi-dimensional difference equations and can be effective tools for dealing with the control of distributed parameter systems. Based on the approximate difference equations obtained from the discretizations, a pole placement controller was designed by applying a 2-D Laplace transform to allow pole assignment (Hernández and Arkun, 1992). However, the dimension of the approximation used is often large and the resulting controllers are potentially complex.

Galerkin approximation procedures have been used to lump DPS for the control and estimation purposes. These methods can produce fewer ODEs in certain cases by finding an appropriate set of basis functions. For example, Sadek (1997) employed orthogonal polynomial expansion to solve a modal/state optimization problem and approximated the state estimation and/or control by finite-term series whose coefficient values were determined optimally (Sadek and Bokhari, 1998). In many cases, these Galerkin methods do not lead to acceptably low dimensional ODEs. In some control methods, model reduction is considered to be an important first step in controller design. Methods such as approximate Inertial Manifolds can be used to obtain the reduced model for the control of DPS (Shvartsman and Kevrekidis, 1998). Combining Galerkin methods with approximate Inertial Manifolds reduces the number of approximate ODEs needed in the approximate models. Armaou and Christofides (1998) designed a geometric control method for parabolic systems using this technique, but computation of the inertial manifolds is complex and not always practical. Singular value decomposition provides a natural framework for low-order modal feedback control system design. However, it is limited to a class of linear DPS described by parabolic PDE models (Chakravarti and Ray, 1999; Gay and Ray, 1995).

The disadvantages of these approximation techniques for distributed parameter systems have motivated the research into control approaches based on the underlying partial differential equation models. A combination of the Method of Characteristics and sliding mode techniques was proposed for processes modelled by first-order hyperbolic PDEs to synthesize a state feedback control (Hanczyc and Palazoglu, 1995; Sira-

Ramirez, 1989). Hanczyc and Palazoglu (1995) proposed a method based on symmetry groups for the design of state feedback control for second-order parabolic systems. The main disadvantage of their techniques is that the selection of infinitesimal generators of the symmetry groups in a PDE system does not contain the effects of initial and boundary conditions. Moreover, these methods only provide the design of state feedback control. Christofides (1996) addressed the synthesis of a nonlinear distributed state feedback controller using geometric control methods and the design of a state observer for first-order hyperbolic DPS. Other PDE-based control approaches include control design for parabolic heat transfer systems using system "flatness", which allows an explicit parameterization of the trajectories as a power series in the spatial variable with coefficients involving time derivatives of the "flat" output (Laroche *et al.*, 1998). A traditional PI controller for a class of nonlinear PDE processes with boundary control was shown to achieve closed-loop stability and output regulation (Alvarez-Ramirez, 2001).

In view of the above discussion, further research into the control of PDE-based distributed parameter systems is necessary to broaden the base of model forms such that their inherent complexity can be addressed. Many problems associated with controller performance, computational tractability and general technical methodology remain.

1.3 Thesis Scope and Objectives

The objective of this thesis is to develop control design techniques for DPS by exploring the geometric properties of the PDEs modelling DPS. The Method of Characteristics, a powerful solution method for hyperbolic systems, is used in the control development to provide a prediction of the process behavior. Standard feedback control, which does not explicitly include prediction horizon in control formulations, and Model Predictive Control (MPC) are the two control techniques considered in this work. High performance control and efficient computation are pursued to attain attractive control methods that can be implemented in industrial applications.

The focus of the thesis is control development for distributed parameter processes

modelled by first order and second order linear, semilinear or quasilinear partial differential equations. These PDEs can model or approximately model many chemical engineering processes and constitute a wide range of PDE models encountered in practical application. Although this thesis presents results for PDE models with a single spatial direction, the methods are easily extendable to two and three dimensional PDEs. Using the Method of Characteristics, the control of hyperbolic and convection-dominated parabolic PDEs is investigated. The focus of the study is on the deterministic processes, and as a result, stochastic behavior is not considered.

The structure of the thesis is as follows. Mathematical preliminaries are provided in Chapter 2. Standard feedback control for first-order hyperbolic system is discussed in Chapter 3. Chapters 4, 5 and 6 focus on characteristic-based MPC for hyperbolic systems and convection-dominant parabolic systems, respectively. Chapter 7 provides the conclusions drawn from this study and suggests future research directions.

Chapter 2

Mathematical Background

In this chapter, a comprehensive review of key mathematical concepts used throughout this thesis is presented. They include the classification of PDEs, the Method of Characteristics and Semigroup theory. The types of PDEs used to model DPS determine the approaches taken for control development. The Method of Characteristics provides the fundamental mathematical tool used in the control design approach proposed here. Semigroup theory allows one to cast the PDE system in an abstract space, which facilitates the design of observers for DPS.

2.1 Classification of Partial Differential Equations

Generally, a PDE model for a distributed parameter system is of the form:

$$F(x_1, ..., x_n, v, v_{x_1}, ...v_{x_n}, v_{x_1x_1}, v_{x_1x_2}, ..., u) = 0, \tag{2.1}$$

where $\mathbf{x} = (x_1, ..., x_n)$ are independent variables such as time and position, v is a dependent variable of $(x_1, ..., x_n)$ and u is the manipulated variable, and $v_{x_1} = \dfrac{\partial v}{\partial x_1}$, $v_{x_1x_2} = \dfrac{\partial^2 v}{\partial x_1 \partial x_2}$, ..., and so on. The order of Equation (2.1) is the order of the highest derivative occurring in the equation. Moreover, the equation is considered linear if it

depends linearly on the states v and its derivatives; if all derivatives of v occur linearly with coefficients depending only on $\mathbf{x}$, then the equation is semilinear; and if the highest-order derivatives of v occur linearly with coefficients depending only on $\mathbf{x}$, u, and lower-order derivatives of v, then the equation is quasilinear (McOwen, 1996). In this study, the primary focus will be on first-order and second-order quasilinear systems.

First-order and second-order PDEs can be classified into hyperbolic, parabolic and elliptic equations. All single first-order PDEs are hyperbolic. The general quasi-linear system of n first-order partial differential equations in two independent variables has the form

$$\sum_{j=1}^{n} a_{ij}\frac{\partial v_j}{\partial x_1} + \sum_{j=1}^{n} b_{ij}\frac{\partial v_j}{\partial x_2} = c_i, \qquad i = 1, 2, ..., n, \tag{2.2}$$

where a_{ij}, b_{ij} and c_i may depend on x_1, x_2, and v_1, v_2, ..., v_n. If $c_i = 0$ for $i = 1, 2, ..., n$, the system is called homogeneous. In terms of the $n \times n$ matrices $\mathbf{A} = [a_{ij}]$ and $\mathbf{B} = [b_{ij}]$ and the column vectors $\mathbf{v} = [v_1, v_2, ..., v_n]^T$ and $\mathbf{c} = [c_1, c_2, ..., c_n]^T$, the system of equations can be written as

$$\mathbf{A}\mathbf{v}_{x_1} + \mathbf{B}\mathbf{v}_{x_2} = \mathbf{c}. \tag{2.3}$$

For a well-posed initial value condition problem (*i.e.*, the initial conditions satisfy the partial differential equations), the matrix $\mathbf{A}$ or $\mathbf{B}$ is nonsingular depending on the initial conditions at $x_1 = 0$ or $x_2 = 0$. Assuming that $det(\mathbf{B}) \neq \mathbf{0}$, the characteristic polynomial can be defined by

$$F(\lambda) = \det(\mathbf{A} - \lambda\mathbf{B}). \tag{2.4}$$

Since $\mathbf{A}$ and $\mathbf{B}$ are $n \times n$ matrices and $det(\mathbf{B}) \neq \mathbf{0}$, the polynomial F is of degree n. If $F(\lambda)$ has n distinct real zeros, the system (2.2) is classified as hyperbolic. The system is also called hyperbolic if $F(\lambda)$ has n non-distinct real zeros and the generalized eigenvalue problem $(\mathbf{A} - \lambda\mathbf{B})\mathbf{x_2} = 0$ has n linearly independent eigenvectors. If $F(\lambda)$ has no real zeros, then the system (2.2) is called elliptic. If $F(\lambda)$ has n non-distinct real zeros and $(\mathbf{A} - \lambda\mathbf{B})\mathbf{x_2} = 0$ does not have n linearly independent solutions, the system may be classified as parabolic. This classification is not possible when $F(\lambda)$ has both real and complex zeros.

A second-order PDE in which the derivatives of second-order all occur linearly can be represented as:

$$a(x_1, x_2)v_{x_1x_1} + b(x_1, x_2)v_{x_1x_2} + c(x_1, x_2)v_{x_2x_2} = d(x_1, x_2, v, v_{x_1}, v_{x_2}), \tag{2.5}$$

with certain initial and/or boundary conditions. Let γ be a line parameterized in (x_1, x_2) space. Cauchy data along γ can be defined as:

$$v|_\gamma = \eta, \qquad \frac{\partial v}{\partial \nu}|_\gamma = \eta_1, \tag{2.6}$$

where ν denotes a choice of unit normal vector along γ. The Cauchy data can also be expressed as

$$v|_\gamma = \eta, \qquad \frac{\partial v}{\partial x_1}|_\gamma = \phi, \qquad \frac{\partial v}{\partial x_2}|_\gamma = \psi, \tag{2.7}$$

provided the compatibility condition holds.

The classification of linear and semilinear second-order PDEs in Equation (2.5) can be associated with the characteristic equation:

$$\frac{dx_2}{dx_1} = \frac{b \pm \sqrt{b^2 - 4ac}}{2a}. \tag{2.8}$$

1. If $b^2 - 4ac > 0$, there are two characteristics and Equation (2.5) is called hyperbolic. An example is the wave equation that describes vibrating membranes and sound and electromagnetic waves.

2. If $b^2 - 4ac = 0$, there is only one characteristic and Equation (2.5) is called parabolic. An example is the heat equation.

3. If $b^2 - 4ac < 0$, there are no characteristics and Equation (2.5) is called elliptic. An example is the Laplace equation that governs the time-independent behavior of solutions to the wave and heat equations, and electrostatic potential.

For quasilinear or fully nonlinear second-order equations, a similar classification can be made by linearization of the highest-order derivatives; but the resulting type (hyperbolic, parabolic, or elliptic) may depend upon the particular solution v being considered. Higher-order systems can be decomposed into one or a combination of the three.

2.2 Method of Characteristics

The Method of Characteristics is a useful technique that is employed to compute integral surfaces of a certain class of DPS. For single first-order PDEs, the solutions can be generated by considering integral curves (or characteristics) of a specific vector field, called the characteristic vector field. By considering this vector field, the solution of a DPS can be readily transformed to the solution of a set of ODEs (Arnold, 1988; McOwen, 1996). In this section, the Method of Characteristics is introduced for scalar first-order PDEs and systems of first-order PDEs.

2.2.1 Scalar First-Order PDEs

Consider the quasilinear equation for a function $v\,(t, x_1, ..., x_n)$ on the manifold $M \times \mathbb{R}$ of R^{n+1}

$$\frac{\partial v}{\partial t} + \sum_{i=1}^{n} a_i(\mathbf{x}, v, \mathbf{u}) \frac{\partial v}{\partial x_i} = f(\mathbf{x}, v, \mathbf{u}), \tag{2.9}$$

where t is the time, $\mathbf{x} = [x_1, \cdots, x_n]$ is a point in the manifold M, $a_1(\mathbf{x}, v, \mathbf{u}), \cdots, a_n(\mathbf{x}, v, \mathbf{u})$ and $f(\mathbf{x}, v, \mathbf{u})$ are continuous (C^0) in $\mathbf{x}$ and v, and $\mathbf{u}$ is the manipulated variable. Given $v\,(t, \mathbf{x})$ as the solution of Equation (2.9), let us consider the graph $z = v\,(t, \mathbf{x})$. This graph has a normal vector

$$\mathbf{N}_0 = [-\frac{\partial v}{\partial t}, -\frac{\partial v}{\partial x_1}, ..., -\frac{\partial v}{\partial x_n}, 1] \tag{2.10}$$

at the point $(t_0, \mathbf{x}_0, v\,(t_0, \mathbf{x}_0))$. Let $z_0 = v\,(t_0, \mathbf{x}_0)$ and take $\mathbf{u}$ as parameters. Then, Equation (2.9) implies that the vector $\xi_0 = [1,\ a_1(\mathbf{x}_0, z_0, \mathbf{u}), \cdots,\ a_n(\mathbf{x}_0, z_0, \mathbf{u}),\ f(\mathbf{x}_0, z_0, \mathbf{u})]$ is perpendicular to the normal vector $\mathbf{N}_0$, and hence, must lie in the tangent plane to the graph of Equation (2.9) at the point $(t_0, \mathbf{x}_0, z_0)$. In other words,

$$\xi(t, \mathbf{x}, v, \mathbf{u}) = [1, a_1(\mathbf{x}, v, \mathbf{u}), \cdots, a_n(\mathbf{x}, v, \mathbf{u}), f(\mathbf{x}, v, \mathbf{u})] \tag{2.11}$$

defines a vector field in R^{n+1}, tangent to the solution graph at each point. This vector field is called the characteristic vector field of the quasilinear Equation (2.9). The integral

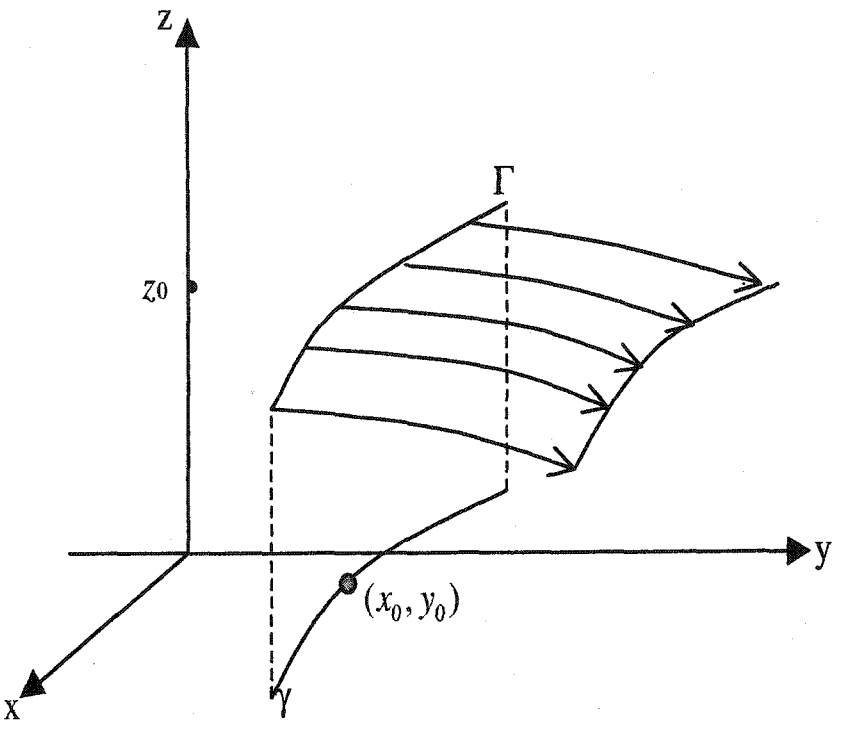

Figure 2.1: Generation of the solution surface by characteristics

curves of the characteristic vector field are called the characteristics of the quasilinear equation. The ordinary differential equation defined by the vector field $\xi(t, \mathbf{x}, v, \mathbf{u})$ is called the characteristic equation and the characteristic equation of the quasilinear Equation (2.9) has the form:

$$\begin{aligned} \dot{t} &= 1, \\ \dot{\mathbf{x}} &= \mathbf{a}(\mathbf{x}, v, \mathbf{u}), \\ \dot{v} &= f(\mathbf{x}, v, \mathbf{u}). \end{aligned} \tag{2.12}$$

If the graph $v = v(t, \mathbf{x}, \mathbf{u})$ is a smooth surface S, which is a union of such characteristic curves, then at each point $(t, \mathbf{x}, v)$, the tangent plane contains the vector $\xi(\mathbf{x}, v, \mathbf{u})$; hence, S must be an integral surface. In other words, a smooth union of characteristic curves is an integral surface of the characteristic vector field. If the given initial condition Γ is non-characteristic (*i.e.,* Γ is nowhere tangent to the vector field), a

simple procedure for solving the first-order PDE problem is to flow out from each point of Γ along the characteristic curve through that point, thereby sweeping out an integral surface (see Figure 2.1). This is *the Method of Characteristics*. It is trivial to show that the function so constructed satisfies the original differential equation. By differentiating along the characteristics, it can be obtained:

$$\dot{v} = f = \frac{\partial v}{\partial t}\dot{t} + \sum_{i=1}^{n} \frac{\partial v}{\partial x_i}\dot{x}_i = \frac{\partial v}{\partial t} + \sum_{i=1}^{n} a_i(\mathbf{x}, v, \mathbf{u})\frac{\partial v}{\partial x_i}. \tag{2.13}$$

This result shows that along the characteristics, the partial derivative terms in Equation (2.9) reduce to a directional derivative of v in that direction.

The characteristics are more complicated for a first-order nonlinear PDE system:

$$\frac{\partial v}{\partial t} + \Phi(v, \mathbf{x}, t, \frac{\partial v}{\partial \mathbf{x}}, u) = 0. \tag{2.14}$$

Equation (2.14) can be interpreted as a hypersurface E^{2n+2} in the manifold $M^{2n+3} = J^1(V^{n+1}, \mathbb{R})$ of 1-jets equipped with the standard contact structure. Let $(\mathbf{x}, t)$ be the local coordinates on V^{n+1} and v be the coordinate in $\mathbb{R}$, $\mathbf{p} = \dfrac{\partial v}{\partial \mathbf{x}}$ and $q = \dfrac{\partial v}{\partial t}$. The corresponding local coordinates are denoted by $(\mathbf{x}, t, v, \mathbf{p}, q)$ in the space of 1-jets. Then, the differential equation can be written in the form:

$$q + \Phi(v, \mathbf{x}, t, \mathbf{p}, u) = 0. \tag{2.15}$$

By the Method of Characteristics, the characteristic equations of PDE (2.14) in the manifold M^{2n+3} can be written as (Arnold, 1988):

$$\begin{aligned} \dot{t} &= 1, \\ \dot{q} &= -q\Phi_v - \Phi_t, \\ \dot{\mathbf{x}} &= \Phi_{\mathbf{p}}, \\ \dot{\mathbf{p}} &= -\Phi_{\mathbf{x}} - p\Phi_v, \\ \dot{v} &= p\Phi_{\mathbf{p}} + q. \end{aligned} \tag{2.16}$$

Substitution of Equation (2.15) can reduce the order of Equation (2.16) by 1:

$$\begin{aligned} \dot{t} &= 1, \\ \dot{\mathbf{x}} &= \Phi_{\mathbf{p}}, \\ \dot{\mathbf{p}} &= -\Phi_{\mathbf{x}} - p\Phi_{v}, \\ \dot{v} &= p\Phi_{\mathbf{p}} - \Phi. \end{aligned} \tag{2.17}$$

For distributed parameter systems, the current control action can affect the states at spatially distributed measurement points before it affects the output. From the spatially distributed measurements, the characteristics in Equation (2.12) allow the prediction of the future process output and the effect of current action on the future process output. The prediction is obtained by examining the orbital curve of the characteristic vector field ξ (*i.e.*, integration of the characteristic ODE).

2.2.2 System of First-Order PDEs

Systems of first-order equations that arise in physical problems are often of hyperbolic type. Therefore, the discussion of systems of first-order equations is confined to systems of hyperbolic PDEs (Duchateau and Zachmann, 1989).

A characteristic of a scalar first-order PDE is defined by the characteristic ordinary differential equations, for which there is no obvious generalization to higher dimensions. For scalar first-order PDEs, however, the partial derivatives are not uniquely defined on the curve that is the projection of a characteristic curve on Cauchy data, this idea can be generalized to determine the characteristics of higher dimensional PDE systems.

Consider a 2×2 system, for which a vector function with components v_1 and v_2 satisfies

$$\mathbf{A}\frac{\partial \mathbf{v}}{\partial x} + \mathbf{B}\frac{\partial \mathbf{v}}{\partial t} = \mathbf{c}, \tag{2.18}$$

where A and B are 2×2 matrices and c is a vector with two components, all of whose entries and components are functions of x, t, v_1 and v_2. A characteristic of Equation

(2.18) is a curve $(x(s), t(s))$ such that Equation (2.18) evaluated on the curve and the differential equations

$$x' \frac{\partial \mathbf{v}}{\partial x} + t' \frac{\partial \mathbf{v}}{\partial t} = \frac{d\mathbf{v}}{ds}, \tag{2.19}$$

where $x' = \frac{dx}{ds}$ and $t' = \frac{dt}{ds}$, do not have unique solutions for $\frac{\partial \mathbf{v}}{\partial x}$ and $\frac{\partial \mathbf{v}}{\partial t}$. Therefore, the left-hand sides of these four equations are linearly dependent. This leads to the expression

$$det(\mathbf{B}x' - \mathbf{A}t') = 0. \tag{2.20}$$

Hence, $(x(s), t(s))$ is a characteristic if Equation (2.20) is satisfied. Unlike the situation in the scalar case, this expression may not yield characteristic directions at each point.

For the solution of Equation (2.18), Cauchy data can be imposed on $t = 0$, so it is crucial that this is not a characteristic. A necessary and sufficient condition that $t = 0$ is not characteristic is that $det(\mathbf{B}x' - \mathbf{A}t') \neq 0$, or that $\mathbf{B}$ is nonsingular. By introducing two new dependent variables into Equation (2.18), the inhomogeneous term $\mathbf{B}^{-1}\mathbf{c}$ can be removed and a homogeneous problem results (Ockendon *et al.*, 1999).

If the system of hyperbolic equations has constant coefficients and is homogeneous, the Method of Characteristics can be used to obtain a complete solution of the system subject to specified initial conditions for each of the unknowns (Duchateau and Zachmann, 1989).

A system of first-order n-dimensional homogeneous PDEs with constant coefficients, along with its initial conditions, can be written as:

$$\mathbf{A}\mathbf{v}_x + \mathbf{B}\mathbf{v}_t = 0, \qquad -\infty < x < \infty, t > 0, \tag{2.21}$$

$$\mathbf{v}(x, 0) = \mathbf{f}, \qquad -\infty < x < \infty. \tag{2.22}$$

The difficulty presented by the system of equations (2.21) is the coupling of the unknowns $v_j(x, t)$ in the sense that, in general, each equation involves all unknowns. The solution method requires the formation of a linear combination of the components of the unknown vector $\mathbf{v}$

$$z_i = \sum_{j=1}^{n} q_{ij} v_j, \qquad i = 1, 2, .., n, \tag{2.23}$$

or

$$\mathbf{z} = \mathbf{Q}\mathbf{v}, \qquad \mathbf{Q} = (q_{ij}), \tag{2.24}$$

where q_{ij} represent constants to be determined. A certain linear combination of the n equations is formed such that the groupings of equations and the groupings of the components of $\mathbf{v}$, dictated by these linear combinations, decouples the unknowns yielding n first-order equation of the form

$$\lambda_i \frac{\partial z_i}{\partial x} + \frac{\partial z_i}{\partial t} = 0, \qquad i = 1, 2, ..., n. \tag{2.25}$$

Since each equation for each z_i is a constant-coefficient advection equation, the Method of Characteristics discussed in the last subsection can be used to determine $z_i(x, t)$. The original unknowns can be recovered from $\mathbf{v} = \mathbf{Q}^{-1}\mathbf{z}$. Let $\mathbf{P} = (p_{ij})$ be an invertible $n \times n$ matrix that satisfies the equation:

$$\mathbf{PA} = \mathbf{\Lambda PB}, \tag{2.26}$$

where $\mathbf{\Lambda}$ represents a diagonal matrix:

$$\mathbf{\Lambda} = \text{diag}(\lambda_i). \tag{2.27}$$

Multiplying each term of Equation (2.21) by the matrix $\mathbf{P}$ gives $\mathbf{PAv_x} + \mathbf{PBv_t} = 0$. Using Equation (5.4), the following is obtained: $\mathbf{\Lambda PBv_x} + \mathbf{PBv_t} = 0$. To determine a linear combination of unknowns that leads to a decoupled system, define a matrix $\mathbf{Q} = \mathbf{PB}$ and set $\mathbf{z} = \mathbf{Qv}$. Then, we have

$$\mathbf{\Lambda PBv_x} + \mathbf{PBv_t} = \mathbf{\Lambda Qv_x} + \mathbf{Qv_t} = \mathbf{\Lambda z_x} + \mathbf{z_t}, \tag{2.28}$$

which implies that the components of the vector $\mathbf{z}$ satisfy the decoupled system

$$\lambda_i \frac{\partial z_i}{\partial x} + \frac{\partial z_i}{\partial t} = 0, \tag{2.29}$$

in which the i^{th} equation involves differentiation only along the i^{th} characteristic. The system of equations asserts that z_i is constant along the characteristics $dx/dt = \lambda_i$. Thus, $z_i,\ i = 1, 2, ..., n$, represent the groupings of the physical variables that remain constant along characteristics. Such groupings are called *Riemann invariants*.

Having grouped the components of the unknown vector $\mathbf{v}$ in Equation (2.21), the same groupings in the initial conditions for $\mathbf{z}$ can be formed:

$$\mathbf{z}(x,0) = \mathbf{Q}\mathbf{v}(x,0), \qquad \text{or} \qquad z_i(x,0) = \sum_{j=1}^{n} q_{ij} f_j(x) = g_i(x). \tag{2.30}$$

Then, the solution to the initial-value problem for $\mathbf{z}$ is given by

$$z_i(x,t) = g_i(x - \lambda_i t), \qquad i = 1, 2, ..., n. \tag{2.31}$$

It can be seen that the entries in the matrix $\mathbf{P}$ fix the linear combination of unknowns that leads to an decoupled system. Since $\mathbf{B}$ has been assumed to be invertible, the product $\mathbf{Q} = \mathbf{PB}$ is invertible. Thus the original unknown $\mathbf{v}(x)$ can be recovered from $\mathbf{v} = \mathbf{Q}^{-1}\mathbf{z}$. All that remains in the solution method for the initial-value problem is a means of determining the matrix $\mathbf{P}$.

The calculation of the matrix $\mathbf{P}$ can be obtained from the property $\mathbf{PA} = \mathbf{\Lambda PB}$, where Λ is diagonal. For the case $n = 2$, the requirement can be written as:

$$\begin{bmatrix} p_{11} & p_{12} \\ p_{21} & p_{22} \end{bmatrix} \begin{bmatrix} a_{11} & a_{12} \\ a_{21} & a_{22} \end{bmatrix} = \begin{bmatrix} \lambda_1 & 0 \\ 0 & \lambda_2 \end{bmatrix} \begin{bmatrix} p_{11} & p_{12} \\ p_{21} & p_{22} \end{bmatrix} \begin{bmatrix} b_{11} & b_{12} \\ b_{21} & b_{22} \end{bmatrix}. \tag{2.32}$$

The transpose of the product of square matrices is the product of the transposes in reverse order, $(\mathbf{PA})^{\mathbf{T}} = \mathbf{A}^{\mathbf{T}}\mathbf{P}^{\mathbf{T}}$. Applying the transpose to both sides of the last matrix equation gives

$$\begin{bmatrix} a_{11} & a_{21} \\ a_{12} & a_{22} \end{bmatrix} \begin{bmatrix} p_{11} \\ p_{12} \end{bmatrix} = \lambda_1 \begin{bmatrix} b_{11} & b_{21} \\ b_{12} & b_{22} \end{bmatrix} \begin{bmatrix} p_{11} \\ p_{12} \end{bmatrix}, \tag{2.33}$$

and

$$\begin{bmatrix} a_{11} & a_{21} \\ a_{12} & a_{22} \end{bmatrix} \begin{bmatrix} p_{21} \\ p_{22} \end{bmatrix} = \lambda_2 \begin{bmatrix} b_{11} & b_{21} \\ b_{12} & b_{22} \end{bmatrix} \begin{bmatrix} p_{21} \\ p_{22} \end{bmatrix}. \tag{2.34}$$

To be able to obtain nonzero vectors $\mathbf{p}_1 = [p_{11}, p_{12}]^T$ and $\mathbf{p}_2 = [p_{21}, p_{22}]^T$, the constants λ_1 and λ_2 must be zeros of the characteristic polynomial:

$$F(\lambda) = det(\mathbf{A} - \lambda\mathbf{B}) = det(\mathbf{A}^T - \lambda\mathbf{B}^T). \tag{2.35}$$

Since the matrix $\mathbf{P}$ is invertible, both $\mathbf{p}_1$ and $\mathbf{p}_2$ are nonzero. The entries of the i^{th} row of the matrix $\mathbf{P}$ can be determined such that they satisfy

$$\mathbf{A^T p_i} = \lambda_i \mathbf{B^T p_i}, \qquad i = 1, 2. \tag{2.36}$$

Therefore, the matrix $\mathbf{P}$ for the case of a system of two equations (*i.e.*, $n = 2$) is constructed from the above equation. The case of general n involves no new ideas. With the determination of the matrix $\mathbf{P}$, the solution method for a constant-coefficient homogeneous hyperbolic system of first-order partial differential equations is straightforward. For a general hyperbolic system, the Method of Characteristics fails to provide an analytical solution. However, it remains possible to apply a numerical approach to the Method of Characteristics for such systems.

2.3 Semigroup Theory

The solution structures for many PDE systems can be expressed by semigroup operators. This can be illustrated by considering a PDE model for a metal bar of length one that is heated along its length:

$$\begin{aligned} &\frac{\partial v}{\partial t}(x,t) = \frac{\partial^2 v}{\partial x^2}(x,t) + u(x,t), \\ &v(x,0) = v_0(x), \\ &\frac{\partial v}{\partial x}(0,t) = 0 = \frac{\partial v}{\partial x}(1,t), \end{aligned} \tag{2.37}$$

where $v(x,t)$ represents the temperature at position x and time t, $v_0(x)$ the initial temperature profile, and $u(x,t)$ the addition of heat along the bar. By choosing $Z = L_2(0,1)$ as the state space and the trajectory segment $v(\cdot,t) = v(x,t), 0 \leq x \leq 1$ as the

state, defining the operators A and B on Z as:

$$\begin{aligned} A\varphi &= \frac{d^2\varphi}{dx^2} \text{ with} \\ \mathbf{D}(A) &= \left\{ \begin{array}{l} \varphi \in L_2(0,1) | \ \varphi, \frac{d\varphi}{dx} \text{ are absolutely} \\ \text{continuous, } \frac{d^2\varphi}{dx^2} \in L_2(0,1) \text{ and} \\ \frac{d\varphi}{dx}(0) = 0 = \frac{d\varphi}{dx}(1) \end{array} \right\}, \\ B &= I, \end{aligned} \tag{2.38}$$

and regarding the input trajectory $u(\cdot, t)$ as the input and the function $v_0(\cdot) \in L_2(0,1)$ as the initial state, Equation (2.37) can be described through an abstract formulation as:

$$\dot{v}(t) = Av(t) + Bu(t), \ t \geq 0, \qquad v(0) = v_0, \tag{2.39}$$

on a Hilbert space Z. This allows a unified treatment of the PDE systems and finite-dimensional systems.

Using the "separation of variables" approach, for sufficiently smooth function v_0 that satisfies the boundary conditions and sufficiently smooth input function $u(x,t)$, the solution of Equation (2.37) is given by

$$v(x,t) = \int_0^1 g(t,x,y)v_0(y)dy + \int_0^t \int_0^1 g(t-s,x,y)u(y,s)dyds, \tag{2.40}$$

where $g(t,x,y)$ represents the Green's function

$$g(t,x,y) = 1 + \sum_{n=1}^{\infty} 2e^{-n^2\pi^2 t} cos(n\pi x)cos(n\pi y). \tag{2.41}$$

For $t \geq 0$, a semigroup operator $T(t) \in \mathfrak{L}(L_2(0,1))$ can be defined as

$$T(t)v_0 = \int_0^1 g(t,x,y)v_0(y)dy. \tag{2.42}$$

Then, the abstract formulation of the solution (2.40) on Z becomes

$$v(t) = T(t)v_0 + \int_0^t T(t-s)u(s)ds. \tag{2.43}$$

For a dynamic system without inputs ($B = 0$), $T(t)$ defined above satisfies the conditions for a strongly continuous semigroup.

A strongly continuous semigroup is an operator-valued function $T(t)$ from R^+ to $\mathfrak{L}(Z)$ that satisfies the following properties (Curtain and Zwart, 1995):

$$\begin{aligned} &T(t+s) = T(t)T(s) \text{ for } t, s \geq 0; \\ &T(0) = I; \\ &\|T(t)z_0 - z_0\| \to 0 \text{ as } t \to 0^+. \end{aligned} \tag{2.44}$$

It can be abbreviated as the C_0-semigroup. Using the C_0-semigroup, the dynamics for a linear, time-invariant, and autonomous infinite-dimensional system can be expressed as:

$$v(t) = T(t)v_0. \tag{2.45}$$

A C_0-semigroup $T(t)$ can be related to the solution of an abstract differential equation as Equation (2.39) through the *infinitesimal generator* A of $T(t)$, which is defined by

$$Av = \lim_{t \to 0^+} \frac{1}{t}(T(t) - I)v, \tag{2.46}$$

whenever the limit exists.

The concept of a semigroup plays an important role in the design of an infinite-dimensional state observer for feedback control in this thesis. Among the semigroups, a contraction semigroup is of special interest ($T(t)$ is a contraction semigroup if it is a C_0-semigroup that satisfies $\|T(t)\| \leq 1$ for all $t \geq 0$).

Chapter 3

Feedback Control for First-order PDE Systems

In the control of distributed parameter systems, researchers have focussed on the design of state feedback or output feedback control for specific classes of PDE models. For processes represented by parabolic PDEs, a finite number of modes may capture the dominant dynamics of the system (Curtain and Zwart, 1995) and modal decomposition techniques can then be used to transform the PDE model into an approximate ODE model, which is subsequently used for controller design. For hyperbolic PDEs, however, all of the eigenmodes of the spatial differential operator contain the same, or nearly the same, amount of energy, and thus an infinite number of modes are required to accurately describe their dynamic behavior (Christofides and Daoutidis, 1998). This prohibits the application of modal decomposition techniques to derive reduced-order ODE models. As a result, the treatment of hyperbolic PDEs requires the analysis of the infinite dimensional nature of the systems.

A control approach based on a combination of the Method of Characteristics and sliding mode techniques was proposed for processes modelled by a first-order, quasi-

linear hyperbolic PDE (Sira-Ramirez, 1989). This method was further developed to synthesize a state feedback controller for a nonlinear hyperbolic PDE model with continuous control action (Hanczyc and Palazoglu, 1995). A nonlinear distributed output feedback controller was also proposed for a quasilinear hyperbolic PDE system using geometric control methods (Christofides and Daoutidis, 1996). However, these methods have focused on either the design of state feedback controllers or specific PDE models. Thus, an output feedback control method that is general for all first-order hyperbolic PDEs is unavailable.

This chapter proposes a PDE-based feedback control for DPS using the Method of Characteristics. An output feedback controller is derived for processes represented by a first-order hyperbolic PDE. The resulting control law guarantees asymptotic output tracking. The proposed approach is applicable to processes modelled by a single linear, quasilinear or nonlinear first-order hyperbolic PDE, and a system of hyperbolic PDEs with a single characteristic. In addition, the resulting control laws efficiently reject disturbances and can deal with some forms of plant-model mismatch. The proposed approach yields a comparatively simple controller design technique and produces control laws that are easy to implement.

3.1 State Feedback Control

Any first-order PDE-based process model can be expressed as

$$\begin{aligned} &\Phi(v, \mathbf{x}, t, \frac{\partial v}{\partial \mathbf{x}}, \frac{\partial v}{\partial t}, u) = 0, \\ &y = h(v, \mathbf{x}, t), \end{aligned} \tag{3.1}$$

where t is time coordinate, $\mathbf{x}$ is the vector of local spatial coordinates (x_i) defining points on an open set in R^n, $v \in L_2(0,1)$ is the distributed state variable which changes in both time and space, $u \in \mathbb{R}$ is the manipulated variable and $y \in \mathbb{R}$ is a scalar-valued output. For each smooth solution v of the system in Equation (3.1), Φ and h are locally smooth functions of their arguments.

Under fixed initial and boundary conditions, Equation (3.1) can be visualized as a surface in R^{n+2} with $(v, \mathbf{x}, t)$ being coordinates and u being a parameter. This surface is dependent on u. The control objective is to have the output function y track a specific trajectory by manipulating u. Without loss of generality, assume the desired output trajectory is $y = 0$, which locally defines an isolated smooth manifold $v = \phi(\mathbf{x}, t)$ such that:

$$h(\phi(\mathbf{x}, t), \mathbf{x}, t) = 0. \tag{3.2}$$

The graph of v is assumed to be a smooth time-varying surface on which the system has the desired behavior. In this section, a state feedback control will be formulated such that the surface determined by Equation (3.1) coincides with the surface specified by Equation (3.2) asymptotically for quasilinear first-order systems and nonlinear first-order systems, separately.

3.1.1 Quasilinear Systems

Consider a dynamic system described by the first-order quasilinear PDE:

$$\begin{aligned} &\frac{\partial v}{\partial t} + \sum_{i=1}^{n} \frac{\partial v}{\partial x_i} a_i(v, \mathbf{x}, t, u) = b(v, \mathbf{x}, t, u), \\ &y = h(v, \mathbf{x}, t), \end{aligned} \tag{3.3}$$

where $a_1, a_2, ..., a_n$ and b are continuous functions. The coefficients in Equation (3.3) constitute a vector field $\xi = [1, a_1, \cdots, a_n, b]^T = [1, \mathbf{a}, b]^T$. As discussed in Chapter 2, this vector field defines a time-varying control-parameterized vector field and is called the characteristic vector field. Surfaces that are tangent at each point to the characteristic vector field are called integral surfaces of the vector field (McOwen, 1996). The controller design problem is to formulate the controller u such that it satisfies a given control objective. The control objective in this section is assumed to be output tracking.

By the Method of Characteristics, the quasilinear PDE system in Equation (3.3) can

be transformed into a nonlinear ODE system:

$$\begin{aligned} \dot{t} &= 1, \\ \dot{\mathbf{x}} &= \mathbf{a}(v, \mathbf{x}, t, u), \\ \dot{v} &= b(v, \mathbf{x}, t, u), \\ y &= h(v, \mathbf{x}, t). \end{aligned} \tag{3.4}$$

To simplify the notation, introduce the vector $\mathbf{z} = [t, \mathbf{x}, v]^T$. For control development, the following assumptions are needed.

Assumption 3.1 The characteristic ODE described by Equation (3.4) can be represented in an affine form:

$$\dot{\mathbf{z}} = \mathbf{f} + \mathbf{g} \cdot u. \tag{3.5}$$

This is a common form assumed often in the nonlinear control literature (Isidori, 1995).

For clarity of discussion, some notation from differential geometry (Doolin, 1990; Bryant *et al.*, 1991) is useful and will be introduced here. The Lie derivative of a scalar function $h(x)$ with respect to a vector function $f(x)$ is defined as

$$L_f h(x) = \frac{\partial h(x)}{\partial x} f(x). \tag{3.6}$$

Since the Lie derivative of a scalar function is also a scalar function, a high order Lie derivative can be defined recursively as:

$$\begin{aligned} L_f^0 h(x) &= h(x), \\ L_f^k h(x) &= \frac{\partial L_f^{k-1} h(x)}{\partial x} f(x). \end{aligned} \tag{3.7}$$

With the definition of a Lie derivative, the relative degree can be defined as the number of times the output must be differentiated so that the input appears explicitly. For a linear system in transfer function form, the relative degree is the difference between the orders of the denominator and numerator polynomials.

Assumption 3.2 There exists an integer γ such that the Lie derivatives of the output function satisfy

$$\begin{aligned} L_{\mathbf{g}} L_{\mathbf{f}}^{\gamma-2} h &= 0, \\ L_{\mathbf{g}} L_{\mathbf{f}}^{\gamma-1} h &\neq 0, \end{aligned} \tag{3.8}$$

$\forall\, x, t, v$. This assumption is required for most nonlinear feedback control methods and is not always explicitly stated.

When Assumption 3.1 and Assumption 3.2 are satisfied, the output function $y = h(v, \mathbf{x}, t)$ has relative degree of γ. Most single PDE systems have relative degree of one and systems of PDEs have relative degree greater than one. When the system modelled by Equation (3.3) has relative degree of one, the Lie derivative of the output function along the characteristic vector field is

$$L_\xi y = L_{\mathbf{f}} h + L_{\mathbf{g}} h \cdot u. \tag{3.9}$$

With these definitions and assumptions, a distributed state feedback control law that ensures offset-free setpoint tracking can be formulated.

Theorem 3.1.1 *Consider the system modelled by the quasi-linear first-order PDE of Equation (3.3). There always exist $k > 0$ and $\tau_I > 0$ such that the distributed state feedback control law:*

$$u = \frac{-k(h + \frac{1}{\tau_I}\int_0^t h d\tau) - L_{\mathbf{f}} h}{L_{\mathbf{g}} h}, \tag{3.10}$$

guarantees closed-loop asymptotic stability.

Proof:

Substituting Equation (3.10) into Equation (3.9) yields:

$$L_\xi y = -k(y + \frac{1}{\tau_I}\int_0^t y d\tau). \tag{3.11}$$

The closed-loop stability can be analyzed by further applying Lie derivative to the above equation:

$$L_\xi L_\xi y + k L_\xi y + \frac{k}{\tau_I} y = 0. \tag{3.12}$$

Along the characteristic vector field ξ, Equation (3.12) can be written in ODE form as:

$$\begin{aligned} \dot{t} &= 1, \\ \dot{\mathbf{x}} &= \mathbf{a}(v_0, \mathbf{x}), \\ \ddot{y} + k\dot{y} + \frac{k}{\tau_I} y &= 0. \end{aligned} \tag{3.13}$$

Therefore, from each point of the current state variable profile v_0, the closed-loop dynamics of the output can be expressed along the characteristic vector field ξ as: $\ddot{y} + k\dot{y} + \frac{k}{\tau_I} y = 0$. Since the time coordinate may not be able to go to infinity along the characteristic line before the spatial coordinate hits the boundary, the asymptotic stability of the closed-loop system cannot be analyzed using Equation (3.13) due to the time scale limitation.

Assume that there exists a residence time $t_R(v_0, x_0)$ (abbreviated as t_R), which indicates the time for the current state variable v_0 at x_0 moving along the characteristic line until it hits the boundary, and assume that t_R satisfies

$$t_R > M, \tag{3.14}$$

where M is a positive number. Hence, along the characteristic vector field ξ, $t \in [0, t_R)$. Define a new time scale variable τ as:

$$\tau = \frac{t_R t}{t_R - t}. \tag{3.15}$$

It can be seen that for $t \in [0, t_R]$, $\tau \in [0, \infty)$. When $t_R \to \infty$, $\tau = t$ and the asymptotic stability of the closed-loop system becomes obvious. Otherwise, it is possible to analyze the closed-loop asymptotic stability in the new time scale τ along the characteristic lines.

From Equation (3.15), the following can be obtained:

$$\begin{aligned} \frac{d\tau}{dt} &= (1 + \tau/t_R)^2, \\ \frac{dy}{dt} &= (1 + \tau/t_R)^2 \frac{dy}{d\tau}, \\ \frac{d^2y}{dt^2} &= (1 + \tau/t_R)^4 \frac{d^2y}{d\tau^2} + \frac{2}{t_R}(1 + \tau/t_R)^3 \frac{dy}{d\tau}. \end{aligned} \tag{3.16}$$

Substituting Equation (3.16) into Equation (3.13), the closed-loop dynamics of the output can be expressed in the new time scale τ along a characteristic line, as:

$$(1+\tau/t_R)^4\frac{d^2y}{d\tau^2}+\left[\frac{2}{t_R}(1+\tau/t_R)^3+k(1+\tau/t_R)^2\right]\frac{dy}{d\tau}+\frac{k}{\tau_I}y=0. \tag{3.17}$$

Since the new time scale τ can go to infinity along the characteristic line, it is convenient to analyze the closed-loop asymptotic stability of the PDE system from this equation.

Define

$$\begin{aligned} y_1 &= y, \\ y_2 &= \frac{dy}{d\tau}, \end{aligned} \tag{3.18}$$

and

$$b=\frac{2}{t_R}(1+\tau/t_R)^3+k(1+\tau/t_R)^2. \tag{3.19}$$

Then, from Equation (3.17) and (3.18), the following can be obtained:

$$\begin{aligned} \frac{dy_1}{d\tau} &= y_2, \\ \frac{dy_2}{d\tau} &= -\frac{b}{(1+\tau/t_R)^4}y_2-\frac{k}{\tau_I(1+\tau/t_R)^4}y_1. \end{aligned} \tag{3.20}$$

Define a function:

$$V=\frac{k}{2\tau_I}y_1^2+\frac{(1+\tau/t_R)^4}{2}y_2^2\geq 0, \qquad \text{for } k,\tau_I>0. \tag{3.21}$$

The derivative of V in terms of τ can be obtained as:

$$\frac{dV}{d\tau}=-k(1+\tau/t_R)^2y_2^2\leq -ky_2^2\leq 0. \tag{3.22}$$

It can be seen that $\frac{dV}{d\tau}=0$ only when $y_2=\frac{dy}{d\tau}=0$. From Equation (3.17), $\frac{dy}{d\tau}=0$ implies $y=0$. From LaSalle's Invariance principle, the largest invariant subspace of $E=\frac{dV}{d\tau}=0$ is the point $y=0$. It can be said that $\frac{dV}{d\tau}<0$ for $y\neq 0$ and $\frac{dV}{d\tau}=0$ for $y=0$. The function V is a Lyapunov function. Therefore, as $\tau\rightarrow 0$, $y\rightarrow 0$. This implies that, as $t\rightarrow t_R$, $y\rightarrow 0$, for the original system. This proves the asymptotic stability of the closed-loop system. ■

The controller in Equation (3.10) is a function of current state variables and output variables. It does not contain derivatives of the state variables as do some of the other existing feedback control methods for quasilinear PDE systems. This simplifies the state observer design problem and makes the proposed feedback control easy to implement.

The proposed controller for quasilinear first-order PDE systems has the form similar to a PI control with a term analogous to dead-time compensation. Since its compensation term is obtained directly from the PDE model, the controller exhibits improved performance, and is capable of dealing with operation variable changes.

3.1.2 Nonlinear Systems

The Method of Characteristics is more involved for first-order nonlinear PDEs than for quasilinear PDEs. The complexity of the state feedback control development using the Method of Characteristics increases correspondingly for a nonlinear system.

Consider a first-order nonlinear PDE control system:

$$\begin{aligned} &\frac{\partial v}{\partial t} + \Phi(v, \mathbf{x}, t, \frac{\partial v}{\partial \mathbf{x}}, u) = 0, \\ &y = h(v, \mathbf{x}, t). \end{aligned} \tag{3.23}$$

Equation (3.23) can be interpreted as a hyper-surface E^{2n+2} in the manifold $M^{2n+3} = J^1(V^{n+1}, R)$ of 1-jets equipped with the standard contact structure. Let $(\mathbf{x}, t)$ be local coordinates on V^{n+1} and v be the coordinate in R, $\mathbf{p} = \frac{\partial v}{\partial \mathbf{x}}$ and $q = \frac{\partial v}{\partial t}$. The corresponding local coordinates are denoted by $(\mathbf{x}, t, v, \mathbf{p}, q)$ in the space of 1-jets. Then, the differential equation can be written locally in the form

$$q + \Phi(v, \mathbf{x}, t, \mathbf{p}, u) = 0. \tag{3.24}$$

By the Method of Characteristics described in Chapter 2, the characteristic equations of

system (3.23) in the manifold M^{2n+3} can be written as (Arnold, 1988):

$$\begin{aligned}
\dot{t} &= 1, \\
\dot{q} &= -q\Phi_v - \Phi_t, \\
\dot{\mathbf{x}} &= \Phi_{\mathbf{p}}, \\
\dot{\mathbf{p}} &= -\Phi_{\mathbf{x}} - \mathbf{p}\Phi_v, \\
\dot{v} &= \mathbf{p}\Phi_{\mathbf{p}} + q,
\end{aligned} \tag{3.25}$$

where the subscript denotes a partial derivative (*e.g.*, $\Phi_v = \frac{\partial \phi}{\partial v}$). In contrast to a quasilinear system, a nonlinear PDE system requires its state variables as well as their first-order derivatives as new variables to describe its characteristics, which complicates the control and state observer design problems.

Based on the characteristic ODEs (3.25) and the underlying PDE (3.24), the characteristics of the nonlinear PDE can be described by the variables t, $\mathbf{x}$, v and $\mathbf{p}$. Denote vector $\mathbf{z}' = [t, \mathbf{x}, v, \mathbf{p}, q]$, $\mathbf{z} = [t, \mathbf{x}, v, \mathbf{p}]$ and vector field $\zeta' = [1, \Phi_{\mathbf{p}}, \mathbf{p}\Phi_{\mathbf{p}} + q, -\Phi_{\mathbf{x}} - \mathbf{p}\Phi_v, -q\Phi_v - \Phi_t]$, $\zeta = [1, \Phi_{\mathbf{p}}, \mathbf{p}\Phi_{\mathbf{p}} - \Phi, -\Phi_{\mathbf{x}} - \mathbf{p}\Phi_v]$. The characteristic ODE can be written in a more compact form:

$$\dot{\mathbf{z}}' = \zeta'(t, \mathbf{x}, v, \mathbf{p}, q, u). \tag{3.26}$$

Substituting Equation (3.24) into Equation (3.26) yields

$$\dot{\mathbf{z}} = \zeta(t, \mathbf{x}, v, \mathbf{p}, u). \tag{3.27}$$

The following assumptions are required for the controller development.

Assumption 3.3 The characteristic vector field ζ for the nonlinear system is affine in the control variable:

$$\dot{z} = \zeta_1(t, \mathbf{x}, v, \mathbf{p}) + \zeta_2(t, \mathbf{x}, v, \mathbf{p}) \cdot u. \tag{3.28}$$

Assumption 3.4 There exists an integer γ such that the Lie derivatives of the output function satisfy:

$$\begin{aligned} L_{\zeta_2} L_{\zeta_1}^{\gamma-2} h &= 0, \\ L_{\zeta_2} L_{\zeta_1}^{\gamma-1} h &\neq 0, \end{aligned} \tag{3.29}$$

$\forall\, x, v, t.$

When Assumption 3.3 and Assumption 3.4 are satisfied, the output function $y = h(v, \mathbf{x}, t)$ has relative degree of γ. When the system has a relative degree of 1, the Lie derivative of the output function along the characteristic vector field ζ is

$$L_\zeta y = L_{\zeta_1} h + L_{\zeta_2} h \cdot u, \tag{3.30}$$

where $L_{\zeta_2} h \neq 0$ by assumption. Then, a distributed state feedback controller for the nonlinear system can be formulated in the same way as that for the quasilinear system:

$$u = \frac{-k(h + \frac{1}{\tau_I}\int_0^t h d\tau) - L_{\zeta_1} h}{L_{\zeta_2} h}. \tag{3.31}$$

The closed-loop stability of the controller can be analyzed by examining the dynamics of the output along the characteristics, which can be obtained by substituting Equation (3.31) into Equation (3.30):

$$L_\zeta y = -k(h + \frac{1}{\tau_I}\int_0^t h d\tau), \tag{3.32}$$

or equivalently,

$$L_\zeta L_\zeta y + k L_\zeta y + \frac{1}{\tau_I} y = 0. \tag{3.33}$$

Assume that there exists a residence time $t_R(v_0, x_0)$ (abbreviated as t_R) such that, along a characteristic vector field ζ,

$$t_R > M \text{ and } t \in [0, t_R], \tag{3.34}$$

where M is a positive number. More complicated than the quasilinear case, the parameter t_R may not have a clear physical interpretation in the nonlinear PDE systems. Defining a

time transformation:

$$\tau = \frac{t_R t}{t_R - t}, \tag{3.35}$$

the closed-loop dynamics of the output in the new time scale can be obtained from Equation (3.33), along a characteristic ζ, as:

$$(1+\tau/t_R)^4 \frac{d^2y}{d\tau^2} + \left[\frac{2}{t_R}(1+\tau/t_R)^3 + k(1+\tau/t_R)^2\right]\frac{dy}{d\tau} + \frac{k}{\tau_I}y = 0. \tag{3.36}$$

The asymptotic stability of the system in Equation (3.36) has been proved in Section 3.1.1. Therefore, the proposed controller in Equation (3.31) has closed-loop asymptotic stability.

The controller (3.31) for the nonlinear system is a function of the state variables and their first-order spatial derivatives. It requires that a state observer estimates both the state variables and their first-order spatial derivatives for its implementation.

3.2 Output Feedback Control

In the previous section, a state feedback controller that enforces output setpoint tracking was formulated. However, such a technique requires the full measurement of infinite dimensional states. Since only a finite set of measurements can be obtained in practice, a state observer is needed to reconstruct the infinite-dimensional state profiles from the finite measurements. This section proposes a state observer structure for quasilinear and nonlinear systems based on Semigroup theory.

3.2.1 Quasilinear Systems

Assuming that a finite number of measurements of the state variables are available for control purposes, the quasilinear PDE system can be expressed as:

$$\begin{aligned} &\frac{\partial v}{\partial t} + \frac{\partial v}{\partial \mathbf{x}}\mathbf{a}(v, \mathbf{x}, t, u) = b(v, \mathbf{x}, t, u), \\ &y = h(v, \mathbf{x}, t), \\ &\mathbf{w} = Qv, \\ &v(\mathbf{x}_0) = v_0, \end{aligned} \tag{3.37}$$

where $\mathbf{w} \in R^m$ is the set of measurements of m elements, Q is an operator: $L_2(0,1) \longrightarrow R^m$, and $v(\mathbf{x}_0) = v_0$ is the boundary condition.

It is always possible to split the term $b(v, \mathbf{x}, t, u)$ into $b_1(v, \mathbf{x}, t, u) + b_2(\mathbf{x}, t, u)$. Then, the PDE in Equation (3.37) can be expressed in the form:

$$\begin{aligned} \frac{\partial v}{\partial t} &= -\frac{\partial v}{\partial \mathbf{x}}\mathbf{a}(v, \mathbf{x}, t, u) + b_1(v, \mathbf{x}, t, u) \\ &\quad + b_2(\mathbf{x}, t, u). \end{aligned} \tag{3.38}$$

Choose $Z = L_2(0,1)$ as the state space. Assume that a nonlinear differentiable operator A can be defined on Z such that

$$A\varphi = -\frac{d\varphi}{d\mathbf{x}}\mathbf{a}(\varphi, \mathbf{x}, t, u) + b_1(\varphi, \mathbf{x}, t, u), \tag{3.39}$$

$$\mathbf{D}(A) = \left\{ \begin{array}{l} \varphi \in L_2(0,1) | \ \varphi, \dfrac{d\varphi}{d\mathbf{x}} \text{ are absolutely} \\ \text{continuous}, \ -\dfrac{d\varphi}{d\mathbf{x}}\mathbf{a}(\varphi, \mathbf{x}, t, u) \\ + b_1(\varphi, \mathbf{x}, t, u) \in L_2(0,1), \\ \varphi(\mathbf{x}_0) = v_0 \end{array} \right\}.$$

Equation (3.38) can be reformulated as a differential operator equation on a Hilbert space Z:

$$\frac{dv}{dt} = Av + b_2(\mathbf{x}, t, u). \tag{3.40}$$

Using Equation (3.40), a state observer can also be designed on the Hilbert space Z in the form:

$$\frac{d\eta}{dt} = A\eta + b_2(x,t,u) + C(\mathbf{w} - Q\eta), \tag{3.41}$$

where η is an estimate of the state v and C is an operator: $R^m \rightarrow Z$. If the operator C can be designed such that the composite operator $(A - CQ)$ is an infinitesimal generator of a contraction semigroup, the state observer in Equation (3.41) guarantees that the estimated state converges to the true state, asymptotically. This can be seen through checking the error between the true process state v and the estimated state η:

$$e = v - \eta, \tag{3.42}$$

where $e \in L_2[0,1]$. Based on Equation (3.37) and (3.41), the equation for e is obtained as follows:

$$\dot{e} = (A - CQ)e. \tag{3.43}$$

If the operator $(A - CQ)$ is an infinitesimal generator of a contraction semigroup, denote the contraction semigroup by $T_e(t) : L_2[0,1] \rightarrow L_2[0,1]$. The error e at any time can be expressed by the semigroup $T_e(t)$ as

$$e(t) = T_e(t)e(0). \tag{3.44}$$

A key property of a contraction semigroup is

$$\|T_e(t)\| < 1. \tag{3.45}$$

From the definition of the module for a semigroup, we have

$$\|T_e(t)\| = \sup_e \frac{\|T_e(t)e\|}{\|e\|}. \tag{3.46}$$

Hence, it holds that

$$\begin{aligned} \|e(t_2)\| &= \|T_e(t_2 - t_1)e(t_1)\| \\ &\leq \|T_e(t_2 - t_1)\| \, \|e(t_1)\| \\ &< \|e(t_1)\| . \end{aligned} \tag{3.47}$$

for any $t_2 > t_1$. Therefore, $e \rightarrow 0$ as $t \rightarrow \infty$. The state observer in Equation (3.41) guarantees that the estimated state converges to the true state asymptotically.

With the proposed structure of the state observer in Equation (3.41), the task of estimating the state variables lies in the design of the operator C. There is no general design method for a general PDE problem and it is not the purpose of this thesis to develop general methods for observer design. In the examples, the operator C designed using Lagrange polynomials is found to be adequate.

If the operator A defined by Equation (3.39) is an infinitesimal generator of a contraction semigroup, the simplest observer can be obtained by choosing $C = 0$. The addition of the term $C(\mathbf{w} - Q\eta)$ in the state observer can accelerate the convergence of the estimation to the true state.

By combining the developed state feedback controller in Equation (3.10) and the state observer in Equation (3.41), an output feedback controller for quasilinear system in Equation (3.37) is obtained:

$$\begin{aligned} &\frac{\partial \eta}{\partial t} + \frac{\partial \eta}{\partial \mathbf{x}}\mathbf{a}(\eta, \mathbf{x}, t, u) = b(\eta, \mathbf{x}, t, u) + C(\mathbf{w} - Q\eta), \\ &u(\mathbf{x}, t) = \frac{-k(h(\eta, \mathbf{x}, t) + \frac{1}{\tau_I}\int_0^t h(\eta, \mathbf{x}, \tau)d\tau)}{L_g h(\eta, \mathbf{x}, t)} \\ &\qquad\qquad - \frac{L_f h(\eta, \mathbf{x}, t)}{L_g h(\eta, \mathbf{x}, t)}, \end{aligned} \tag{3.48}$$

where η is the estimated state.

3.2.2 Nonlinear Systems

The implementation of the state feedback control in Equation (3.31) for a nonlinear system requires the estimation of both the infinite state variables and their spatial derivatives of the state variables, which are also infinite dimensional. Assuming the the state variables in the DPS can be measured at a finite number of points, the nonlinear PDE

system can be expressed as:

$$\begin{aligned} &\frac{\partial v}{\partial t} + \Phi(v, \mathbf{x}, t, \frac{\partial v}{\partial \mathbf{x}}, u) = 0, \\ &y = h(v, \mathbf{x}, t), \\ &\mathbf{w} = Qv, \\ &v(\mathbf{x}_0) = v_0, \end{aligned} \tag{3.49}$$

where $\mathbf{w}$ is the set of measurements of m elements, Q is an operator $L_2(0,1) \longrightarrow R^m$, and $v(\mathbf{x}_0) = v_0$ is the boundary condition.

Splitting Φ in Equation (3.49) into a term containing the state variable v and a term independent of the state variable v, the state equation for the nonlinear system can be expressed in the form:

$$\frac{\partial v}{\partial t} = \Phi_1(v, \mathbf{x}, t, \frac{\partial v}{\partial \mathbf{x}}, u) + \Phi_2(\mathbf{x}, t, u). \tag{3.50}$$

Choose $Z = L_2(0,1)$ as the state space. An operator A on Z can be defined such that

$$A\varphi = \Phi_1(\varphi, \mathbf{x}, t, \frac{d\varphi}{d\mathbf{x}}, u), \tag{3.51}$$

$$D(A) = \left\{ \begin{array}{l} \varphi \in L_2(0,1) | \ \Phi_1(\varphi, \mathbf{x}, t, \frac{d\varphi}{d\mathbf{x}}, u) \\ \text{is continuous,} \\ \Phi_1(\varphi, \mathbf{x}, t, \frac{d\varphi}{d\mathbf{x}}, u) \in L_2(0,1) \\ \varphi(\mathbf{x}_0) = v_0 \end{array} \right\}.$$

The state observer for the nonlinear PDE system in Equation (3.50) can be constructed in the same way as that for a quasilinear PDE, and has the form:

$$\frac{d\eta}{dt} = A\eta + \Phi_2(x, t, u) + C(\mathbf{w} - Q\eta), \tag{3.52}$$

where η is the estimation for state variable v and C: $R^m \rightarrow Z$. If the operator C can be designed such that the composite operator $(A - CQ)$ is an infinitesimal generator of a contraction semigroup, the state observer (3.52) guarantees that the estimated state

converges to the true state asymptotically. The estimated state variables can then be used to estimate the spatial derivatives of the state variables, which is required for nonlinear control implementation. Since the operator A has a more complicated form for nonlinear systems than for quasilinear systems, the design of the operator C is more difficult.

By combining the developed state feedback controller (3.31) and state observer (3.52), an output feedback controller for the nonlinear system in Equation (3.49) is obtained:

$$\begin{aligned} &\frac{\partial \eta}{\partial t} + \Phi(\eta, \mathbf{x}, t, \frac{\partial \eta}{\partial \mathbf{x}}, u) = C(\mathbf{w} - Q\eta), \\ &u(\mathbf{x}, t) = \frac{-k(h(\eta, \mathbf{x}, t) + \frac{1}{\tau_I}\int_0^t h(\eta, \mathbf{x}, \tau)d\tau)}{L_{\zeta_2} h(\eta, \mathbf{x}, t)} \\ &\qquad - \frac{L_{\zeta_1} h(\eta, \mathbf{x}, t)}{L_{\zeta_2} h(\eta, \mathbf{x}, t)}, \end{aligned} \tag{3.53}$$

where η is the estimate of the state v.

3.3 Examples

In this section, the proposed feedback controller is illustrated through two examples, and the closed-loop performance is investigated. The two example processes are a heat exchanger modelled by a single PDE and a plug-flow reactor modelled by a system of first-order PDEs.

3.3.1 Heat Exchanger

Consider a forced-flow steam-jacketed tabular heat exchanger. The fluid within the tube is heated using steam without condensation. The dynamic model of the process in deviation form can be expressed as (Hanczyc and Palazoglu, 1995):

$$\frac{\partial T}{\partial t} + u\frac{\partial T}{\partial x} + H(T - T_j) = 0, \tag{3.54}$$

where $T(x, t)$ denotes the temperature of the heat exchanger within the tube, $x \in [0, 1]$, T_j denotes the jacket temperature, u, the manipulated variable, is the fluid velocity in

the exchanger, and H is a positive constant. For simplicity, the steam temperature is considered to be spatially uniform. Temperature T at the exit is the variable to be controlled. Note that the model given in Equation (3.54) is quasilinear.

State Feedback Control

The characteristic vector field for Equation (3.54) is $\xi = [1, u, -H(T - T_j)]$. The output function is defined as:

$$y = T - T_{sp}(x), \tag{3.55}$$

where T_{sp} denotes the setpoint temperature profile. The control objective is $y = 0$. The Lie derivative of the output is:

$$L_\xi y = -H(T - T_j) - \frac{\partial T_{sp}}{\partial x} u. \tag{3.56}$$

A state feedback control for the heat exchanger can be obtained by applying the control law (3.10) and can be formulated as:

$$\begin{aligned} u(x,t) &= \frac{k}{\frac{\partial T_{sp}(x)}{\partial x}} \left[(T(x,t) - T_{sp}(x)) + \frac{1}{\tau_I} \int_0^t (T(x,\tau) - T_{sp}(x)) d\tau \right. \\ &\quad \left. - \frac{H}{k} (T(x,t) - T_j) \right], \end{aligned} \tag{3.57}$$

where $\frac{\partial T_{sp}(x)}{\partial x}$ is the spatial derivative of the setpoint temperature profile, which is specified. To avoid the singularity, $\frac{\partial T_{sp}(x)}{\partial x} \neq 0$ has to hold and setpoint profiles must not be constant. Although this is a spatially distributed controller, the manipulated variable u is spatially uniform throughout the heat exchanger due to the assumption of well-mixed heating gas. Since the control objective is to have the exit temperature of the exchanger reach its setpoint, a modification can be made by simply replacing the spatially distributed variables by their values at $x = 1$. The resulting spatially uniform controller can be written as

$$\begin{aligned} u &= K \left[(T(1,t) - T_{sp}) + \frac{1}{\tau_I} \int_0^t (T(1,\tau) - T_{sp}) d\tau \right. \\ &\quad \left. - \frac{H}{k} (T(1,t) - T_j) \right], \end{aligned} \tag{3.58}$$

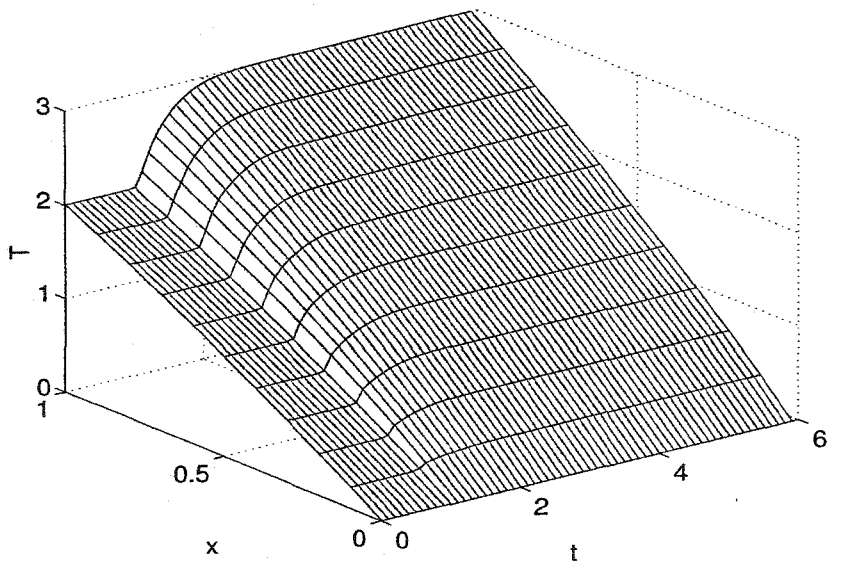

Figure 3.1: Setpoint tracking performance in the heat exchanger using state feedback

where $K = k/\frac{\partial T_{sp}}{\partial x}|_{x=1}$. Note that the control law in Equation (3.58) is a PI form plus a term to correct for disturbances in jacket temperature and heat coefficient.

A simulation was performed to evaluate the performance of the state feedback controller of Equation (3.58). The parameters used for simulation were: $H = 1, T_j = 10$. The tuning parameters were chosen to be $K = 2, \tau_I = 0.2$. The initial temperature profile is $T(x, 0) = 2x$ and the boundary condition were $T(0, t) = 0$. The specification of the exit temperature and its spatial derivative was taken as $T_{sp} = 3$ and $\frac{\partial T_{sp}}{\partial x} = 3$. For simulation purposes, the finite difference method was used to derive a finite-dimensional approximation of the original PDE equation, with a choice of 10 discretization points. Simulation results are shown in Figure 3.1. It is observed that the exit temperature, (*i.e.*, T at $x = 1$), tracks the setpoint well and the temperature profile at other points is stabilized and reaches its steady state quickly.

The performance of the proposed state feedback control was compared with that of the traditional PI control. The same tuning parameters, $K = 2$ and $\tau_I = 0.2$, were taken in both control methods. These tuning parameters are consistent with the tuning formula for PI controllers based on the open loop step test (Smith and Corripio, 1985). Figure 3.2

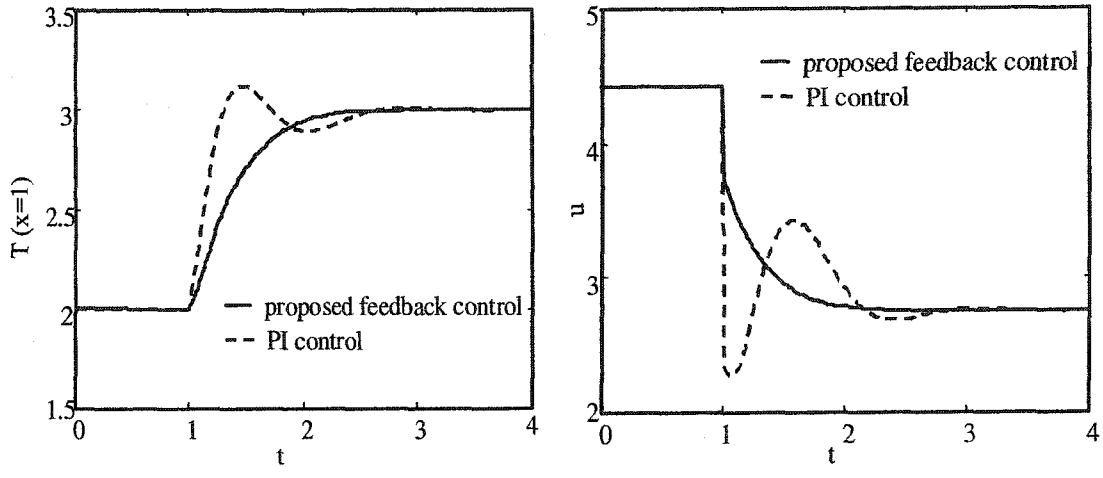

(a) Exit Temperature

(b) Manipulated variable

Figure 3.2: Comparison of the proposed state feedback *vs.* the conventional PI control

compares the output response to a setpoint change using these two control methods. It is observed that, in comparison to the traditional PI control, the proposed state feedback control yields smooth convergence to the setpoint with little overshoot and oscillation. The improved performance of the proposed state feedback control over the traditional PI control results from the dead-time compensation term $\frac{H}{k}(T(1,t) - T_j)$ in the controller, which prevents the output from having large overshoot.

The performance of the proposed control method for disturbances in process parameters or operating variables were investigated. Figure 3.3 and 3.4 compare the process performance of the traditional PI control and the proposed state feedback control when the jacket temperature increases from 10 to 15, and decreases from 10 to 8 at time $t = 1$, respectively. It is observed that the proposed feedback control responds to the disturbances in operating variables quickly.

The performance of both control methods to the disturbances in process variables was also studied. Figure 3.5 and 3.6 compare the control performance of the proposed feedback control and PI control if the process parameter H increases 20% and decreases 20% at time $t = 1$, respectively. The proposed feedback control displays quick rejection

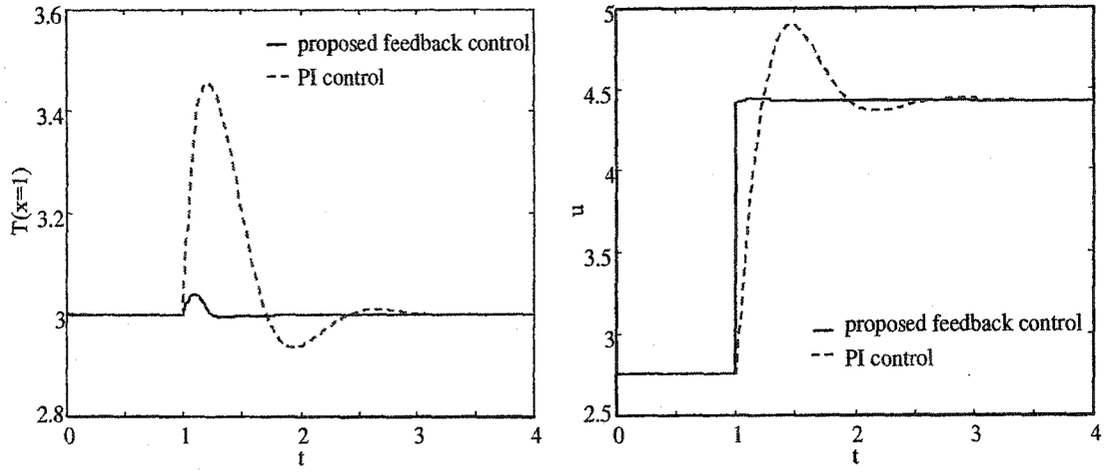

(a) Exit Temperature (b) Manipulated variable

Figure 3.3: Comparison of the proposed state feedback control and the traditional PI control in the heat exchanger (T_j increases from 10 to 15 at $t = 1$)

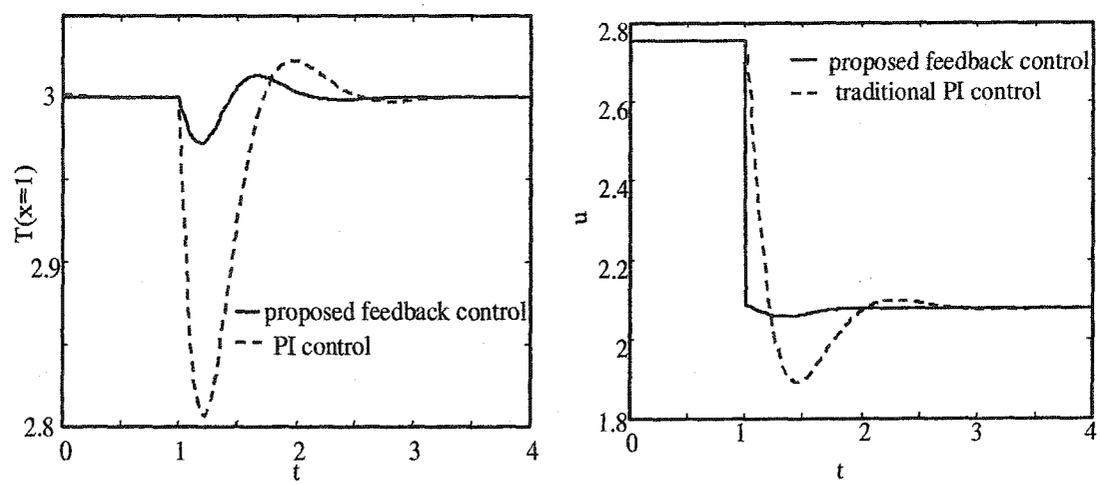

(a) Exit Temperature (b) Manipulated variable

Figure 3.4: Comparison of the proposed state feedback control *vs.* the conventional PI control in the heat exchanger (T_j decreases from 10 to 8 at $t = 1$)

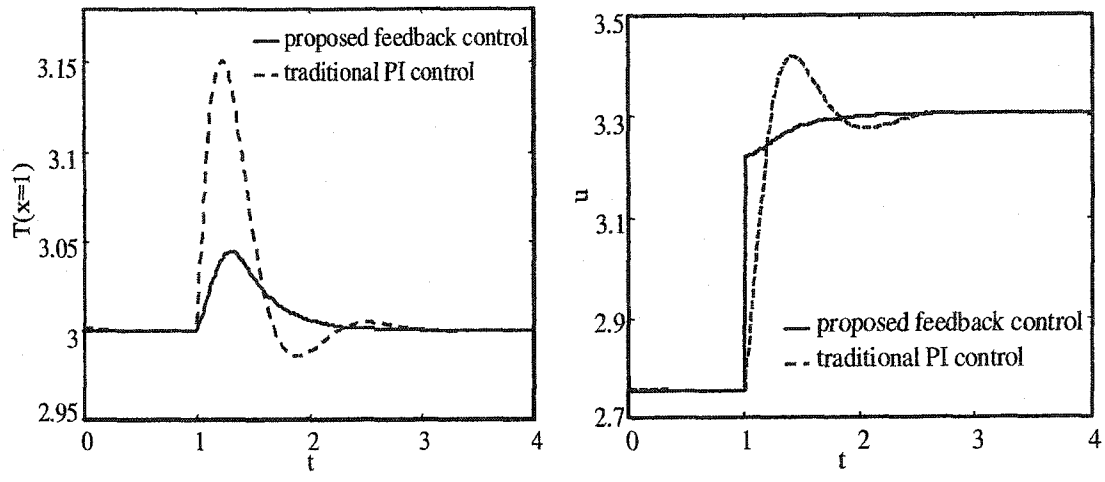

(a) Exit Temperature (b) Manipulated variable

Figure 3.5: Comparison of the proposed state feedback control *vs.* the traditional PI control in the heat exchanger (H increases from 1 to 1.2 at $t = 1$)

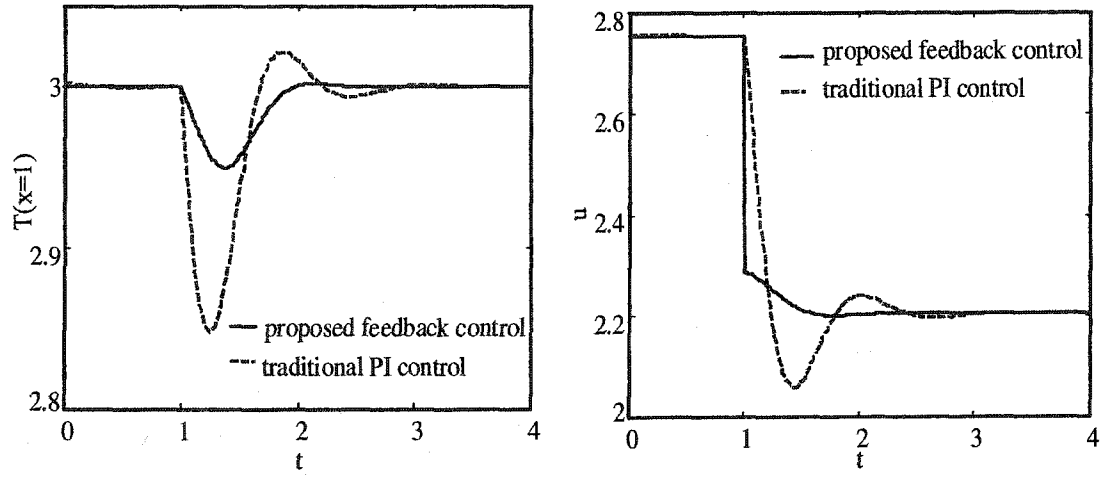

(a) Exit Temperature (b) Manipulated variable

Figure 3.6: Comparison of the proposed state feedback control *vs.* the traditional PI control in the heat exchanger (H decreases from 1 to 0.8 at t=1)

to the disturbances in the process variable and returns to normal operation in a very short time. Simulation results show that the proposed state feedback control provides remarkable advantages over the traditional PI control when there are disturbances in process parameters or operating variables.

Output Feedback Control

An output feedback control law can be obtained by combining the developed state feedback control with the design of a state observer. Assume that temperature in the heat exchanger can be measured at 5 points $x = 0, 0.2, 0.4, 0.6, 0.8$. The state observer for system (3.54) can be designed as

$$\frac{\partial T'}{\partial t} = -u\frac{\partial T'}{\partial x} - H(T' - T_j) - C(T_m - QT'), \tag{3.59}$$

where T_m is the temperature measurement vector in R^5, T' is the estimated temperature profile in the heat exchanger. Operator Q maps the estimated temperature profile into temperature at 5 points. Design an operator $C : R^5 \longrightarrow Z$ as

$$Cy = \sum_{i}^{5} \prod_{j \neq i}^{5} c\frac{(x - x_j)}{(x_i - x_j)} y_i, \tag{3.60}$$

where parameter c is adjusted to reach the desired convergence rate.

For the simulation, it is assumed that the true initial temperature profile is $T_0 = 1 - e^{-5x}$ and the estimated initial temperature profile is $T_0' = 5x$.

Figure 3.7 shows that the estimated temperature profile converges to the true temperature profile for any negative value of the parameter c. The more negative value of c, the faster the convergence; however, large absolute values of c can cause a strong oscillation in the temperature estimate and is deemed undesirable. So a trade-off has to be considered between fast convergence and oscillation in the temperature estimate.

An output feedback controller is obtained by combining the state feedback control (3.58) with the state observer (3.59). A simulation is run using $c = -10$, $k = 5$ and $\tau = 2$. Figure (3.8) shows that the output feedback control produces more oscillation than the state feedback control but tracks the setpoint well.

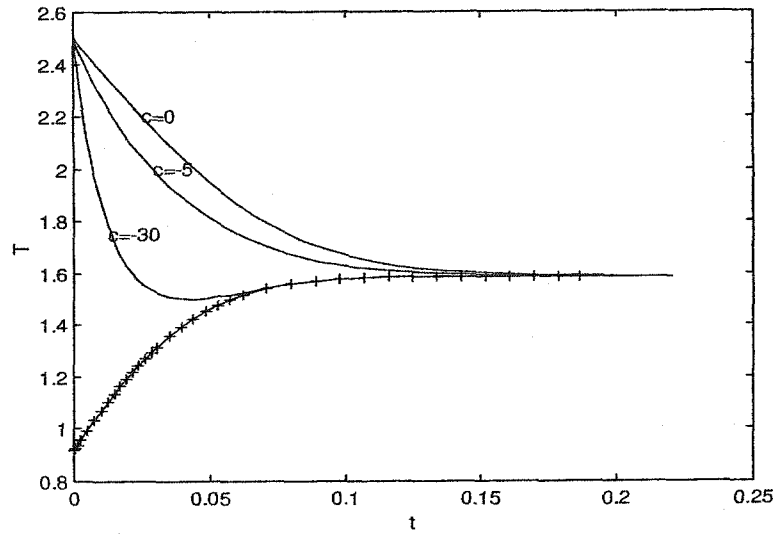

Figure 3.7: Comparison of true temperature evolution (+) *vs.* temperature evolution from the state observer at x=0.5 in the heat exchanger

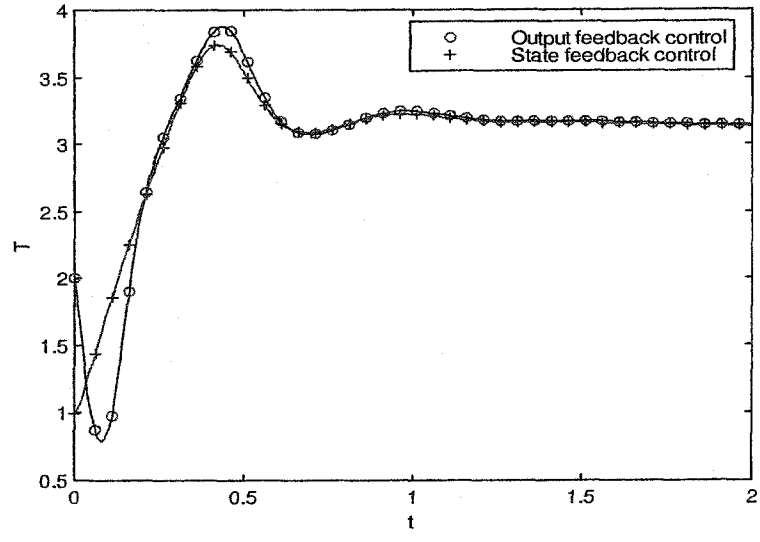

Figure 3.8: Comparison of temperature evolution at x=1 by output feedback control *vs.* state feedback control in the heat exchanger

3.3.2 Plug-flow Reactor

In contrast to the continuous stirred tank reactor (CSTR), a plug flow reactor (PFR) is such that reactants pass through a reactor with little mixing (Aris, 1969). In the ideal case, each element of the reaction mixture would have a reaction time precisely equal to the residence time of the reactor. In this section, the proposed feedback control will be applied on a plug-flow reactor with uniform heating in the jacket.

Consider the non-isothermal plug-flow reactor where two first-order reactions in series take place:

$$A \longrightarrow B \longrightarrow C,$$

where A is the reactant species, B is the desired product and C is an undesired product. The reaction rates follow an Arrhenius expression:

$$r_1 = -k_{10}e^{-E_1/RT_r}C_A,$$

$$r_2 = -k_{20}e^{-E_2/RT_r}C_B,$$

where k_{10}, k_{20}, E_1, E_2 are Arrhenius constants and the activation energies of the reactions. The reactions are assume to be endothermic. The reactor is heated with a jacket.

Under the assumptions of no radial concentration gradients in the reactor, constant volume of the liquid in the reactor, constant density and heat capacity of the reactants, and negligible diffusion and dispersion, the following model can be obtained using material and energy balance:

$$\begin{aligned}
\frac{\partial C_A}{\partial t} &= -v_l\frac{\partial C_A}{\partial x} - k_{10}e^{-E_1/RT_r}C_A, \\
\frac{\partial C_B}{\partial t} &= -v_l\frac{\partial C_B}{\partial x} + k_{10}e^{-E_1/RT_r}C_A - k_{20}e^{-E_2/RT_r}C_B, \\
\frac{\partial T_r}{\partial t} &= -v_l\frac{\partial T_r}{\partial x} + \frac{(-\Delta H_{r_1})}{\rho_m c_{pm}}k_{10}e^{-E_1/RT_r}C_A \\
&\quad + \frac{(-\Delta H_{r_2})}{\rho_m c_{pm}}k_{20}e^{-E_2/RT_r}C_B + \frac{U_w}{\rho_m c_{pm}V_r}(T_j - T_r),
\end{aligned} \tag{3.61}$$

subject to the boundary conditions:

$$C_A(0,t) = C_{A0}, \quad C_B(0,t) = 0, \quad T_r(0,t) = T_{r0}, \tag{3.62}$$

where C_A and C_B are the concentrations of the species A and B in the reactor, T_r is the temperature of the reactor, ΔH_{r_1} and ΔH_{r_2} are enthalpies of the two reactions, ρ_m and c_{pm} is the density and heat capacity of the fluid in the reactor, V_r is the volume of the reactor, U_w is the heat-transfer coefficient, C_{A0} and T_{A0} are concentration and temperature of the inlet stream in the reactor, T_j is the spatially uniform temperature in the jacket and manipulated to control the concentrations, x is the spacial coordinate along the reactor and $x \in [0, 1]$.

Define the vector field $\xi_1 = \frac{\partial}{\partial t} + v_l \frac{\partial}{\partial x}$ in the space of (t, x), and the system in Equation (3.61) can be described by ODEs along the vector field ξ_1:

$$\begin{aligned}
\dot{t} &= 1, \\
\dot{x} &= v_l, \\
\dot{C}_A &= -k_{10} e^{-E_1/RT_r} C_A, \\
\dot{C}_B &= k_{10} e^{-E_1/RT_r} C_A - k_{20} e^{-E_2/RT_r} C_B, \\
\dot{T}_r &= \frac{(-\Delta H_{r_1})}{\rho_m c_{pm}} k_{10} e^{-E_1/RT_r} C_A + \\
&\quad \frac{(-\Delta H_{r_2})}{\rho_m c_{pm}} k_{20} e^{-E_2/RT_r} C_B + \frac{U_w}{\rho_m c_{pm} V_r} (T_j - T_r),
\end{aligned} \tag{3.63}$$

and the corresponding vector field in the space of (t, x, C_A, C_B, T_r) is denoted as ξ.

Define an output function as:

$$y = C_B - C_B^r(x), \tag{3.64}$$

where $C_B^r(x)$ is the desired concentration trajectory of species B. Then the first-order and

second-order Lie derivatives of the output function along the vector field ξ are:

$$
\begin{aligned}
L_\xi y &= k_{10}e^{-E_1/RT_r}C_A - k_{20}e^{-E_2/RT_r}C_B - \frac{dC_B^r}{dx}v_l, \\
L_\xi L_\xi y &= -k_{10}^2 e^{-2E_1/RT_r}C_A + k_{20}^2 e^{-2E_2/RT_r}C_B - k_{10}k_{20}e^{-(E_1+E_2)/RT_r}C_A \\
&+(\frac{k_{10}E_1C_A}{RT_r^2}e^{-E_1/RT_r} - \frac{k_{20}E_2C_B}{RT_r^2}e^{-E_2/RT_r}) \\
&\left[\frac{(-\Delta H_{r_1})}{\rho_m c_{pm}}k_{10}e^{-E_1/RT_r}C_A + \frac{(-\Delta H_{r_2})}{\rho_m c_{pm}}k_{20}e^{-E_2/RT_r}C_B + \frac{U_w}{\rho_m c_{pm}V_r}(T_j - T_r)\right].
\end{aligned}
\tag{3.65}
$$

The input appears in the second-order Lie derivative of the output function, and thus, the system can be said to have relative degree 2. The task is to design a controller such that the output response along the vector field ξ is

$$
L_\xi L_\xi y + L_\xi y + k_1(y + \frac{1}{\tau_I}\int_0^t y d\tau) = 0, \tag{3.66}
$$

where k_1, k_2 and τ_I are parameters to be selected. The three parameters in Equation (3.66) complicate the tuning process. For the convenience of tuning, it is assumed that $k_1 = k_2$.

Let

$$
\begin{aligned}
\varpi_1 &= (\frac{k_{10}E_1C_A}{RT_r^2}e^{-E_1/RT_r} - \frac{k_{20}E_2C_B}{RT_r^2}e^{-E_2/RT_r}), \\
\varpi_2 &= \varpi_1\left[\frac{(-\Delta H_{r_1})}{\rho_m c_{pm}}k_{10}e^{-E_1/RT_r}C_A + \frac{(-\Delta H_{r_2})}{\rho_m c_{pm}}k_{20}e^{-E_2/RT_r}C_B\right].
\end{aligned}
\tag{3.67}
$$

If $\varpi_1 \neq 0$, a state feedback controller can be designed using the proposed characteristic-based feedback control method. The formulation for T_j can be obtained from Equation (3.65) and (3.66):

$$
\begin{aligned}
T_j &= T_r - \frac{\rho_m c_{pm}V_r}{U_w\varpi_1}[\varpi_2 + k_2k_{10}e^{-E_1/RT_r}C_A - k_2k_{20}e^{-E_2/RT_r}C_B \\
&\quad -k_2\frac{\partial r}{\partial x}v_l + k_1(y + \frac{1}{\tau_I}\int_0^t y d\tau)].
\end{aligned}
\tag{3.68}
$$

Since the concentration of B at the exit is to be controlled, the jacket temperature can be computed based on the above equation using the values at $x = 1$ for the distributed variables.

Table 3.1: Model parameters for a PFR

v_l	=	1	m/min	R	=	1.987	kcal/(min ∘ K)
L	=	1.0	m	ρ_m	=	0.09	kg/l
V_r	=	10.0	l	U_w	=	0.20	kcal/(min ∘ K)
E_1	=	20000.0	kcal/kmol	C_{pm}	=	0.231	kcal/(kg∘K)
E_2	=	50000.0	kcal/kmol	C_{A0}	=	4	mol/l
k_{10}	=	5.0×10^{12}	min^{-1}	C_{B0}	=	0	mol/l
k_{20}	=	5.0×10^{2}	min^{-1}	T_{r0}	=	320	K
H_{r_1}	=	0.5480	kcal/kmol	H_{r_2}	=	0.9860	kcal/kmol

In simulation, the model parameters used are listed in Table (3.1). The setpoint tracking performance of the proposed controller was examined with the control parameters $k_1 = 2$, $k_2 = 2$ and $\tau_I = 1$ and the initial state variable profiles are shown in Figure 3.9. Figure 3.10 shows the response of the state variable profiles and the manipulated variable when the outlet concentration setpoint of product B increases from 0.8 mol/l to 1 mol/l. It can be seen that the state variable profiles respond quickly to setpoint changes with a smooth evolution. Further, the process is stable under the proposed feedback control in the simulation. The output response for setpoint change is further illustrated in Figure 3.11 with different setpoint changes. The proposed feedback control yields offset-free output response. The output converges to the setpoint quickly and smoothly with some overshoot.

The performance of the proposed feedback control in the presence of the measured disturbances was also investigated. Figure 3.12 shows the output response and the control

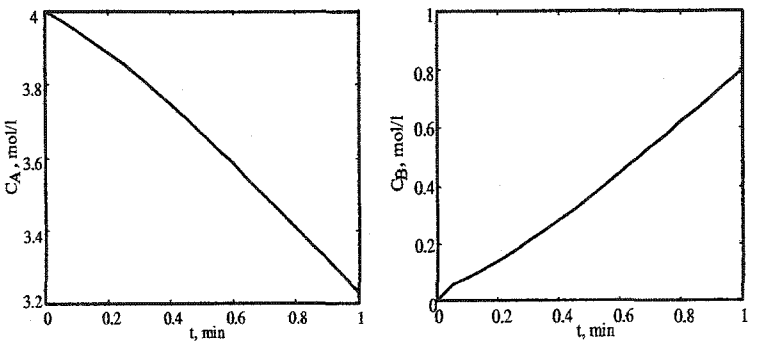

(a) C_A (b) C_B

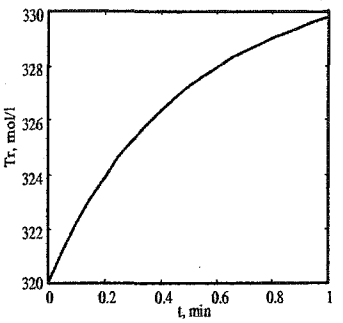

(c) T_r

Figure 3.9: Initial process variable profiles in PFR

action when flow rate v_l changes from 1 m/min to 1.2 m/min at time $t = 1$ min and from 1.2 m/min to 0.8 at time $t = 7$ m/min. Note that the process output returns to the setpoint after a short period of time. The behavior of the proposed feedback control to the unmeasured process variable disturbances is shown in Figure 3.13. When the process variable U_w changes from 0.2 kcal/(min.K) to 0.22 kcal/(min.K) at time $t = 1$ min and from 0.22 kcal/(min.K) to 0.18 kcal/(min.K), the proposed feedback control rejects these disturbances well. Overall, the proposed feedback control is shown to provide satisfactory performance and reject measured or unmeasured process disturbances.

In the control of the reactor, concentrations cannot be measured along the reactor

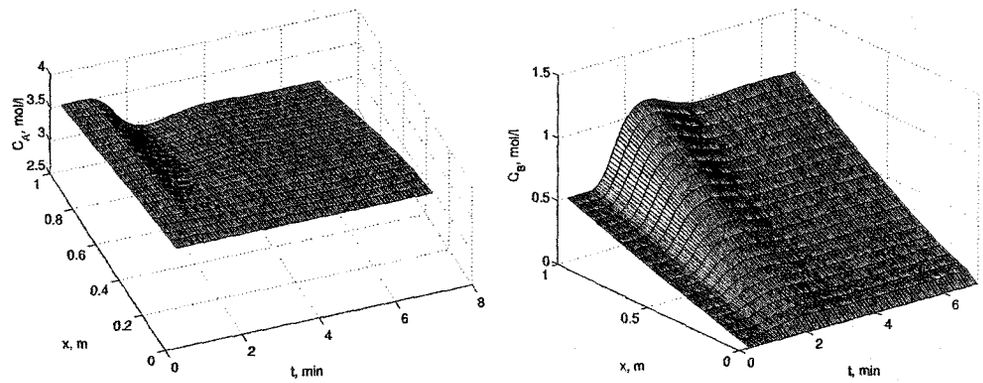

(a) C_A (b) C_B

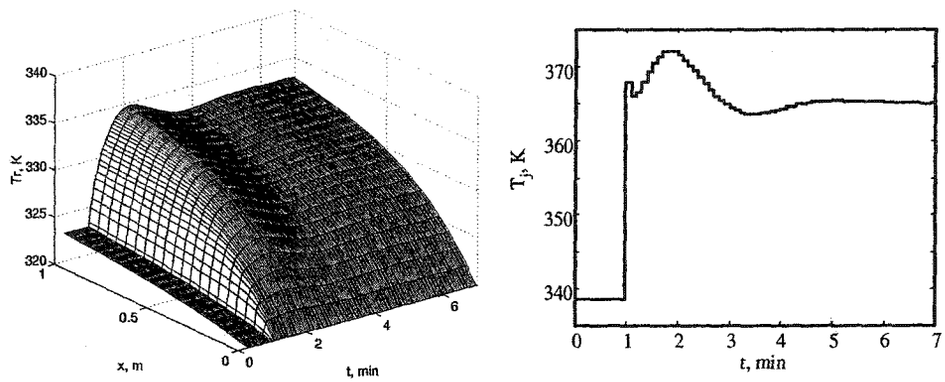

(c) T_r (d) T_j

Figure 3.10: Evolution of the state variable profiles under the state feedback control in PFR

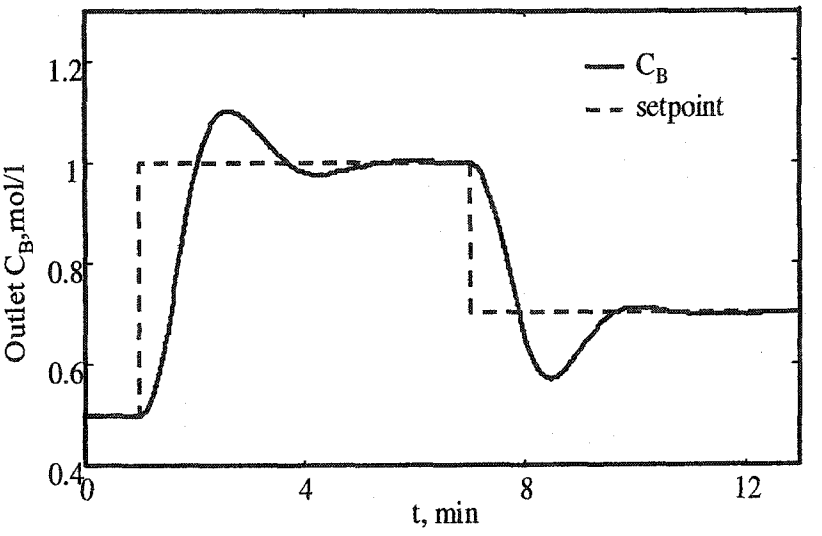

Figure 3.11: Output response to setpoint changes in PFR

while temperature can be easily measured at many points along the reactor. So output feedback control can be implemented based on the estimated concentration. Take the true initial conditions as: $C_A(0,x) = 4$ mol/l, $C_B(0,x) = 0$ mol/l, $T_r(0,x) = 330$ K and the estimated initial concentration profiles as: $\hat{C}_A(0,x) = 3$ mol/l, $\hat{C}_B(0,x) = 1$ mol/l. The control parameters are taken as: $k_1 = 20$, $k_2 = 20$, $\tau_I = 1$. The setpoint is $C_B^r(x=1) = 1$, $\frac{dC_B^r}{dx}(x=1) = r$. Figure 3.14 shows that output feedback control converges to the state feedback control and the concentration of B at the exit tracks the setpoint well, with only a slight degradation in performance.

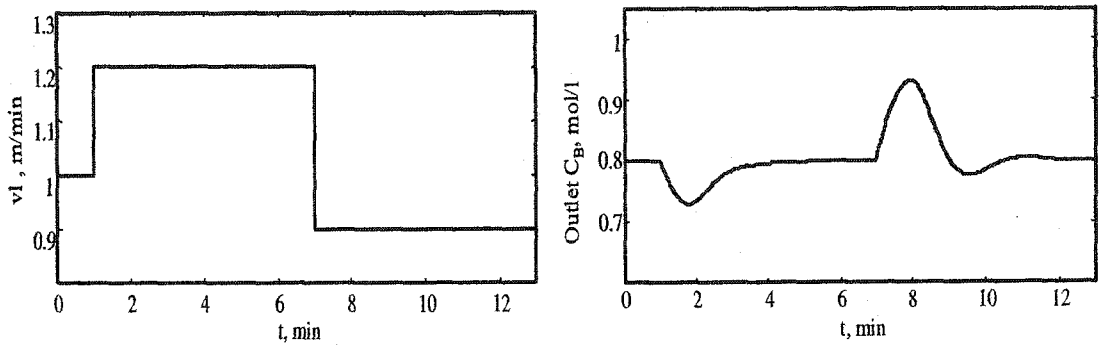

(a) operation variable changes (b) output

Figure 3.12: Output response to flow changes in PFR

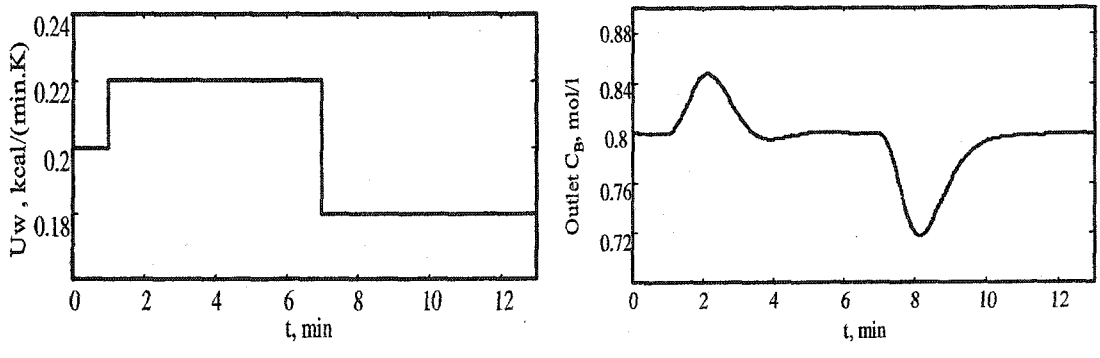

(a) unmeasured process variable changes (b) output

Figure 3.13: Output response to heat transfer coefficient changes in PFR

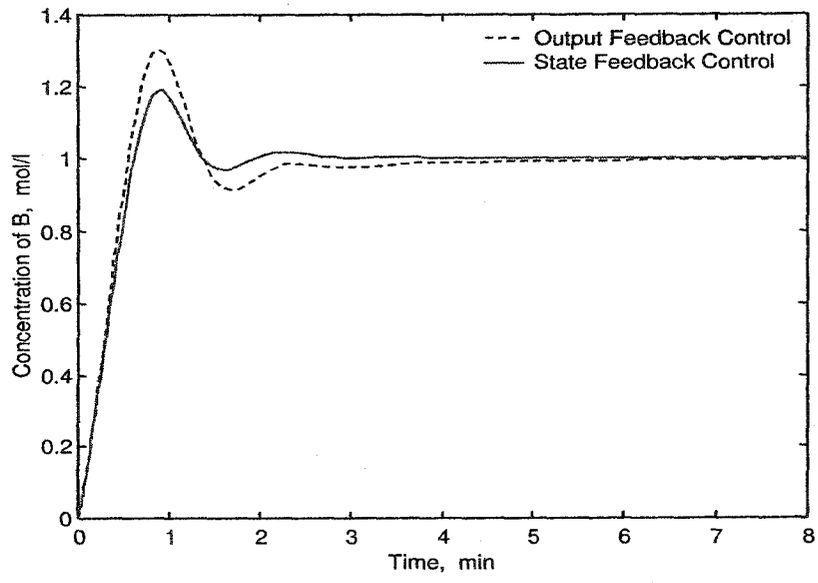

Figure 3.14: Comparison of state feedback control *vs.* output feedback control in PFR

3.4 Discussions

In this chapter, feedback control methods for systems described by a single first-order hyperbolic PDE were developed. The central idea of this control approach is the combination of the Method of Characteristics and geometric control. The Method of Characteristics is employed for a general first-order PDE system to derive a nonlinear ODE control system. Based on the characteristic ODEs, nonlinear output tracking control schemes are used to drive the system towards the desired behavior. The proposed state feedback control and output feedback control are shown, via simulation, to provide good performance. In comparison to other available methods, the proposed controller has a simple form and is easy to implement. The proposed feedback control can respond to disturbances quickly while maintaining normal process operation well. The calculation of control action does not require high order spatial derivatives of the state variable, which reduces sensor system requirements.

In spite of the advantages of the proposed control method, in comparison to the existing feedback control methods and traditional PI control, some inherent problems exist for this method. The idea of feedback control development using the Method of Characteristics is to formulate the controller such that the process output moves towards the desired setpoint along the characteristic direction. Unlike similar methods in lumped parameter systems, this movement pattern cannot be kept as time goes on due to the boundary limitation and will be broken at the boundary. This causes offset in process response. Thus, adding an integral term is necessary to eliminate offset in this method. The dynamics of DPS are such that the inputs of the process affect the infinite-dimensional state variables; however, it may take some time for the influence of the input to be observed in the process output, a situation analogous to the effect of time-delay in finite dimensional systems. The feedback control methods compute control actions based on the current process output value and ignore the long-term effect of the control action on process output, and thus lead to a short-sighted controller. The shortsightedness also makes the proposed feedback control difficult to apply to boundary control problems and the conservative tuning required for stability, *etc.*, results in sluggish process response to

boundary condition changes.

Output feedback control is obtained by combining the state feedback control and an infinite-dimensional state observer. The development of an infinite-dimensional state observer is a very challenging issue in the control of DPS. Even though it has been explored for first-order PDE systems in this work, some specific algorithms remain unsolved.

The above disadvantages of the proposed feedback control may limit its applications. An alternative control method, which overcomes these disadvantages, is required to achieve good control performance in the DPS.

Model Predictive Control takes into consideration the long term effect of control actions on process outputs in the controller design, thus can overcome the shortsightedness of the feedback control. The Method of Characteristics provides a geometric way of viewing the solution structure of PDE systems, and it can help to build an insight into how the process output evolves in the future. Therefore, it may be an effective tool in developing Model Predictive Control algorithms for some DPS. Use of the Method of Characteristics in Model Predictive Control should be able to deliver better performance.

The focus of this chapter, to this point, has been limited to the first-order PDE systems with a single characteristic. Next, the method is extended to more complex systems such as first-order PDE systems with multiple characteristics and certain higher-order systems.

3.4.1 Extensions to More Complex PDE Systems

The convenience of developing feedback control methods for first-order PDE systems with a single characteristic lies in that the Cauchy characteristic exists and the PDE models can be exactly transformed into a system of ODEs along one characteristic direction. However, many distributed parameter systems are modelled by a system of first-order PDEs in which Cauchy characteristics do not exist. The possibility of extending the proposed feedback control to these complex systems and the potential problems are

explored in this section.

First-order PDE Systems with Multiple Characteristics

Distributed parameter systems modelled by a system of PDEs usually cannot be transformed into a set of ODEs along one characteristic direction. They have to be described by more than one characteristic. These systems include counter-flow heat exchangers, counter-flow reactors and chemical absorbers, *etc.* Research on model-based feedback control of these systems has been very limited.

Consider a quasi-linear PDE model with two infinite-dimensional state variables:

$$\begin{aligned} &\frac{\partial v_1}{\partial t} + \sum_{i=1}^{n} \frac{\partial v_1}{\partial x_i} a_{1i}(v_1, v_2, \mathbf{x}, u) = b_1(v_1, v_2, \mathbf{x}, u), \\ &\frac{\partial v_2}{\partial t} + \sum_{i=1}^{n} \frac{\partial v_1}{\partial x_i} a_{2i}(v_1, v_2, \mathbf{x}, u) = b_2(v_1, v_2, \mathbf{x}, u), \\ &y = h(v_1, v_2, \mathbf{x}), \end{aligned} \tag{3.69}$$

where t is time, $\mathbf{x} = \{x_1, x_2, ..., x_n\}$ is spatial coordinates, $a_{11}, ..., a_{1n}, a_{21}, ..., a_{2n}$, and b_1, b_2 are continuous functions. Assume that condition $y = 0$ defines a smooth surface, which serves as the desired process setpoint.

Since $a_{1i} \neq a_{2i}$, $i = 1, 2, ..., n$ holds almost everywhere, Equation (3.69) cannot be described by a set of ODEs along a certain direction. However, the two PDEs in (3.69) can be described by ODEs along two different characteristic directions, separately. Vector $\xi_1 = [1, a_{11}, \cdots, a_{1n}, b_1]^T = [1, \mathbf{a_1}, b_1]^T$ in space $[t, x, v_1]$ and $\xi_2 = [1, a_{21}, \cdots, a_{2n}, b_2]^T = [1, \mathbf{a_2}, b_2]^T$ in space $[t, x, v_2]$ define two time-varying control-parameterized vector fields and are called characteristic vector fields. These two vector fields can be expressed in $t - x$ space as:

$$\begin{aligned} \xi_1 &= \frac{\partial}{\partial t} + \mathbf{a_1} \frac{\partial}{\partial x}, \\ \xi_2 &= \frac{\partial}{\partial t} + \mathbf{a_2} \frac{\partial}{\partial x}. \end{aligned} \tag{3.70}$$

The Lie derivatives of state variables v_1 and v_2 along the vector fields ξ_1 and ξ_2 can be

expressed as:

$$\begin{aligned} L_{\xi_1} v_1 &= b_1, \\ L_{\xi_1} v_2 &= f_2 + (\mathbf{a_1} - \mathbf{a_2}) \frac{\partial v_2}{\partial \mathbf{x}}, \\ L_{\xi_2} v_2 &= b_2, \\ L_{\xi_2} v_1 &= f_1 + (\mathbf{a_2} - \mathbf{a_1}) \frac{\partial v_1}{\partial \mathbf{x}}. \end{aligned} \tag{3.71}$$

With the above equations, the Lie derivative of the output along the two vector fields ξ_1 and ξ_2 are:

$$\begin{aligned} L_{\xi_1} y &= \frac{\partial h}{\partial v_1} b_1 + \frac{\partial h}{\partial v_2} (f_2 + (\mathbf{a_1} - \mathbf{a_2}) \frac{\partial v_2}{\partial \mathbf{x}}) + \frac{\partial h}{\partial \mathbf{x}} \mathbf{a_1}, \\ L_{\xi_2} y &= \frac{\partial h}{\partial v_2} b_2 + \frac{\partial h}{\partial v_1} (f_1 + (\mathbf{a_2} - \mathbf{a_1}) \frac{\partial v_1}{\partial \mathbf{x}}) + \frac{\partial h}{\partial \mathbf{x}} \mathbf{a_2}. \end{aligned} \tag{3.72}$$

If $a_1 = a_2$, Equation (3.72) is greatly simplified and becomes an algebraic equation without derivative terms. For PDE models with multiple characteristics, $a_1 \neq a_2$ and the Lie derivative of the output along each of the two characteristic vector fields cannot be simplified. When the output function contains only one infinite-dimensional state variable (*i.e.*, either $\frac{\partial h}{\partial v_2} = 0$ or $\frac{\partial h}{\partial v_1} = 0$), one of $L_{\xi_1} y$ and $L_{\xi_1} y$ has a simple formula. Assume that the control objective is to regulate variables associated with v_1 only. Then, $L_{\xi_1} y$ can be written as :

$$L_{\xi_1} y = \frac{\partial h}{\partial v_1} b_1 + \frac{\partial h}{\partial \mathbf{x}} \mathbf{a_1}. \tag{3.73}$$

The first-order Lie derivatives only partially display the process information. There exists four different second-order Lie derivatives of the output corresponding to the two characteristics of the systems. The term $L_{\xi_2} L_{\xi_1} y$ is the one that contains the most information of the systems and also has the simplest form. It is calculated as:

$$L_{\xi_2} L_{\xi_1} y = L_{\xi_2} \frac{\partial h}{\partial v_1} b_1 + \frac{\partial h}{\partial v_1} L_{\xi_2} b_1 + L_{\xi_2} \frac{\partial h}{\partial x} \mathbf{a_1} + \frac{\partial h}{\partial x} L_{\xi_2} \mathbf{a_1}. \tag{3.74}$$

The controller can be formulated such that:

$$L_{\xi_2} L_{\xi_1} y + k_1 L_{\xi_1} y + k_0 (y + \frac{1}{\tau_I} \int_0^t y d\tau) = 0. \tag{3.75}$$

The method can be illustrated by applying it to a counter-flow double pipe heat exchanger modelled by

$$\begin{aligned}
&\frac{\partial T_1}{\partial t} + u_1 \frac{\partial T_1}{\partial x} + h_1(T_1 - T_2) = 0, \\
&\frac{\partial T_2}{\partial t} - u_2 \frac{\partial T_2}{\partial x} - h_2(T_1 - T_2) = 0, \\
&y = T_2(x,t) - T_{2sp}(x),
\end{aligned} \tag{3.76}$$

where T_1 and T_2 represent the temperature profiles inside and outside of the tube, u_1, the flow rate of the fluid inside the tube, is manipulated to control the temperature T_2. The first-order and second-order Lie derivatives of the output along the two characteristics can be expressed as:

$$\begin{aligned}
&L_{\xi_2} y = h_2(T_1 - T_2) + u_2 \frac{\partial T_{2sp}}{\partial x}, \\
&L_{\xi_1} L_{\xi_2} y = -h_2(h_1 + h_2)(T_1 - T_2) - h_2(u_1 + u_2)\frac{\partial T_2}{\partial x} + u_2 u_1 \frac{\partial^2 T_{2sp}}{\partial x^2}.
\end{aligned} \tag{3.77}$$

Assuming $x \in [0,1]$, the controller can be formulated based on Equation (3.75) and (3.77):

$$\begin{aligned}
u_1 \;=\; &\Big\{-h_2(h_1 + h_2 + k_1 h_2)E(T_1 - T_2) - h_2 u_2 T_2|_{x=0}^{x=1} \\
&+k_1 u_2 T_{2sp}|_{x=0}^{x=1} + k_0 E(T_2 - T_{2sp}) \\
&+ \frac{k_0}{\tau_I}\int_0^t E(T_2 - T_{2sp})dt\Big\} \Big/ \left\{h_2 T_2|_{x=0}^{x=1} - u_2 \frac{\partial T_{2sp}}{\partial x}|_{x=0}^{x=1}|\right\},
\end{aligned} \tag{3.78}$$

where $T_2|_{x=0}^{x=1} = T_2(x=1) - T_2(x=0)$ and $T_{2sp}|_{x=0}^{x=1} = T_{2sp}(x=1) - T_{2sp}(x=0)$. This complex control formula does not have as clear geometric meaning as the one for a single characteristic case. It involves complicated computations. In simulation, it is hard to tune to get satisfactory process performance. Hanczyc and Palazoglu (1995a) proposed a nonlinear state feedback control for a double-pipe heat exchanger using the Method of Characteristics by extending the sliding feedback control algorithm in single characteristic case to multiple characteristics. At the current time, the effort of extending the feedback control technique by using the Method of Characteristics to multiple characteristic cases does not appear to be promising. Further research is required to address this complex problem.

Second and Higher Order Systems

Most second-order or higher-order PDE systems cannot be described by a single characteristic, but there are some special cases. Consider a second-order quasi-linear parabolic system:

$$\begin{aligned} & a^2(t,x,u)v_{tt} + 2a(t,x,u)b(t,x,u)v_{tx} + b^2(t,x,u)v_{xx} \\ & +c(t,x,u)v_t + d(t,x,u)v_x = f(x,u), \\ & y = h(v,x), \end{aligned} \tag{3.79}$$

where $a(t,x,u) \neq 0$, $b(t,x,u)$ and $c(t,x,u)$ are C^∞-continuous functions of their arguments. Define a vector field in the space of (t,x) as $\xi = a(t,x,u)\frac{\partial}{\partial t} + b(t,x,u)\frac{\partial}{\partial x}$. Then, Equation (3.79) can be written as:

$$L_\xi L_\xi v + (a\frac{\partial a}{\partial t} + b\frac{\partial a}{\partial x} + c)\frac{\partial v}{\partial t} + (a\frac{\partial b}{\partial t} + b\frac{\partial b}{\partial x} + d)\frac{\partial v}{\partial x} = f(x,u). \tag{3.80}$$

If

$$\frac{a\frac{\partial a}{\partial t} + b\frac{\partial a}{\partial x} + c}{a\frac{\partial b}{\partial t} + b\frac{\partial b}{\partial x} + d} = \frac{a}{b}, \tag{3.81}$$

Equation (3.79) becomes

$$L_\xi L_\xi v + e(x,y,u)L_\xi v = f(x,u), \tag{3.82}$$

where $e(x,y,u) = \frac{\partial a}{\partial t} + \frac{b}{a}\frac{\partial a}{\partial x} + \frac{c}{a} = \frac{a}{b}\frac{\partial b}{\partial t} + \frac{\partial b}{\partial x} + \frac{c}{b}$. Then, the system in Equation (3.79) can be exactly described by one characteristic:

$$\begin{aligned} \dot{t} &= 1, \\ \dot{x} &= \frac{b}{a}, \\ \dot{v} &= \omega, \\ \dot{\omega} &= e(x,y,u)\omega + \frac{f(x,u)}{a}. \end{aligned} \tag{3.83}$$

The first-order Lie derivative of the output y along the vector field ξ can be calculated from Equation (3.83):

$$L_\xi y = \frac{\partial h}{\partial v}\omega + \frac{\partial h}{\partial x}\frac{b}{a}. \tag{3.84}$$

With the assumption that $\frac{\partial h}{\partial v}$ is constant, the second-order Lie derivative of output can be obtained:

$$L_\xi L_\xi y = \frac{\partial h}{\partial v}\left[e(x,y,u)\omega + \frac{f(x,u)}{a}\right] + L_\xi\left(\frac{\partial h}{\partial x}\frac{b}{a}\right). \tag{3.85}$$

Normally, the second-order Lie derivative includes all information of the original systems and calculation of the higher-order Lie derivatives is not necessary. A controller can be designed such that

$$L_\xi L_\xi y + k_1 L_\xi y + k_0(y + \frac{1}{\tau_I}\int_0^t y d\tau) = 0. \tag{3.86}$$

The controller has a clearer geometric interpretention than the one for first-order systems with multiple characteristics, but the disadvantage of this controller is that it contains a new variable ω, which requires a complicated state observer. In addition, this method is only applicable when the condition in Equation (3.81) holds. Obviously, this is a very restrictive limitation and may not be satisfied in many practical applications.

Similarly, for n^{th} order system, if we can define a vector field ξ in the space of (t,x) such that the system can be described as:

$$L_\xi L_\xi ... L_\xi v + a_{n-1} L_\xi ... L_\xi v + ... + a_1 L_\xi v = f(x,u), \tag{3.87}$$

the n-th order PDE systems can be controlled using the feedback control strategy based on the Method of Characteristics. As above, the controller requires an additional $(n-1)$ variables that must be estimated. Such a controller is highly restrictive and potentially complex.

Given these limitations on the use of the proposed feedback controller, an alternative approach is required to extend the class of processes that can be considered. As previously discussed, the MPC paradigm can address some of the key characteristics of DPS. Thus,

in the next chapter, Model Predictive Control is developed for different PDE systems using the Method of Characteristics.

Chapter 4

CBMPC for Hyperbolic Systems - Single Characteristic

A significant number of practical processes can be modelled by first-order hyperbolic PDEs with single characteristics (*e.g.*, heat-exchangers, continuum models of traffic flow, evolution of an age-structured population, flow in a porous media, *etc*). As discussed in the last chapter, the Method of Characteristics has been used in the development of state feedback control or output feedback control for these systems (Godasi *et al.*, 1999; Shang *et al.*, 2000). The resulting controllers have comparatively good setpoint tracking behavior and robust performance; however, implementation of the control law requires the estimation of the infinite-dimensional state despite the fact that only a portion of the information is used in the final control action. Thus, the available information is not fully exploited in the control strategies.

This chapter proposes a Characteristics-Based Model Predictive Control (CBMPC) for hyperbolic PDE systems with single characteristics. It uses the Method of Characteristics to predict the future process outputs from the current state variable profiles and formulates the controller such that this prediction is as close as possible to the desired process

response. The transformation of PDEs to nonlinear ODEs is exploited in the proposed approach to facilitate the computation of the control actions using a nonlinear quadratic MPC algorithm. The main advantage of the approach is the increased computational efficiency and improved prediction accuracy compared with the conventional finite-difference approach. The CBMPC approach takes into account the long-term effect of the current control action on the process output in the controller formulation, and thus, can overcome the shortsightedness of simple feedback control methods.

The chapter is structured as follows. In section 4.1, a brief review of MPC is presented. In section 4.2, the CBMPC algorithm is developed in details for linear and quasilinear systems. Section 4.3 discusses the stability issue of this control method. A simulation study is presented in section 4.4. The chapter concludes with a brief discussion of the result in section 4.5.

4.1 MPC Background

Model Predictive Control (MPC) refers to a control scheme in which a sequence of manipulated variable adjustments is determined by optimizing some open-loop performance objective on a time interval extending from the current time through some specified prediction horizon. The computed settings for the manipulated variables are implemented until plant measurements become available, usually at the next control interval. Feedback is incorporated by using the measurements to update the disturbance estimate in the optimization problem for the next time step. The defining features of MPC include the direct use of a process model for optimizing the open-loop process performance objective over a finite horizon (Eaton and Rawlings, 1992; Garcia and Morshedi, 1986). The explicit use of a prediction horizon in the control law formulation distinguishes MPC from standard feedback control.

The MPC control law can be most easily described by referring to Figure 4.1. For the single-input-single-output case, the control calculation consists of the following

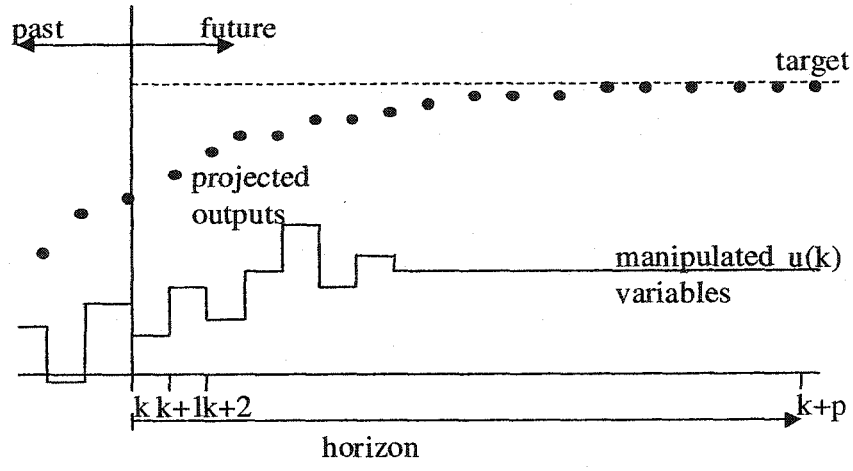

Figure 4.1: Introduction of model predictive control

optimization problem:

$$\min_{\Delta u(k),\ldots,\Delta u(k+m_c-1)} \left[\sum_{i=1}^{p} q(i) \left(y^{sp}(k+i) - \hat{y}(k+i) \right)^2 + \sum_{j=1}^{m_c} r(j) \left(\Delta u(k+j-1) \right)^2 \right], \tag{4.1}$$

where y^{sp} is the setpoint, $\hat{y}$ is the model prediction, $q(i)$ and $r(j)$ are weighting factors, p is the prediction horizon and m_c is the control horizon or the number of future moves to be computed, Δu is the change in manipulated variables, which is defined as $\Delta u(k) = u(k) - u(k-1)$. In general, $m_c \leq p$ and therefore $u(k+m_c-1) = u(k+m_c) = \ldots = u(k+p-1)$. The model prediction $\hat{y}$ can be written as:

$$\hat{y}(k+j) = y_0(k+j) + \sum_{i=1}^{j} S_{mi} \Delta u(k+j-1) + w(k+j), \tag{4.2}$$

where $y_0(k+j)$ is the contribution to the future values due to past input moves (up to time $k-1$), S_{mi} are the step response coefficients for the manipulated variables and $w(k+j)$ captures all unmodelled effects. To predict the output value using Equation (4.2), the disturbance $w(k+j)$ must be estimated, which is carried out as follows:

$$w(k+j) = w(k) = y^m(k) - y_0(k), \qquad j = 1, 2, \ldots, p, \tag{4.3}$$

where $y^m(k)$ is the current measurement. The control problem as presented in Problem

(4.1) using Equation (4.2) through (4.3) is the well known Quadratic Dynamic Matrix Control (QDMC) form (Garcia and Morshedi, 1986).

MPC began with an attempt to improve the control of processes that are constrained, multi-variable and uncertain (Chen and Allgower, 1998). The use of MPC in the chemical engineering field started in the process industries in the 1970s (Culter and Ramaker, 1979; Richalet *et al.*, 1976) and in the past three decades, MPC has found wide acceptance in industrial practice. MPC, using a linear model, has been the technology of choice in the petrochemical and chemical industry since the advent of the technique. A number of approaches now exist including: linear time-domain, input/output, step response or impulse response modelling approaches and Generalized Predictive Control (GPC) (Clarke *et al.*, 1987*a*; Clarke *et al.*, 1987*b*; Garcia, 1984; Richalet *et al.*, 1994). Recent developments have seen the emerging use of state-space formulations of the MPC approach (Rawlings, 2000). An account of current trends in linear MPC are discussed in a number of survey papers (Badgewell, 1997; Mayne *et al.*, 2000; Rani and Unbehauen, 1997; Rao and Rawlings, 2000).

Since the essence of MPC is to optimize forecasts of process behavior based on a process model over values for the manipulated input variables, the model is a critical element of a MPC controller (Rawlings, 2000). Typically, linear models are used for this task, despite the fact that essentially all industrial processes exhibit some degree of nonlinear behavior. The use of nonlinear models in process control is motivated by the possibility of performance enhancement through improved quality of forecasting. Active research on Nonlinear Model Predictive Control (NLMPC) has resulted in a number of algorithms (Chen and Allgower, 1998; Henson, 1998; Mayne *et al.*, 2000; Scokaert *et al.*, 1999; Sistu and Bequette, 1996). Some of these algorithms attempt to deal with nonlinear systems by modifying the linear algorithm, in particular the prediction equation, while retaining the advantage of Linear Model Predictive Control (LMPC). Nonlinear quadratic dynamic matrix control is proposed for the control of nonlinear processes and uses a nonlinear model to compute the manipulated variable values and achieves optimal quadratic performance (Garcia, 1984). A NLMPC algorithm based on a reinterpretation

of the process output prediction equation as a Taylor series expansion for non-affine, nonlinear systems showed improved computational efficiency and performance (Mutha *et al.*, 1997). Other NLMPC approaches have included the use of second-order Volterra model series and other nonlinear models such as Wiener models and Hammerstein models (Maner *et al.*, 1996; Norquay *et al.*, 1998). These MPC techniques focus on lumped parameter models and limited results are available for MPC methods based on distributed parameter models.

Traditionally, distributed parameter systems have been approximated by linear models that can be used to design linear model based control strategies (Patwardhan *et al.*, 1992). Satisfactory control can be achieved using these low-order linear models when the process nonlinearity and spatial variation of the state variable are mild. When the processes have large spatial variation, the use of partial differential equation models in model based control for DPS may provide tighter control of the process and improved constraint handling. Unfortunately, model predictive control techniques for distributed parameter systems are relatively scarce due, in part, to the mathematical complexity arising from the partial differential equation models. Some researchers have addressed the design of model predictive control for distributed parameter systems (Bhattacharyya *et al.*, 1996; VanAntwerp and Braatz, 2000); however, most of these strategies use an approximate ordinary differential equation (ODE) model or a discretization of the underlying partial differential equations into a system of ODEs, in order to apply nonlinear MPC techniques to the resulting high-dimensional lumped parameter systems. These methods can produce a control performance that is superior to traditional lumped parameter controller for some distributed parameter systems; however, discretization of partial differential equations usually leads to a large number of ODEs, which drastically increases the complexity of the calculations. The computational cost associated with this lumping approach can be prohibitive for some processes and may not provide an improvement in performance that warrants the additional computational cost.

The MPC scheme presented in this chapter addresses processes modelled by first-order hyperbolic PDEs with single characteristics. The MPC scheme for processes modelled

by hyperbolic PDEs with multiple characteristics and parabolic PDEs are presented in chapters 5 and 6, respectively. The Method of Characteristics is the fundamental basis for future output prediction. This prediction approach is then reformulated into the framework of existing nonlinear model predictive control and a control action is calculated using available nonlinear model predictive control algorithms.

4.2 CBMPC Development

For processes modelled by a scalar PDE or some specific systems of PDEs, Cauchy characteristics exist and the PDE models can be described by their characteristic ODEs along single characteristic curves. This provides a convenient and efficient way to predict the future output from current state variable profiles. This geometric solution method is used in this section, to develop a characteristic-based MPC scheme.

4.2.1 Linear Systems

Consider a system modelled by a linear first-order scalar PDE:

$$\begin{aligned} &\frac{\partial v}{\partial t} + a\frac{\partial v}{\partial x} = bv + cu, \\ &v(x=0) = v_b, \\ &y = v(x_{out}, t), \end{aligned} \tag{4.4}$$

where t is time, x is a normalized spatial coordinate and $x \in [0, 1]$, a, b, c are constants, u is a spatially uniform input, v is the distributed state variable, v_b is the value of the state variable v at boundary $x = 0$ and the output y is the state variable v at position x_{out}.

The PDE in Equation (4.4) has a system of linear characteristic ODEs:

$$\begin{aligned} \dot{t} &= 1, \\ \dot{x} &= a, \\ \dot{v} &= bv + cu. \end{aligned} \tag{4.5}$$

Equation (4.5) represents a set of orbital curves, which are in the solution surface of the PDE model. With the initial condition $t(0) = t_0, x(0) = x_0, v(0) = v_0$, the above system of ODEs can be integrated analytically:

$$\begin{aligned} t &= t_0 + \Delta t, \\ x &= x_0 + a\Delta t, \\ v &= (v_0 + \frac{c}{b}u)e^{b\Delta t} - \frac{c}{b}u. \end{aligned} \tag{4.6}$$

This equation indicates that the state variable v evolves along each characteristic curve. The variation of v is determined by the initial condition on the same characteristic curve and not affected by other characteristic curves.

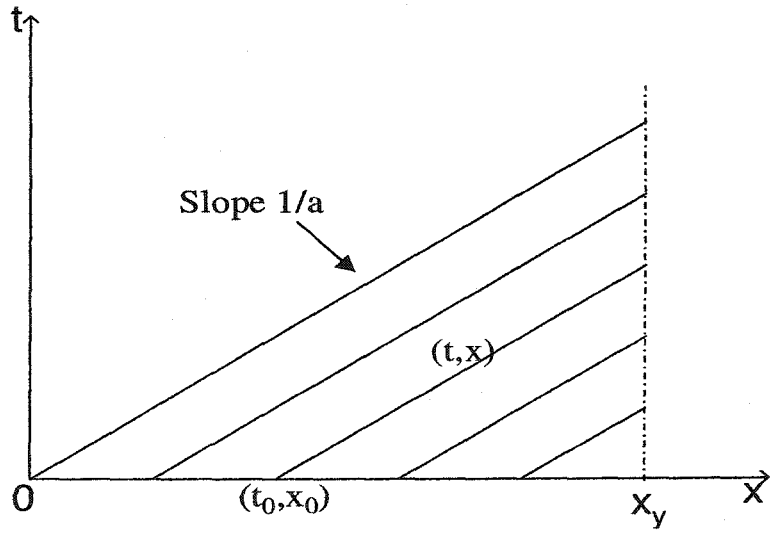

Figure 4.2: Projection of characteristic curves for scalar PDEs

Equation (4.6) allows prediction of the sampled future output in high accuracy. It is possible to predict the future output in a continuous time, but it involves more complex computation and can be impossible as the model complexity increases. Therefore, the MPC methods in this thesis optimize the sampled future outputs predicted based on the continuous PDE model. The prediction of a sampled future output can be obtained from the value of current state variable profile v_0 at some discrete spatial points, as shown in Figure 4.2. From Equation (4.6) and given a sampling time t_s, the output at sample instants: t_0+it_s, $i = 1, 2, \cdots$, can be determined from the initial value of the current state variable at spatial points: $x_{01} = x_{out}-at_s, x_{02} = x_{out}-2at_s, \cdots$. On the other hand, if the current state variable v_0 is estimated or measured at discrete points $x_1, ..., x_m$, the output can be determined at future sample instants $t_0+\frac{x_{out}-x_m}{a}, ..., t_0+\frac{x_{out}-x_1}{a}$. Since time and spatial coordinates are correlated along characteristic curves, either sampling time or spatial discretization grid of the initial state variable profile can be freely specified, but not both. In this chapter, the spatial discretization points of the initial state variable profile are specified and sampling time is determined and can be adjusted through discretization grids. The control approach, however, applies to the case with specified sampling time. The selection of sampling time in CBMPC follows the same rules as MPC in LPS and is not discussed in this thesis.

Assuming that the value of the current state variable at spatial points $x_1 = 0, x_2, ..., x_m$, is known, the next m sample instants $t_0 + \Delta t_1, t_0 + \Delta t_2, ..., t_0 + \Delta t_m$, at which the output can be predicted, are

$$\Delta t_1 = \frac{x_{out} - x_m}{a}, \Delta t_2 = \frac{x_{out} - x_{m-1}}{a}, ..., \Delta t_m = \frac{x_{out} - x_1}{a}. \tag{4.7}$$

Since the current control actions affect the output only until time $t_0 + \Delta t_m$ for systems modelled by Equation (4.4), the prediction horizon is chosen to be equal to Δt_m. When the space is uniformly discretized with a spacing Δx, the prediction sampling time becomes

$$t_s = \frac{\Delta x}{a}, \tag{4.8}$$

and the sampling times are: $\Delta t_1 = t_s, \Delta t_2 = 2t_s, ..., \Delta t_m = mt_s$. It is easy to see that the discretization spacing can be used to adjust the sampling times.

Assuming that the control actions in the next m_c sample instants are $u_0, u_1, ..., u_{m_c-1}$ and $u_{m_c-1} = u_{m_c} = ... = u_{m-1}$, the output $y = v(x_{out})$ at the future sample instants can be formulated from Equation (4.6) as:

$$\begin{aligned}
y(t_0+\Delta t_1) &= e^{b\Delta t_1}v_0(x_m) + (e^{b\Delta t_1}-1)\frac{c}{b}u_0, \\
y(t_0+\Delta t_2) &= e^{b\Delta t_2}v_0(x_{m-1}) + (e^{b\Delta t_2} - e^{b(\Delta t_2-\Delta t_1)})\frac{c}{b}u_0 \\
&\quad +(e^{b(\Delta t_2-\Delta t_1)}-1)\frac{c}{b}u_1, \\
&\cdots\cdots \\
y(t_0+\Delta t_{m_c}) &= e^{b\Delta t_{m_c}}v_0(x_{m-m_c+1}) + (e^{b\Delta t_{m_c}} - e^{b(\Delta t_{m_c}-\Delta t_1)})\frac{c}{b}u_0 \\
&\quad +... + (e^{b(\Delta t_{m_c}-\Delta t_{m_c-1})}-1)\frac{c}{b}u_{m_c-1}, \\
&\cdots\cdots \\
y(t_0+\Delta t_m) &= e^{b\Delta t_m}v_0(x_1) + (e^{b\Delta t_m} - e^{b(\Delta t_m-\Delta t_1)})\frac{c}{b}u_0 \\
&\quad +... + (e^{b(\Delta t_m-\Delta t_{m_c-1})}-1)\frac{c}{b}u_{m_c-1}.
\end{aligned} \tag{4.9}$$

From this equation, the future output values can be calculated using current and some of the future control actions, as well as the current state variable profiles.

By defining the vectors

$$\hat{\mathbf{y}} = [y_{t_0+\Delta t_1}, y_{t_0+\Delta t_2}, \cdots, y_{t_0+\Delta t_m}]^T, \tag{4.10}$$

$$\mathbf{y_0} = [e^{b\Delta t_1}v_0(x_m), e^{b\Delta t_2}v_0(x_{m-1}), ..., e^{b\Delta t_m}v_0(x_1)]^T, \tag{4.11}$$

$$\mathbf{u} = [u_0, u_1, ..., u_{m_c-1}]^T, \tag{4.12}$$

and a matrix

$$\mathbf{S} = \frac{c}{b}\begin{bmatrix} e^{b\Delta t_1} - 1 & 0 & \dots & 0 \\ e^{b\Delta t_2} - e^{b(\Delta t_2 - \Delta t_1)} & e^{b(\Delta t_2 - \Delta t_1)} - 1 & \dots & 0 \\ \dots & & & \\ e^{b\Delta t_{m_c}} - e^{b(\Delta t_{m_c} - \Delta t_1)} & e^{b(\Delta t_{m_c} - \Delta t_1)} - e^{b(\Delta t_{m_c} - \Delta t_2)} & \dots & e^{b(\Delta t_{m_c} - \Delta t_{m_c-1})} - 1 \\ \dots & & & \\ e^{b\Delta t_m} - e^{b(\Delta t_m - \Delta t_1)} & e^{b(\Delta t_m - \Delta t_1)} - e^{b(\Delta t_m - \Delta t_2)} & & e^{b(\Delta t_m - \Delta t_{m_c-1})} - 1 \end{bmatrix}, \tag{4.13}$$

Equation (4.9) can be expressed in a compact form:

$$\hat{\mathbf{y}} = \mathbf{y}_0 + \mathbf{S}\mathbf{u}. \tag{4.14}$$

This equation gives an exact prediction of future output modelled by Equation (4.4). The dimension of the equation is determined by the spatial discretization of the initial state variable profile, which only affects the sampling time. Using other numerical methods such as the finite difference method on Equation (4.4) may also yield a linear matrix prediction equation similar to Equation (4.14), but a much higher dimension would be required to get an acceptable prediction accuracy. Equation (4.19) has the form of typical linear models, and therefore, it is straightforward to construct the control formula for the unconstrained MPC.

Given the specified sampling time and current state variable profiles at some discretized spatial points, $\mathbf{y}_0$ and $\mathbf{S}$ can be determined in Equation (4.19). The future control sequence $\mathbf{u}$ is calculated to make $\hat{\mathbf{y}}$ as close as possible to output setpoint $\mathbf{y}^r$. An optimization problem with an objective function can be set up:

$$\begin{aligned} &\min_{\mathbf{u}} \|\hat{\mathbf{y}} - \mathbf{y}^r\| \\ &= \min_{\mathbf{u}} \|\mathbf{y}_0 + \mathbf{S}\mathbf{u} - \mathbf{y}^r\|. \end{aligned} \tag{4.15}$$

With $m > m_c$, the control moves can be computed using the least-square solution:

$$\mathbf{u} = (\mathbf{S}^T\mathbf{S})^{-1}\mathbf{S}^T(\mathbf{y}^r - \mathbf{y}_0). \tag{4.16}$$

Then, the first element of $\mathbf{u}$ is implemented.

To be consistent with the CBMPC for more complex PDE systems discussed in the rest of the thesis, the control increments from the past control action can also be calculated. Denote the immediate past control action as u_{-1}. Define

$$\hat{\mathbf{y}}_0 = \mathbf{y}_0 + \mathbf{S}[u_{-1}, u_{-1}, \cdots, u_{-1}]^T, \tag{4.17}$$

and

$$\Delta\mathbf{u} = [u_0 - u_{-1}, u_1 - u_{-1}, ..., u_{m_c-1} - u_{-1}]^T, \tag{4.18}$$

where u_{-1} indicates the past control action at t_{-1}. Equation (4.14) can then be written as:

$$\hat{\mathbf{y}} = \hat{\mathbf{y}}_0 + \mathbf{S}\Delta\mathbf{u}. \tag{4.19}$$

Note that $\Delta\mathbf{u}$ is defined as the control increment from the past control action u_{-1}, different from the definition as in DMC. Therefore, Equation (4.19) is not an integral equation. The control increments from u_{-1} is obtained as:

$$\Delta\mathbf{u} = (\mathbf{S}^T\mathbf{S})^{-1}\mathbf{S}^T(\mathbf{y}^r - \hat{\mathbf{y}}_0). \tag{4.20}$$

In the control law described by Equation (4.16) or (4.20), $\mathbf{S}$ can be calculated off-line and $\mathbf{y}_0$ needs to be updated based on the available new measurement, using Equation (4.11). Therefore, the control calculation is easy and the control law has the simple form of an analytical off-line control law. An example of heat exchangers in Section 4.4 will illustrate the design technique and performance of this proposed control method.

4.2.2 Quasilinear Systems

In a first-order quasilinear PDE model, the partial derivatives of the dependent variables occur linearly in the equations, with coefficients and non-homogeneous terms being functions of independent variables and dependent variables, which can be nonlinear.

Processes described by such models can be represented as:

$$\begin{aligned} &\frac{\partial v}{\partial t} + a(x, v, u)\frac{\partial v}{\partial x} = f(x, v, u), \\ &v(x = 0) = v_b, \\ &y = v(x_{out}, t), \end{aligned} \tag{4.21}$$

where $a(x, v, u)$ and $f(x, v, u)$ are smooth functions.

In the space with coordinates (t, x, v), the PDE model in Equation (4.21) possesses a characteristic vector field $\xi = [1, a(x, v, u), f(x, v, u)]$, which defines the characteristic ODEs:

$$\begin{aligned} &\dot{t} = 1, \\ &\dot{x} = a(v, u, x), \\ &\dot{v} = f(v, u, x). \end{aligned} \tag{4.22}$$

In contrast to linear systems discussed in the last subsection, the characteristic ODEs for quasilinear systems are nonlinear and cannot be integrated analytically. Numerical integration methods are required to obtain a sampled future output from the value of the current state variable at discrete spatial points. Assuming that the value of the current state variable at spatial coordinate value x_0 is $v_0(x_0)$, the output at a future time instant can be obtained by simultaneously integrating Equation (4.22) with initial conditions $t(0) = t_0$, $x(0) = x_0$ and $v(0) = v_0(x_0)$:

$$t = t_0 + \Delta t, \tag{4.23}$$

$$x = \int_{t_0}^{t} a(v, u, x)d\tau = \phi_x(v_0, u, x_0, \Delta t), \tag{4.24}$$

$$v = \int_{t_0}^{t} f(v, u, x)d\tau = \phi_v(v_0, u, x_0, \Delta t), \tag{4.25}$$

where $\Delta t = t - t_0$. Integration can proceed until x reaches x_{out}, and corresponding state variable value is the output at time t. The output at a different future time can be obtained by varying the initial point x_0. The prediction horizon time can be taken to be equal to the residence time, since the current value of the state variable and control action can only

affect the output within one residence time. Increasing the prediction horizon beyond the residence time will be equivalent to increasing the weighting factor for the terminal output in objective functions. This leads to a prediction horizon p equal to the number of initial discretization points m. The manipulated variable can be kept constant or varying during the integration. In typical MPC calculation, control actions for the first m_c instants are to be determined assuming the control action is kept the same after m_c control horizon time.

This procedure of predicting the future output can be described mathematically by assuming that the values of the current state variable v_0 at m spatial points $x_1, x_2, ..., x_m$, are $v_0(x_1), v_0(x_2), ..., v_0(x_m)$. Since $a(v, u, x) \neq 0$ in Equation (4.21), it is clear that

$$\frac{\partial \phi_x}{\partial \Delta t} = a(v, u, x) \neq 0. \tag{4.26}$$

By the Implicit Function Theorem, $\Delta t = t - t_0$ can be expressed from Equation (4.24) as

$$\Delta t = \alpha(x, v_0, u, x_0), \tag{4.27}$$

and therefore the next m sampling times, at which the output can be predicted, are:

$$\begin{aligned} \Delta t_1 &= t_1 - t_0 = \alpha(x_{out}, v_0(x_1), u, x_1), \\ \Delta t_2 &= t_2 - t_0 = \alpha(x_{out}, v_0(x_2), u, x_2), \\ &..... \\ \Delta t_m &= t_m - t_0 = \alpha(x_{out}, v_0(x_m), u, x_m). \end{aligned} \tag{4.28}$$

The output at the next m sample instants, $t_i = t + \Delta t_i,\ i = 1, 2, \cdots, m$, can be expressed as:

$$\begin{aligned} y(t_1) &= \phi_v(v_0(x_1), u, x_1, \Delta t_1), \\ y(t_2) &= \phi_v(v_0(x_2), u, x_2, \Delta t_2), \\ &.... \\ y(t_m) &= \phi_v(v_0(x_m), u, x_m, \Delta t_m). \end{aligned} \tag{4.29}$$

Thus, from the current m-dimensional measurements or discretizations, the output is predicted for the next m time instants.

When the coefficient function a is a constant, the PDE in Equation (4.21) becomes semi-linear and the first two equations of the characteristic ODE (4.22) can be integrated analytically to give:

$$\begin{aligned} t &= t_0 + \Delta t, \\ x &= x_0 + a\Delta t. \end{aligned} \tag{4.30}$$

In this case, the next m time intervals, at which the future output can be predicted, are expressed explicitly from Equation (4.30) as:

$$\Delta t_1 = \frac{x_{out} - x_m}{a}, \Delta t_2 = \frac{x_{out} - x_{m-1}}{a}, ..., \Delta t_m = \frac{x_{out} - x_1}{a}. \tag{4.31}$$

Using the current state variable v_0 at different spatial points as initial conditions, the output at time $t_0 + \Delta t_1, t_0 + \Delta t_2, ..., t_0 + \Delta t_m$ $(m \geq m_c)$, can be obtained by numerically integrating the third equation of the characteristic ODEs (4.22):

$$y(t_i) = \int_{t_0}^{t_i} f(v, u, x_{m+1-i} + a(\tau - t_0))d\tau, \qquad i = 1, 2, \cdots, m. \tag{4.32}$$

Using the above procedure, the prediction of the output by numerical integration of the characteristic ODEs is decoupled for each spatial point and prediction time instant. This decoupling property allows one to predict the future output with relatively high accuracy at no cost of demanding computational requirement.

Given the control action u, Equation (4.29) or (4.32) can be used to predict the output for future sample instants. Therefore, the value of u can be obtained by minimizing the objective function:

$$\mathbf{J} = \sum_{i=1}^{p} (y^r - y(t_i))^2, \tag{4.33}$$

subject to either (4.29) or (4.32), depending on the quasilinear or semi-linear characteristics of the system. The more general objective function can also be used:

$$(\mathbf{y}^r - \mathbf{y})^T \mathbf{Q} (\mathbf{y}^r - \mathbf{y}) + \Delta \mathbf{u}^T \mathbf{R} \Delta \mathbf{u}, \tag{4.34}$$

where $\mathbf{y}^r$ is the desired output trajectory in future time, $\mathbf{Q}$ and $\mathbf{R}$ are two positive definite weighting matrices, $\Delta \mathbf{u}$ is the control increment from the past control action u_{-1}.

4.3 Stability

The general form of MPC does not guarantee closed-loop stability, because a finite horizon criterion is not designed to deliver an asymptotic property such as stability. Closed-loop stability can only be achieved by a suitable tuning of design parameters such as prediction horizon, control horizon and weighting matrices (Chen and Allgower, 1998). In this section, the closed-loop stability of the proposed CBMPC is analyzed for linear and quasilinear PDE systems via different routes.

4.3.1 Linear Systems

As discussed in the last section, the unconstrained CBMPC for linear PDE systems has the form of an offline control law. Hence, it is possible to analyze the closed loop stability by examining the denominator polynomials of the closed-loop transfer functions. This method was used to establish stability result for unconstrained MPC based on impulse response models (Garcia and Morari, 1982).

The output prediction for linear systems can be explicitly expressed in terms of the current state variable profiles and the future output, as in Equation (4.9). Since the current state variable value at every spatial point can be determined by the boundary condition value v_b and the past control actions, the future output can as well be formulated in terms of both past and future control actions as well as the boundary condition value v_b (see Figure 4.3). Using a uniform sampling time t_s, the time intervals in Equation (4.9) are:

$$\Delta t_1 = t_s,\ \Delta t_2 = 2t_s,\ \cdots,\ \Delta t_m = mt_s. \tag{4.35}$$

Then, the output for the next m time instants, $t_i = t_0 + it_s,\ i = 1, \cdots, m$, can be

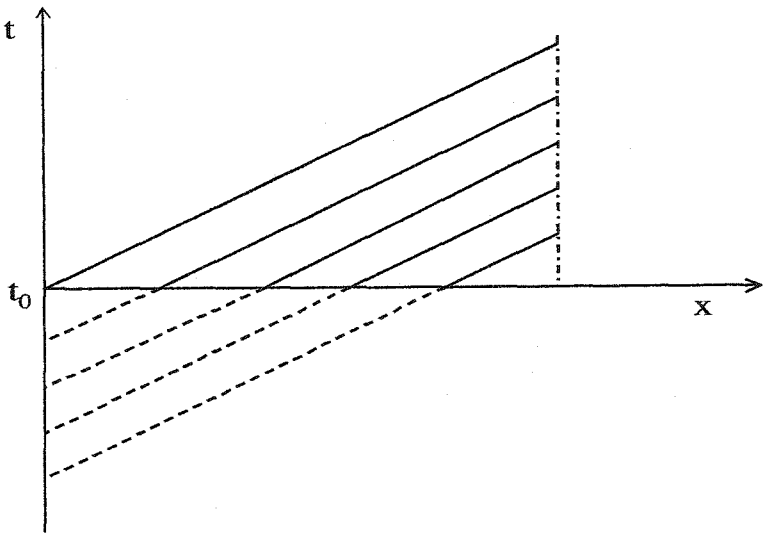

Figure 4.3: Output prediction from characteristic curves for scalar linear PDEs

formulated as:

$$
\begin{aligned}
y(t_1) &= e^{mbt_s}v_b + (e^{bt_s}-1)\frac{c}{b}u_0 \\
&\quad +(e^{2bt_s}-e^{bt_s})\frac{c}{b}u_{-1} + \cdots + (e^{mbt_s}-e^{(m-1)bt_s})\frac{c}{b}u_{-(m-1)}, \\
y(t_2) &= e^{mbt_s}v_b + (e^{2bt_s}-e^{bt_s})\frac{c}{b}u_0 + (e^{bt_s}-1)\frac{c}{b}u_1 \\
&\quad +(e^{3bt_s}-e^{2bt_s})\frac{c}{b}u_{-1} + \cdots + (e^{mbt_s}-e^{(m-1)bt_s})\frac{c}{b}u_{-(m-2)}, \\
&\cdots\cdots \\
y(t_{m_c}) &= e^{mbt_s}v_b + (e^{m_cbt_s}-e^{(m_c-1)bt_s})\frac{c}{b}u_0 + \cdots + (e^{bt_s}-1)\frac{c}{b}u_{m_c-1} \\
&\quad +(e^{(m_c+1)bt_s}-e^{m_cbt_s})\frac{c}{b}u_{-1} + \cdots + (e^{mbt_s}-e^{(m-1)bt_s})\frac{c}{b}u_{-(m-m_c)}, \\
&\cdots\cdots \\
y(t_m) &= e^{mbt_s}v_b + (e^{mbt_s}-e^{(m-1)bt_s})\frac{c}{b}u_0 + \cdots + (e^{(m-m_c+1)bt_s}-1)\frac{c}{b}u_{m_c-1},
\end{aligned}
\tag{4.36}
$$

where $u_0, u_1, \cdots, u_{m_c-1}$ indicate current and future control actions at t_i, and $u_{-1}, u_{-2}, \cdots, u_{-(m-1)}$ indicate the control actions in the past $(m-1)$ sample instants.

By defining

$$h_i = (e^{ibt_s} - e^{(i-1)bt_s})\frac{c}{b}, \qquad i = 1, \cdots, m, \tag{4.37}$$

Equation (4.36) can be written concisely in the matrix form as:

$$\hat{\mathbf{y}} = \mathbf{v_b} + \mathbf{S_1 u} + \mathbf{S_2 u_{-1}}, \tag{4.38}$$

where $\hat{\mathbf{y}}$ and $\mathbf{u}$ are defined as in Equation (4.11), and

$$\mathbf{u_{-1}} = [u_{-1}, u_{-2}, \cdots, u_{-(m-1)}]^T, \tag{4.39}$$

$$\mathbf{v_b} = [e^{mbt_s} v_b, e^{mbt_s} v_b, \cdots, e^{mbt_s} v_b]^T, \tag{4.40}$$

$$\mathbf{S_1} = \begin{bmatrix} h_1 & 0 & \cdots & 0 & 0 \\ h_2 & h_1 & \cdots & 0 & 0 \\ & & & \ddots & \\ h_{m_c} & h_{m_c-1} & \cdots & h_2 & h_1 \\ \vdots & & & & \\ h_{m-1} & h_{m-2} & \cdots & h_{m-m_c+1} & \sum_{i=1}^{m-m_c} h_i \\ h_m & h_{m-1} & \cdots & h_{m-m_c+2} & \sum_{i=1}^{m-m_c+1} h_i \end{bmatrix}, \tag{4.41}$$

$$\mathbf{S_2} = \begin{bmatrix} h_2 & h_3 & \cdots & h_{m-1} & h_m \\ h_3 & h_4 & \cdots & h_m & 0 \\ \vdots & & & & \\ h_m & 0 & \cdots & 0 & 0 \\ 0 & 0 & \cdots & 0 & 0 \end{bmatrix}. \tag{4.42}$$

The CBMPC calculation in the last section was performed in terms of S and $\mathbf{y_0}$. Comparing Equation (4.38) and (4.14), it is easy to see that

$$\mathbf{S} = \mathbf{S_1}, \tag{4.43}$$

$$\mathbf{y_0} = \mathbf{v_b} + \mathbf{S_2 u_{-1}}. \tag{4.44}$$

In the CBMPC for linear PDE systems, a sequence of control actions are obtained explicitly, as in Equation (4.16). The input to be implemented is obtained by selecting the first element of the sequence. Hence, the control law developed for the linear PDE systems can be written as:

$$\begin{aligned} u_0 &= \mathbf{b^T u} \\ &= \mathbf{b^T}(\mathbf{S_1}^T\mathbf{S_1})^{-1}\mathbf{S_1}^T(\mathbf{y}^r - \mathbf{v_b} - \mathbf{S_2 u_{-1}}), \end{aligned} \tag{4.45}$$

where $\mathbf{b^T} = [1, 0, \cdots, 0]^T$. To prove the stability of this control law, the following lemma is needed, which can be found in the book by Jury (1964, p116).

Lemma 4.3.1 ***Monotonic Conditions*** *(Jury, 1964). The real polynomial*

$$P(x) = \alpha_n x^n + \alpha_{n-1}x^{n-1} + \cdots + \alpha_1 x + \alpha_0 \tag{4.46}$$

has roots outside the unit circle if $\alpha_0 > \alpha_1 > \cdots > \alpha_n > 0$.

Based on the formulation of the control law in Equation (4.45), the following theorem establishes the stability of the proposed CBMPC for linear PDE systems.

Theorem 4.3.1 *For control horizon* m_c *chosen sufficiently small, the control law in Equation (4.45) is stable for the linear PDE system (4.4).*

Proof:

The control law in Z-transform can be obtained by applying Z-transforms to Equation (4.45), which has the general form as:

$$D_c(z)u_0(z) = N_{cr}(z)y^r(z) - N_{cb}(z)v_b(z). \tag{4.47}$$

Stability of the scheme is determined by the roots of $D_c(z)$. By defining the backward shift operator $q = z^{-1}$, the equivalent stability condition requires that the characteristic polynomial:

$$C(q) = 1 + \mathbf{b^T}(\mathbf{S_1}^T\mathbf{S_1})^{-1}\mathbf{S_1}^T\mathbf{S_2}[q, q^2, \cdots, q^{m-1}]^T = 0 \tag{4.48}$$

has roots outside of the unit circle. We will establish the result by showing stability for $m_c = 1$.

From Equation (4.41) through (4.40), it can be obtained that:

$$\mathbf{S_1^T S_1} = h_1^2 + \left(\sum_{i=1}^{2} h_i\right)^2 + \cdots + \left(\sum_{i=1}^{m} h_i\right)^2 = \sum_{j=1}^{m}\left(\sum_{i=1}^{j} h_i\right)^2, \tag{4.49}$$

$$\begin{aligned}\mathbf{S_1}^T\mathbf{S_2}\,[q, q^2, \cdots, q^{m-1}]^T &= h_1(h_2 q + h_3 q^2 + \cdots + h_m q^{m-1}) \\ &+ \sum_{i=1}^{2} h_i(h_3 q + h_4 q^2 + \cdots + h_m q^{m-2}) + \cdots + \sum_{i=1}^{m-1} h_i(h_m q).\end{aligned} \tag{4.50}$$

Substituting the above two expressions to Equation (4.48) yields:

$$\begin{aligned}&\sum_{j=1}^{m}\left(\sum_{i=1}^{j} h_i\right)^2 + \left(\sum_{j=1}^{m-1}\sum_{i=1}^{j} h_i h_{j+1}\right) q + \cdots \\ &+ \left(\sum_{j=1}^{m-k}\sum_{i=1}^{j} h_i h_{j+k}\right) q^k + \cdots + h_1 h_m q^{m-1} = 0.\end{aligned} \tag{4.51}$$

Starting with the last coefficient $(h_1 h_m)$, one can verify that all the terms in each coefficient are included in the next. From the definition of h_i in Equation (4.37), it is clear that h_i, $i = 1, \cdots, m$, have the same sign. Consequently, the monotonic condition of Lemma 4.3.1 are satisfied. Therefore, the roots of the characteristic polynomial lie all outside of the unit circle. This proves the stability of the CBMPC for linear PDE sytems. ■

4.3.2 Quasilinear Systems

Unlike that for linear PDE systems, the CBMPC for quasilinear PDE systems does not have the closed form of control laws. Hence, it is not possible to analyze its stability

based on the closed-loop transfer functions. In fact, stability of nonlinear MPC has been an issue. Some modifications such as terminal constraint or terminal cost are usually added to ensure the closed-loop stability. In this subsection, stability of the quasilinear systems will be considered by adding a terminal constraint and examining the objective functions.

Consider the first-order quasilinear hyperbolic system described by Equation (4.21). Assume that the system has constant boundary condition at $x = 0$ (*i.e.*, $v(x = 0) =$ const.), and $x \in [0, 1]$. In the design of the characteristic-based MPC, the infinite dimensional state variable v is discretized at spatial points $x_1, x_2, ..., x_m$. The output for the next p sample instants is obtained by integrating characteristic ODEs with initial values $v(x_m), ..., v(x_2), v(x_1)$ and boundary value v_b (see Figure 4.4).

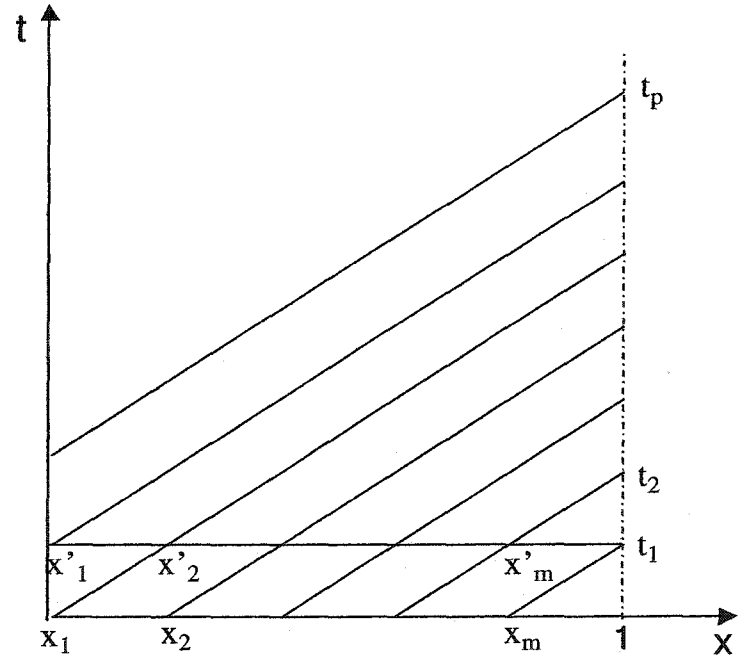

Figure 4.4: Output prediction along characteristic curves for scalar PDEs

The design parameters of the CBMPC are chosen such that $p \geq m + m_c - 1$, where p is the prediction horizon, m_c is the control horizon and m is the number of the discretization points. The control action in the first m_c sample instants are free variables

and the remaining $p - m_c$ variables are specified as $u_{m_c-1} = u_{m_c} = ... = u_{p-1}$, or $\Delta u_{m_c} = \Delta u_{m_c+1} = ... = \Delta u_{p-1} = 0$. The selection $p \geq m + m_c - 1$ ensures that the effect of chosen control actions is included in the prediction horizon.

Based on the current state variable profile v, the CBMPC can be designed to minimize a performance objective function. For simplicity of discussion, the objective function takes the form as:

$$\begin{aligned} J^0(v) &= \min_{\Delta u} J(v,u) \\ &= \min_{\Delta u} \sum_{i=1}^{p} \left[y^r - y(t_i, v, u)\right]^2, \end{aligned} \tag{4.52}$$

with no penalty on the control increments. But the discussion below applies to the case with small cost parameters for control increments, as well. Defining

$$l(t_i, v, u) = \left[y^r - y(t_i, v, u)\right]^2, \tag{4.53}$$

Equation (4.52) can be written as:

$$J^0(v) = \min_{\Delta u} \sum_{i=1}^{p} l(t_i, v, u). \tag{4.54}$$

One way of ensuring stability for finite horizon MPC is to add a 'terminal constraint' which forces the states or output to a particular value or a set at the end of the prediction horizon. In this subsection, the following terminal constraint is used to ensure the stability of the CBMPC for quasilinear systems:

$$l(t_p, v, u) \leq \min\left\{l(t_1, v, u_1), l(t_2, v, u_2), ..., l(t_{p-1}, v, u_{p-1})\right\}. \tag{4.55}$$

This constraint requires that the terminal cost term be the smallest among the cost terms within prediction horizon. With this constraint, if a control sequence $(u_0, u_1, \cdots, u_{m_c-1})$ satisfies Equation (4.55), it is also satisfied by the control sequence $(u_1, u_2, \cdots, u_{m_c-1}, u_{m_c-1})$ at the next sample instant. This property will be seen from the output prediction expression in the proof of the following theorem and is important for the guaranteed closed-loop stability of the CBMPC.

Theorem 4.3.2 *The CBMPC that satisfies (4.52) subject to (4.21) and (4.55) is stabilizing if the process in Equation (4.21) is controllable at $y = y^r$.*

Proof:

Suppose that the control problem of minimizing the cost function (4.52) subject to (4.21) and the constraint (4.55) is solved from the current state variable value $v(x_1), v(x_2), ..., v(x_m)$, yielding the optimal control sequence:

$$\mathbf{u}^0(v) = \left\{u_0^0(v), u_1^0(v), ..., u_{m_c-1}^0(v)\right\}, \tag{4.56}$$

where the superscript ^{0} indicate the optimal value. Under this optimal control sequence, the optimal objective function and the optimal output trajectory can be obtained as:

$$J^0(v) = J(v, \mathbf{u}^0(v)), \tag{4.57}$$

$$\mathbf{y}^0(v) = \left\{y_0^0(v), y_1^0(v), ..., y_p^0(v)\right\}. \tag{4.58}$$

Using the mathematical description in Equation (4.29) of the last section, the output trajectory under the optimal control sequence can be written as:

$$\begin{aligned}
&y^0(t_1, v) = \phi_v(v_{x_m}, u_0^0),\\
&y^0(t_2, v) = \phi_v(v_{x_{m-1}}, u_0^0, u_1^0),\\
&\qquad \cdots\cdots\\
&y^0(t_{m_c}, v) = \phi_v(v_{x_{m-m_c+1}}, u_0^0, u_1^0, ..., u_{m_c-1}^0),\\
&\qquad \cdots\cdots\\
&y^0(t_m, v) = \phi_v(v_b, u_0^0, u_1^0, ..., u_{m_c-1}^0),\\
&y^0(t_{m+1}, v) = \phi_v(v_b, u_1^0, ..., u_{m_c-1}^0),\\
&\qquad \cdots\cdots\\
&y^0(t_{m+m_c-1}, v) = \phi_v(v_b, u_{m_c-1}^0),\\
&y^0(t_p, v) = \phi_v(v_b, u_{m_c-1}^0).
\end{aligned} \tag{4.59}$$

Note that the predicted output at $t \geq t_{m+m_c-1}$ is a function of only $u_{m_c-1}^0$ for constant v_b.

Implementing the first control move u_0^0 of the optimal control sequence from t_0 through t_1, we get the output $y(t_1) = y^0(t_1, v)$, and a new state variable profile v' at spatial points x_i', $i = 1, \cdots, m$ at t_1. Then the problem of minimizing the cost function subject to the constraints is solved at t_1 from the new state variable values at discrete spatial points: $v'(x_1'), v'(x_2'), ..., v'(x_m')$. Define a control sequence $\tilde{\mathbf{u}}$ at t_1 based on the optimal control sequence obtained at t_0 as:

$$\tilde{\mathbf{u}} = \left\{u_1^0, u_2^0, \cdots, u_{m_c-2}^0, u_{m_c-1}^0, u_{m_c-1}^0\right\}. \tag{4.60}$$

Then the output trajectory using $\tilde{\mathbf{u}}$ at t_1 can be obtained

$$\mathbf{y}(v', \tilde{\mathbf{u}}) = \{y^0(t_2, v), ..., y^0(t_p, v), y^0(t_{p+1}, v)\}. \tag{4.61}$$

From Equation (4.59), it is easy to see that $y^0(t_{p+1}, v) = y^0(t_p, v)$. Then $\tilde{\mathbf{u}}$ satisfies the process model (4.21) and the constraint (4.55) at t_1. Therefore, the optimal value of the objective function at t_1 is not greater than the objective function using $\tilde{\mathbf{u}}$. The following inequality holds:

$$J^0(v') \leq J(v', \tilde{\mathbf{u}}). \tag{4.62}$$

Since

$$\begin{aligned} J(v', \tilde{\mathbf{u}}) &= \sum_{i=2}^{p} [y^r - y^0(t_i, v)]^2 + [y^r - y^0(t_p, v)]^2 \\ &= J^0(v) - l^0(t_1, v)) + l^0(t_p, v), \end{aligned} \tag{4.63}$$

and $l^0(t_p, v) \leq l^0(t_1, v))$ (due to the terminal constraint at t_0), the optimal objective function value at two consecutive sample instants satisfy:

$$J^0(v') \leq J^0(v). \tag{4.64}$$

Therefore, the cost function J^0 is non-increasing, which implies that the cost function J^0 converges to zero or a positive value.

When $J^0(v)$ converges to a steady state positive value, $J^0(v') = J^0(v)$ and $l^0(t_1, v)) = l^0(t_2, v)) = \cdots = l^0(t_p, v)) \neq 0$. Therefore, the output converges to a steady state value $y_s^0 \neq y^r$, and the optimal control sequence satisfies $u_{s0}^0 = u_{s1}^0 = \cdots = u_{sp}^0 = u_s^0$. Since

the process is controllable at $y = y^r$, there exists a control action u^0 such that $y = y^r$ at the steady state. The objective function value using u^0 is less than that using u_s^0. This conflict with that u_s^0 is the optimal control action. Therefore, $J^0(v)$ converges to zero, not a positive number. $J^0(v)$ is a Lyapunove function and the output converges to the setpoint y^r. This proves that the developed CBMPC is stabilizing. ■

4.4 Implementation Issue

As discussed in Section 4.2, the CBMPC provides an explicit formula of offline control law for linear systems. For quasilinear systems, however, calculation of the control actions in CBMPC requires to solve an optimization problem involving nonlinear integral equations at each sample instant. The corresponding computational requirement may be demanding and make the resulting control hard to implement. There are a variety of nonlinear MPC algorithms available which can be used to simplify the calculation of the control action based on the nonlinear output prediction. In this section, a nonlinear quadratic MPC algorithm is used by assuming a locally linearized expression for output and input:

$$\hat{\mathbf{y}} = \hat{\mathbf{y}}_0 + \mathbf{S}\Delta\mathbf{u}, \tag{4.65}$$

where: $\hat{\mathbf{y}}_0$ is the vector of predicted outputs due to the past control actions in the prediction horizon time, $\Delta\mathbf{u}$ is the vector of future control increments in the next m_c sample instants, $\hat{\mathbf{y}}$ is the vector of the predicted outputs for the control increments $\Delta\mathbf{u}$ in the prediction horizon time, and $\mathbf{S}$ is the rate of output variation about the past control actions.

As discussed in the last section, the analytical expression for output prediction in the form of Equation (4.65) can be obtained for linear PDE systems. There may exist different nonlinear MPC algorithms that can be used in the proposed CBMPC for quasilinear PDE systems. In this thesis, the similar algorithm to linear PDE systems is used for quasilinear systems because of its simplicity and convenience.

Due to the nonlinearity of the system, Equation (4.65) needs to be updated at each sample instants for prediction accuracy. In this expression, $\hat{\mathbf{y}}_0$ and $\mathbf{S}$ have to be calculated numerically using the described output prediction approach. The calculation of $\hat{\mathbf{y}}_0$ can be carried out numerically by integrating the characteristic ODEs using the current state variable values as initial conditions and the past control action u_{-1}. The elements of $\mathbf{S}$ can be computed via perturbation

$$\mathbf{S} = \left(\frac{\partial \hat{\mathbf{y}}}{\partial \mathbf{u}}\right)_0 = \frac{\hat{\mathbf{y}}|_{\mathbf{u}_{-1}+\delta} - \hat{\mathbf{y}}|_{\mathbf{u}_{-1}}}{\delta}, \tag{4.66}$$

where δ is the numerical perturbation on past input $\mathbf{u}_{-1}$, $\hat{\mathbf{y}}|_{\mathbf{u}_{-1}+\delta}$ and $\hat{\mathbf{y}}|_{\mathbf{u}_{-1}}$ are the predicted future output under the control actions $\mathbf{u}_{-1}+\delta$ and $\mathbf{u}_{-1}$.

Equation (4.65) is an approximate expression for the output. The prediction error of this equation decreases to zero as the output moves towards setpoint and the required control increment $\Delta\mathbf{u}$ vanishes gradually. With the linearized expression for the output, the control action can be designed to minimize the objective function:

$$\mathbf{J} = (\mathbf{y}^r - \hat{\mathbf{y}})^T \mathbf{Q} (\mathbf{y}^r - \hat{\mathbf{y}}) + \Delta\mathbf{u}^T \mathbf{R} \Delta\mathbf{u}, \tag{4.67}$$

where $\mathbf{y}^r$ is the desired output trajectory in future time, and, $\mathbf{Q}$ and $\mathbf{R}$ are two positive definite weighting matrices. The control action minimizing the above objective function subject to the linearized prediction equation (4.65) can be obtained:

$$\Delta\mathbf{u} = (\mathbf{S}^T\mathbf{Q}^T\mathbf{Q}\mathbf{S} + \mathbf{R}^T\mathbf{R})^{-1}\mathbf{S}^T\mathbf{Q}^T\mathbf{Q}(\mathbf{y}^r - \hat{\mathbf{y}}_0). \tag{4.68}$$

Then, the first element of Δu is implemented at the next sample instant.

In the control law described by Equation (4.68), online computation is required to update $\mathbf{S}$ and $\hat{\mathbf{y}}_0$ at every sample instant. The prediction horizon p and m_c affect the dimensions of $\mathbf{S}$ and $\hat{\mathbf{y}}_0$, and therefore, can significantly affect the online computational demand of the proposed CBMPC. As discussed above, it is reasonable to choose a prediction horizon time equal to the residence time (*i.e.*, $p = m$). The control horizon can be chosen to be a small number to reduce the dimension of $\mathbf{S}$ and $\hat{\mathbf{y}}_0$, and also in favor of stable and smooth operation (Brosilow and Joseph, 2002). If $m_c = 1$, $p = m$

and SISO control is used, the control action in Equation (4.68) can be calculated via the following procedure:

Step I Get the current value of the state variable at m spatial points based on the measurement.

Step II Using the past control action u_{-1}, calculate the future output $\hat{\mathbf{y}}_0$ in the next m sample time instants by integrating the characteristic ODEs via using Equation (4.23) through (4.25), or Equation (4.32) for the semilinear case.

Step III Using the control action $u_{-1} + \delta$, calculate the future output $\hat{\mathbf{y}}|_{u_{-1}+\delta}$in the next m sample time.

Step IV Calculate S using Equation (4.66).

Step V Substitute the obtained S and $\hat{\mathbf{y}}_0$ into Equation (4.68) to get the required control action.

These steps are repeated at every sample instant to update the control action based on new measurement. It also applies to MIMO control or the case with larger control horizon and prediction horizon.

The proposed CBMPC can produce improved performance with efficient online computation. Unlike other numerical methods, the discretization of the state variable in this CBMPC does not sacrifice prediction accuracy, but only affects the prediction sampling time. Therefore, high prediction accuracy can be obtained with small dimension of calculation, which, along with the decoupled nature in the output prediction, makes the control method computationally efficient. High performance of the CBMPC comes from the high prediction accuracy of this method.

4.5 Examples

In this section, the proposed CBMPC algorithm for hyperbolic PDE systems with a single characteristic is evaluated by performing simulations on two systems: a heat exchanger

and a Plug-Flow Reactor (PFR) with uniform heating. The CBMPC development for linear and quasilinear systems are illustrated using the two examples.

4.5.1 Heat Exchanger

The heat exchanger discussed in Section 3.3.1 is also considered in this section. The system is modelled as:

$$\begin{aligned} &\frac{\partial T}{\partial t} + u\frac{\partial T}{\partial x} + H(T - T_j) = 0, \\ &y = T(x = 1). \end{aligned} \tag{4.69}$$

Integrating the characteristic ODEs of this system yields the following analytical expression for the characteristic curves:

$$\begin{aligned} t &= t_0 + \Delta t, \\ x &= x_0 + u\Delta t, \\ T &= (T_0 - T_j)e^{-H\Delta t} + T_j. \end{aligned} \tag{4.70}$$

The solution T can then be obtained from the above expression as:

$$T(t_0 + \Delta t, x) = (T(t_0, x - u\Delta t) - T_j)e^{-H\Delta t} + T_j. \tag{4.71}$$

From this equation, it can be seen that the outlet temperature (at $x = 1$) in the future sample instants $t_0 + \Delta t$ can be predicted from the current value of temperature at $x_0 = 1 - u\Delta t$. If the current temperature is uniformly discretized into m points $x_{0i} = 1 - \frac{i}{m}$, $i = 1, ..., m$, in the spatial range $[0, 1]$, the outlet temperature can be predicted at the sample instants $\Delta t_i = \frac{i}{mu}$, $i = 1, ..., m$.

Let $\Delta t = t - t_0$ and $\Delta x = x - x_0$. From Equation (4.71), the solution of the PDE can be written as:

$$T(t_0 + \Delta t, x) = (T(t_0, x - u\Delta t) - T_j)e^{-H\Delta x/u} + T_j. \tag{4.72}$$

For the CBMPC design of the system, the control horizon is chosen to be $m_c = 1$, the prediction horizon is equal to the number of discretization points (*i.e.*, $p = m$) with a

sampling time: $t_s = \Delta t = \dfrac{1}{mu}$. From Equation (4.72), the future output for the next m sample instants can be predicted as:

$$\begin{aligned} \hat{T}(t_0 + \Delta t_i, 1) &= (T(t_0, x_i) - T_j)e^{-H(1-x_i)/u} + T_j, \\ & \qquad i = 1, 2, \cdots, m. \end{aligned} \tag{4.73}$$

Note that the manipulated variable u appears in the exponential term. In order to develop a controller that has an analytical formula, it is convenient to design a cost function as:

$$\mathbf{J} = \sum_{i=1}^{m} \log^2 \left| \frac{\hat{T}(t_0 + \Delta t_i, 1) - T_j}{T_{sp} - T_j} \right|. \tag{4.74}$$

This cost function provides a convenient approach for an analytical offline control formulation. Denote vectors as:

$$\begin{aligned} \hat{\mathbf{T}} &= \left[\hat{T}(t_0 + \Delta t_1, 1), ..., \hat{T}(t_0 + \Delta t_m, 1)\right]^T, \\ \mathbf{T}_0 &= \left[T(t_0, x_1), ..., T(t_0, x_m)\right]^T, \\ \mathbf{\Delta x} &= \left[1 - x_1, 1 - x_2, ..., 1 - x_m\right], \\ \mathbf{T}_j &= \left[T_j, T_j, \cdots, T_j\right], \\ \mathbf{T}_{sp} &= \left[T_{sp}, T_{sp}, \cdots, T_{sp}\right]. \end{aligned} \tag{4.75}$$

Then the solution of minimizing the objective function in Equation (4.74) is given by:

$$u = \frac{[\log(\mathbf{T}_0 - \mathbf{T}_j) - \log(\mathbf{T}_{sp} - \mathbf{T}_j)]^T H \mathbf{\Delta x}}{[\log(\mathbf{T}_0 - \mathbf{T}_j) - \log(\mathbf{T}_{sp} - \mathbf{T}_j)]^T [\log(\mathbf{T}_0 - \mathbf{T}_j) - \log(\mathbf{T}_{sp} - \mathbf{T}_j)]}. \tag{4.76}$$

This formulation of u provides an analytical off-line control law for the heat-exchanger and does not involve complicated computation.

A simulation was performed to evaluate the performance of the controller in Equation (4.76). The parameters used for simulation were: $H = 1, T_j = 10$. The initial temperature profile was chosen as $T(0, x) = 2x$ and the boundary condition as $T(t, 0) = 0$. For the simulation purpose, the finite difference method was used to derive a finite-dimensional approximation of the original PDE equation, with 100 discretization points.

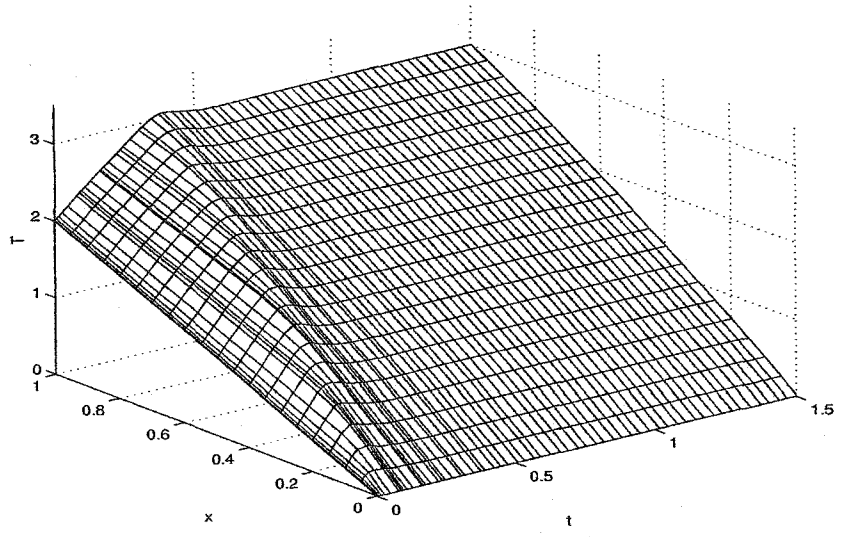

Figure 4.5: Output tracking performance of the heat exchanger using CBMPC

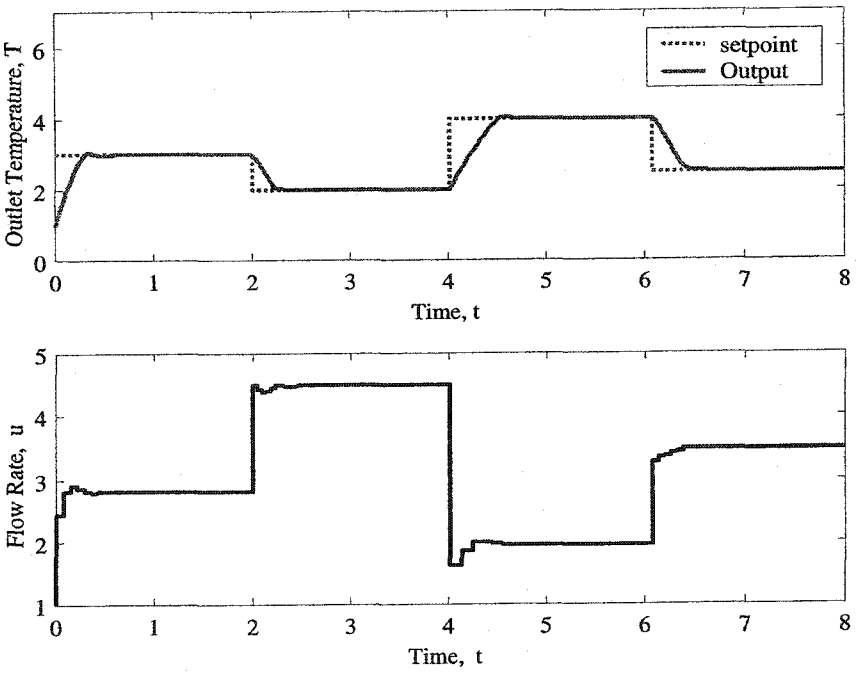

Figure 4.6: Setpoint tracking response of CBMPC in the heat exchanger

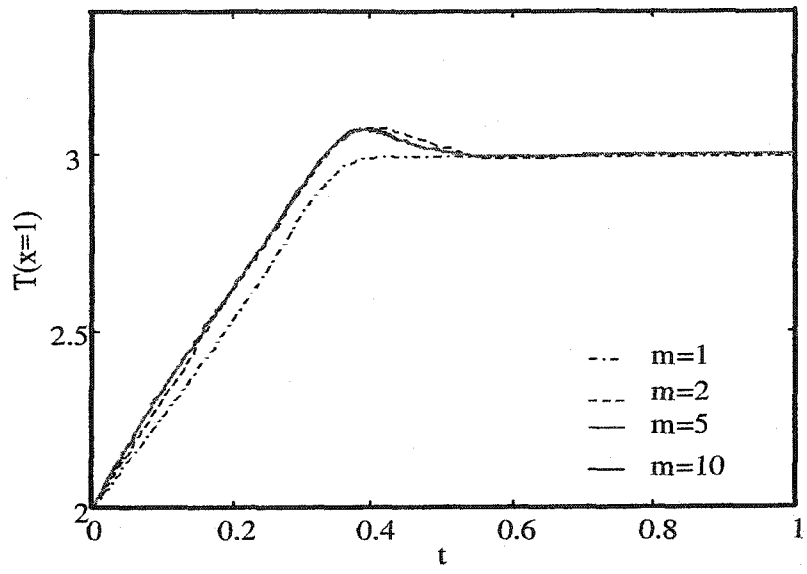

Figure 4.7: Output response of CBMPC for different discretizations in the heat-exchanger

Table 4.1: Computations for different discretizations: heat-exchanger problem

discretization m	1	2	5	10	20
flops	29	65	167	337	677

Figure 4.5 shows the temperature profile of the heat exchanger subject to the proposed predictive control law. The outlet temperature setpoint is specified as: $T_{sp}(x = 1) = 3$, and the discretization number $m = 5$. It can be seen that temperature profile converges to the setpoint smoothly and quickly with reasonable control action. A filter was applied to the setpoint to prevent aggressive control action. This is achieved by substituting the expression $\alpha T_{sp} + (1-\alpha)T(1,t)$ for T_{sp} in Equation (4.76). Figure 4.6 shows the tracking performance of the controller with the filtered setpoint for a value of $\alpha = 0.9$.

In CBMPC, the discretization of the state variables corresponds to the number of the future sample instants. Since the prediction horizon is designed to be fixed by the residence time of the heat exchanger, the discretization only affects the required number of

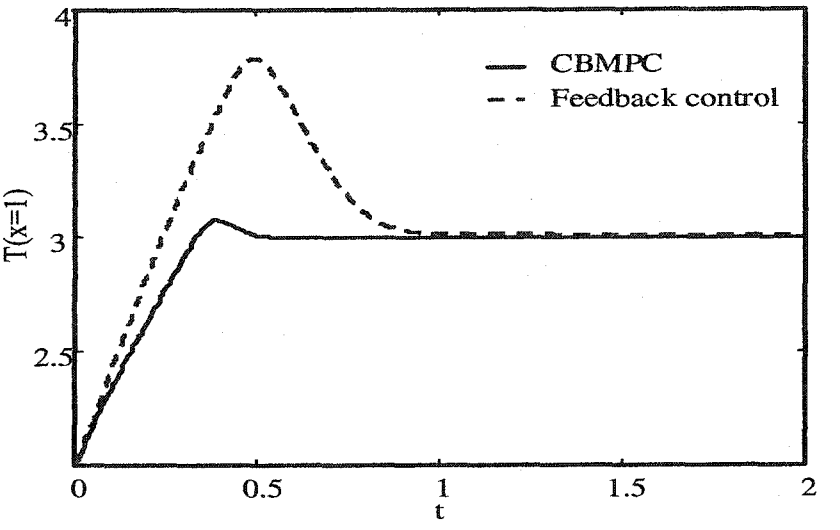

Figure 4.8: Performance comparison of CBMPC *vs.* standard feedback control

sampling intervals. It is of interest to consider the effect of the increase in computational requirements on the tracking performance. Figure 4.7 shows the tracking performance that results from different discretizations ($m = 1, 2, 5$ and 10). In each case, the output converges to a neighborhood of the setpoint. This simulation suggests that the choice of discretization has a small effect on the ability of the controller to reach the setpoint. In fact, only a very coarse discretization of the domain would be required in the present case. This property is quite advantageous in light of the corresponding change in computational requirements, shown in Table 4.1.

The performance of the predictive controller in Equation (4.76) is compared with the feedback control in Equation (3.58) developed in Chapter 3, with $m = 5$. From Figure 4.8, it is noted that the characteristic-based MPC produces quick convergence to the setpoint with small overshoot. The improved performance of the CBMPC results from that it overcomes the inherent shortsightedness of the feedback control. In this specific process, the CBMPC is obtained without additional demanding computational requirement since the CBMPC controller in Equation (4.76) only requires simple algebraic calculation.

In an attempt to test the response of the proposed controller to disturbances, the

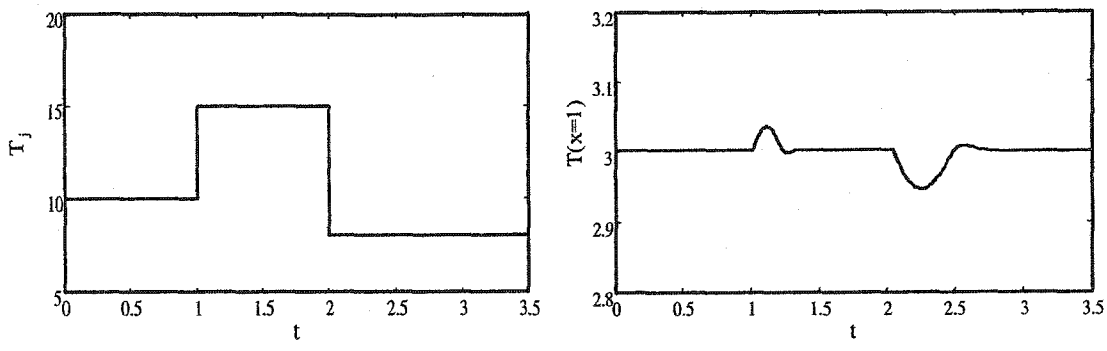

(a) Jacket Temperature Change

(b) Exit Temperature

Figure 4.9: Process response to T_j changes in the heat exchanger under CBMPC

effect of the disturbances in the jacket temperature on the tracking performance was investigated. Figure 4.9 shows the result of a change of T_j from 10 to 15 at time $t = 1$ and from 15 to 8 at time $t = 2$. It is noted that the proposed controller rejects the disturbances in jacket temperature effectively. The CBMPC provides a desirable response to the disturbances in process operating conditions.

The results indicate that the CBMPC yields simple controller formulation for flow rate without approximation. It provides a computationally efficient methodology for MPC of distributed parameter systems.

4.5.2 Plug-flow Reactor

As a second example, the control of a plug-flow reactor with uniform jacket temperature is considered. The output feedback controller in Chapter 3 is also considered to provide

a comparative basis for the CBMPC. This process can be modelled as:

$$\begin{aligned}
\frac{\partial C_A}{\partial t} &= -v_l \frac{\partial C_A}{\partial x} - k_{10} e^{-E_1/RT_r} C_A, \\
\frac{\partial C_B}{\partial t} &= -v_l \frac{\partial C_B}{\partial x} + k_{10} e^{-E_1/RT_r} C_A - k_{20} e^{-E_2/RT_r} C_B, \\
\frac{\partial T_r}{\partial t} &= -v_l \frac{\partial T_r}{\partial x} + \frac{(-\Delta H_{r_1})}{\rho_m c_{pm}} k_{10} e^{-E_1/RT_r} C_A + \\
&\quad \frac{(-\Delta H_{r_2})}{\rho_m c_{pm}} k_{20} e^{-E_2/RT_r} C_B + \frac{U_w}{\rho_m c_{pm} V_r} (T_j - T_r),
\end{aligned} \tag{4.77}$$

subject to the boundary conditions:

$$C_A(0,t) = C_{A0}, \quad C_B(0,t) = 0, \quad T_r(0,t) = T_{r0}. \tag{4.78}$$

The nonlinear PDE (4.77) provides a significant challenge for MPC applications. In this subsection, the effectiveness of the CBMPC technique is demonstrated. An emphasis is put on computational requirements in order to demonstrate, in particular, that CBMPC is a viable alternative for some nonlinear PDE models.

The vector field $\xi_1 = \dfrac{\partial}{\partial t} + v_l \dfrac{\partial}{\partial x}$ is the characteristic vector field of the system. Following the Method of Characteristics, the system in Equation (4.77) can be described by a set of ODEs:

$$\begin{aligned}
\dot{t} &= 1, \\
\dot{x} &= v_l, \\
\dot{C}_A &= -k_{10} e^{-E_1/RT_r} C_A, \\
\dot{C}_B &= k_{10} e^{-E_1/RT_r} C_A - k_{20} e^{-E_2/RT_r} C_B, \\
\dot{T}_r &= -v_l \frac{\partial T_r}{\partial x} + \frac{(-\Delta H_{r_1})}{\rho_m c_{pm}} k_{10} e^{-E_1/RT_r} C_A + \\
&\quad \frac{(-\Delta H_{r_2})}{\rho_m c_{pm}} k_{20} e^{-E_2/RT_r} C_B + \frac{U_w}{\rho_m c_{pm} V_r} (T_j - T_r).
\end{aligned} \tag{4.79}$$

Prediction of the future output is obtained by numerical integration of the characteristic ODE (4.79) for a finite number of discrete points, as described in Equation (4.31) and

(4.32) in the last section. The infinite dimensional process variables at the current time are discretized into m spatially uniform points in the x-space. It is assumed that the temperature of the reactor can be measured at these m points x_i, $i = 1, ..., m$, along the reactor. The concentrations C_A and C_B at these points can be estimated from the inlet concentration value and temperature measurements. The control action is calculated to minimize the objective function:

$$J = \sum_{i=1}^{m} [C_B^r - C_B(t_0 + \Delta t_i, x = 1)]^2, \tag{4.80}$$

where C_B^r is the setpoint of the outlet concentration C_B, $\Delta t_i = \dfrac{1 - x_i}{v_l}$, and $C_B(t_0 + \Delta t_i, x = 1)$ are the predicted output in the next m time instants.

For simulation, the constants in Equation (4.77) are those listed in Table 3.1. The simulation is carried out by discretizing the PDE along the space into 500 points. The control horizon m_c is set to 1. The prediction horizon is taken to be equal to the residence time with sampling time being $1/(mv_l)$. In most cases, $m = 5$ is used.

At initial state, the jacket temperature of the reactor is $T_j = 359.5K$, and a steady state profile similar to the profiles shown in Figure 3.9 is used. Figure 4.10 illustrates the simulation of the response of the state variables to an output setpoint change from $C_B(x = 1) = 0.8$ mol/l to $C_B(x = 1) = 1$ mol/l. The simulation results indicate that the CBMPC provides good tracking performance.

The effect of the prediction horizon was investigated. For a prediction horizon that is less than the residence time, the closed-loop response is oscillatory and aggressive. Increasing the prediction horizon beyond the residence time does not improve the process response significantly. For a control horizon that is greater than 1, a penalty on the control action can be added in the performance function to improve the smoothness of the response. In general, the following objective function is considered:

$$J = \sum_{i=1}^{m} [C_B^r - C_B(t_0 + \Delta t_i, x = 1)]^2 + \sum_{i=1}^{m_c} \lambda (\Delta T_j)_i^2. \tag{4.81}$$

where λ is a tuning parameter. Figure 4.10 discussed previously shows the simulation results for a value of 0.8.

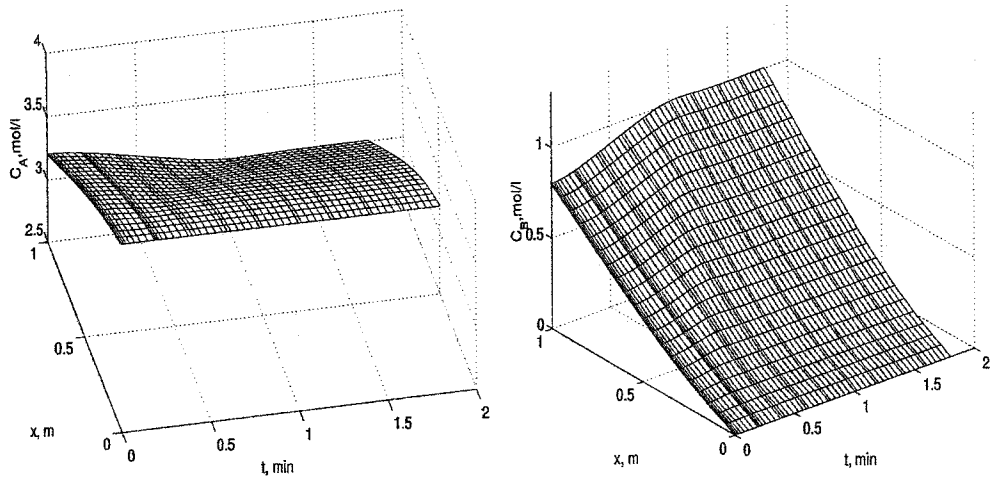

(a) C_A (b) C_B

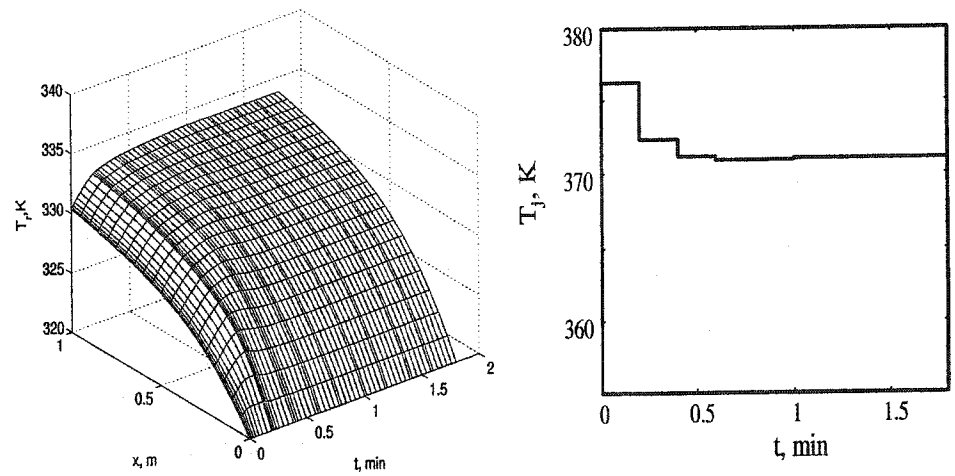

(c) T_r (d) T_j

Figure 4.10: Simulation results of the PFR using CBMPC for a setpoint change from $C_B(x=1) = 0.8$ to $C_B(x=1) = 1$

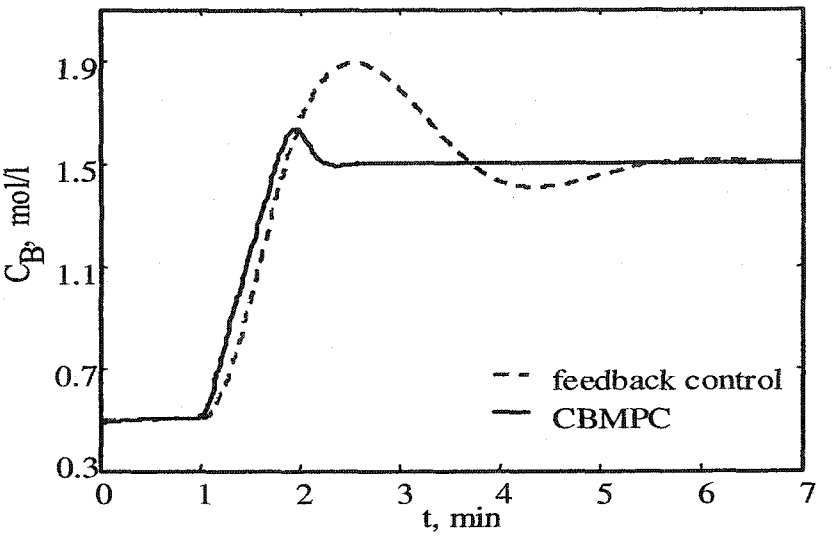

Figure 4.11: Performance comparison of the CBMPC and the state feedback control in PFR

Figure 4.11 provides a comparison of the proposed CBMPC and the state feedback controller developed in Chapter 3. The simulation results indicate that the CBMPC provides satisfactory tracking performance without undesirable overshoot and oscillation as displayed by the feedback control. The improved performance of the CBMPC over the state feedback control results from taking the long-term effect of current control action into control development and overcoming the shortsightedness of the feedback control.

The performance of the CBMPC to the disturbances in operating condition changes was also studied. Figure 4.12 shows the results of a change of v_l from 1 m/min to 1.2 m/min and 1.2 m/min to 0.9 m/min. It can be observed that the CBMPC responds adequately to the disturbances in operating variables. In a second simulation exercise, the process response to the boundary condition changes under the CBMPC was examined. The results of a change of the boundary condition $T_r(x = 0)$ from 320 K to 340 K and 340 K to 300 K is shown in Figure 4.13. It can be seen that the CBMPC also responds satisfactorily to the boundary condition changes, steering the process output to the setpoint.

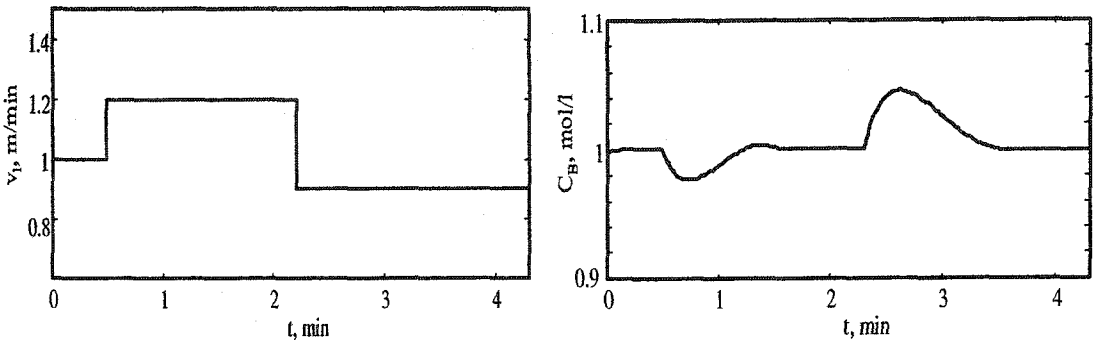

(a) operation variable changes (b) output

Figure 4.12: Output response to operation variable changes under CBMPC in PFR

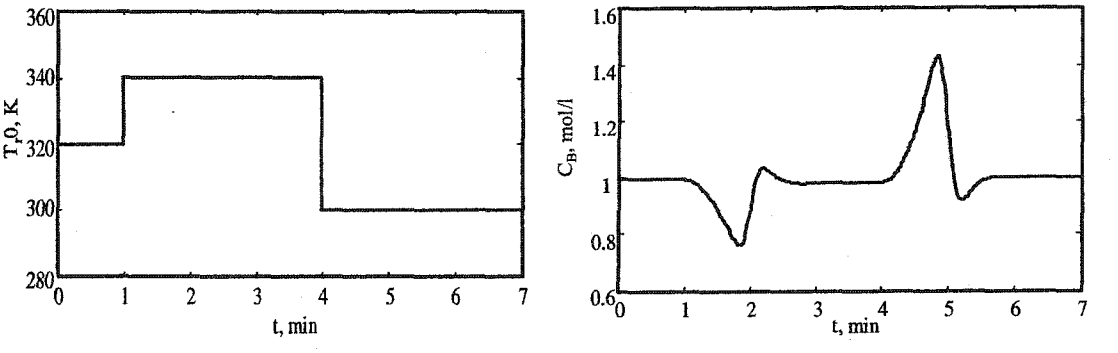

(a) boundary condition changes (b) output

Figure 4.13: Output response to boundary condition changes under CBMPC in PFR

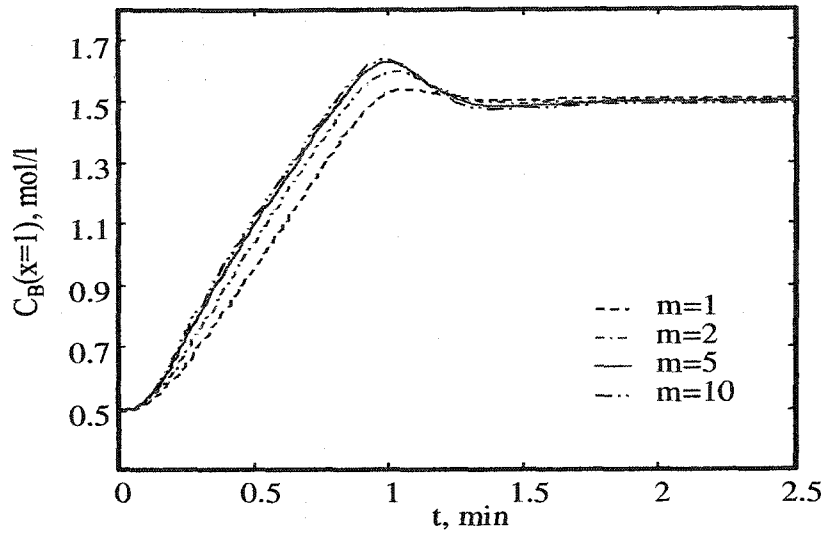

Figure 4.14: Output response of CBMPC using different discretizations in PFR

Table 4.2: Computations for different discretizations: PFR problem

control method	flops (Matlab ©)
CBMPC ($m = 1$)	1.4870×10^4
CBMPC ($m = 2$)	2.3024×10^4
CBMPC ($m = 5$)	4.7200×10^4
CBMPC ($m = 10$)	8.8412×10^4
CBMPC ($m = 20$)	1.7021×10^5

As in previous example, the effect of the number of discretization points was investigated. From Figure 4.14, it can be seen that the effect of discretization on the process output response is minor. The process displays an acceptable output response even when a small number of discretization points are used. A larger number of discretizations tends to produce a more aggressive control action when there is no penalty on the input moves. This results from including the effect of the more immediate process output in the control calculations using a larger number of discretizations. A compilation of the computational requirements for different numbers of discretization points is shown in Table 4.2. As expected, the computational demand increases proportionally with the number of discretization points. Therefore, the full advantage of the CBMPC can be realized by using a small number of discretization points. To emphasize this point, a traditional MPC algorithm was applied to control the PFR model. The model used for the traditional MPC was generated by discretizing the PDE model to a higher order ODE approximation. Since a large number of ODEs are normally required to generate a good approximate model, this approach significantly increase the computational demand. It is not clear whether this approach provides a good controller. To investigate this, simulations were performed using each approach and a performance metric, the ISM, was computed. The ISM is the integral of the square of the error given by:

$$\text{ISM} = \int_0^{t_{\text{ISM}}} [C_B^r - C_B(\tau, x = 1)]^2 d\tau \tag{4.82}$$

In each case, the control action was computed by minimizing the objective function (4.80). The computation of the control action by discretization was conducted by discretizing the PDE model into 50 points. The time interval for the integration of Equation (4.82) was $[0, 2.2]$ min. The ISM values are listed in Table 4.3. Results indicate that the proposed CBMPC is advantageous due to its computational efficiency, high accuracy and relatively simple requirement of state estimation.

Table 4.3: Computations of CBMPC *vs.* conventional MPC in PFR

	MPC using Characteristics	Traditional MPC
flops (Matlab ©)	4.73×10^4	4.7×10^7
ISM	0.098	0.103
State Estimation	5 points	50 points

4.6 Summary

Distributed parameter systems modelled by PDEs which admit Cauchy characteristics can be fully characterized by the corresponding characteristic ODEs. This property of the PDE model was used in Chapter 3 to develop a characteristic-based feedback control method. In this chapter, the Method of Characteristics was used to develop the MPC for the hyperbolic systems, which overcomes the inherent limitations of the feedback control by including the prediction horizon in the control formulation. The proposed CBMPC provides a control approach suitable for the dynamics of DPS, and it fully exploits the information provided by the Method of Characteristics.

This chapter has focused on the CBMPC development for systems modelled by linear or quasilinear PDEs with single characteristics. For linear PDE models, the application of the Method of Characteristics can lead to an analytical expression for output prediction, which can be used to develop the off-line MPC formulation. The resulting control law does not require more complicated computation than standard feedback control, but provides high performance as a MPC approach. The complexity of the CBMPC for quasilinear PDE systems increases significantly in comparison to the linear PDE systems. In quasilinear systems, the output prediction is obtained by integrating numerically the nonlinear characteristic ODEs, and the control action is calculated using standard nonlinear MPC schemes. In spite of the relative complexity of quasilinear systems, the

characteristic ODEs of the quasilinear systems discussed in this chapter are decoupled for different characteristic curves. This decoupled nature reduces the need for high order discretizations of the current state variable profiles in spatial domain in order to obtain the prediction accuracy. Thus, the good performance of the CBMPC reported in this chapter can be realized without the need for demanding computational requirements..

Similar to most MPC schemes, the proposed CBMPC can only guarantee closed-loop stability when a series of restrictive assumptions are made. A stabilizing modification of the CBMPC is proposed using a terminal constraint in the CBMPC.

Overall, the proposed MPC scheme for hyperbolic systems with single characteristics provides reasonable tracking performance, comparatively simple on-line computation, easy requirement of state estimation, and robustness to disturbances. The proposed CBMPC provides a promising control method in implemention into industrial practice. The success of the CBMPC for systems with single characteristics motivates the research on the CBMPC for more complex systems of multiple characteristics, which is the subject of the next chapter.

Chapter 5

CBMPC for Hyperbolic Systems-Multiple Characteristics

The last two chapters were devoted to the problem of designing controllers for systems modelled by scalar first-order PDEs or some systems of first-order PDEs with single characteristics. For many problems encountered in practice, more than one dependent variables are required to model the physical systems. In such cases, the integral manifold of the PDEs cannot be presented by the solution of unique characteristics (*e.g.*, a counter-flow heat exchanger, a plug-flow reactor with counter flow heating jacket, a counter flow gas absorber and one-dimensional flow of ideal gas, *etc*). The main objective of this chapter is to develop characteristic-based MPC to more complex systems having multiple characteristics. In particular, we consider those processes that can be modelled by vector systems of first-order PDEs of discrete characteristic values, and second or higher order hyperbolic PDEs.

The Method of Characteristics has not received much attention for those systems and only limited results are available in the literature. Among them is the state feedback control proposed by Hancyc and Palazoglu (1995) for controlling the outlet temperature of

a counter-flow exchanger. This strategy leads to a complex control structure and provides limited performance. In this chapter, it is demonstrated the characteristic-based MPC introduced in the previous chapter provides a mechanism to overcome the limitations and significantly improve performance. The CBMPC for more complicated systems is developed in this chapter.

The focus of the study is on systems modelled by 2×2 systems of first-order PDEs and second-order scalar hyperbolic PDEs. These relatively simple systems are used to generate a framework for the systems of multiple characteristics. The chapter is structured as follows. Section 5.1 presents some preliminary discussions of multiple characteristics. In section 5.2, the development of CBMPC is studied for first-order and second-order systems. Section 5.3 presents a simulation of applying the CBMPC on a counter-flow PFR. The chapter closes with a discussion of the proposed approach.

5.1 Effect of Multiple Characteristics

Consider a system modelled by n first-order semi-linear PDEs in two independent variables:

$$\frac{\partial v_i}{\partial t} + \sum_{j=1}^{n} a_{ij}(x)\frac{\partial v_j}{\partial x} = f_i(x, \mathbf{v}), \qquad i = 1, ..., n, \tag{5.1}$$

where: $\mathbf{v} = [v_1, ..., v_n]^T$ is the vector of distributed state variables, t is time, x is space, a_{ij} and $f_i(x, \mathbf{v}, u)$ are analytical functions. Compared with DPS modelled by scalar first-order PDEs, such systems usually require multiple infinite dimensional state variables that have to be described along multiple characteristics.

In order to use the Method of Characteristics for the solution of the PDE (5.1), some transformation is required to convert the PDE into a characteristic normal form. In terms of the $n \times n$ matrix $\mathbf{A} = [a_{ij}]$, the column vectors $\mathbf{v} = [v_1, v_2, ..., v_n]$ and $\mathbf{f} = [f_1, f_2, ..., f_n]$, the PDE can be written as:

$$\mathbf{v}_t + \mathbf{A}\mathbf{v}_x = \mathbf{f}, \tag{5.2}$$

whose *characteristic polynomial* (Duchateau and Zachmann, 1989) is defined as:

$$F(\lambda) = \det(\mathbf{A} - \lambda \mathbf{I}). \tag{5.3}$$

When $F(\lambda)$ has n real zeros and A has n linearly independent eigenvectors, the system in Equation (5.1) is hyperbolic and the matrix A is diagonalizable. Let $\lambda_1, \lambda_2, ..., \lambda_n$ be the n real zeros of the characteristic polynomial in Equation (5.3). The characteristics for the system in Equation (5.1) are the curves in the (x, t) plane satisfying

$$\frac{dx}{dt} = \lambda_i, \qquad i = 1, 2, ..., n. \tag{5.4}$$

These characteristic curves reflect the structure of the solution manifold of Equation (5.1).

Let $\mathbf{\Lambda}$ represent the diagonal matrix of eigenvalues of A

$$\Lambda = diag[\lambda_{ij}], \tag{5.5}$$

and let P represent the matrix of eigenvectors of A. The matrices $\mathbf{\Lambda}$ and P satisfy the eigenvalue problem:

$$\mathbf{PA} = \mathbf{\Lambda P}. \tag{5.6}$$

Multiplying Equation (5.2) by P yields

$$(\mathbf{Pv})_t + \mathbf{\Lambda}(\mathbf{Pv})_x = \mathbf{Pf} + \mathbf{\Lambda P}_x\mathbf{v}. \tag{5.7}$$

By defining new infinite-dimensional variables $\mathbf{v}' = \mathbf{Pv}$, Equation (5.7) becomes:

$$\mathbf{v'}_t + \mathbf{\Lambda v'}_x = \mathbf{Pf} + \mathbf{\Lambda P}_x\mathbf{v}. \tag{5.8}$$

In the PDEs (5.8), the i^{th} equation involves differentiation along the i^{th} characteristics only, which provides the possibility of simplifying the required computations.

For PDE systems with multiple characteristics, n characteristic directions exist at each point of the solution surface and the value of the solution at each point is regulated by the characteristic curves passing through it. If the boundary data $\mathbf{v} = \mathbf{v}_0(s)$ is given as the initial curve Γ and if P is the intersection of the extreme characteristics through $s = s_1$ and $s = s_2$ (see Figure 5.1 for the case $n = 4$), the domain enclosed by the boundary and

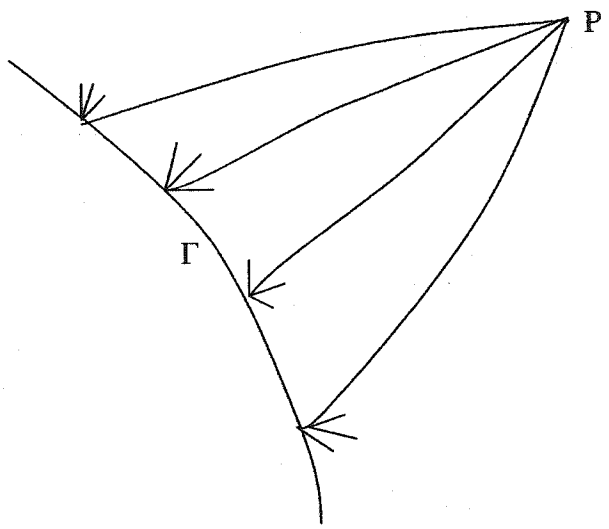

Figure 5.1: Domain of dependence of P

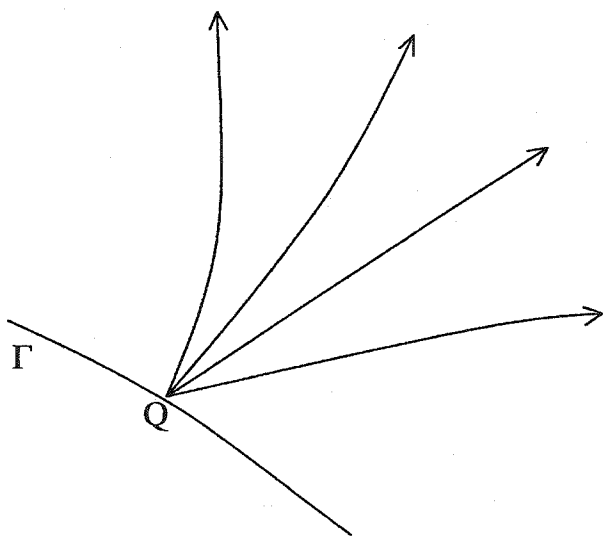

Figure 5.2: Region of influence of Q

these extreme characteristics is called the *domain of dependence* of P. The solution at P depends on the boundary data given within its domain of dependence and is independent of boundary data given on sections of the boundary outside it. As well, a given point Q on the initial curve has a *region of influence* defined by the extreme characteristics through it, as shown in Figure 5.2; a change in the boundary data would change the solution everywhere in its region of influence and only there.

The solutions of the PDE systems may be constructed numerically by approximating the characteristic curves by straight lines and approximating the differential relations in Equation (5.8) along the characteristics by algebraic relations. In Figure 5.1, the solution at P may be obtained from a knowledge of v at four different points on the initial curves for the case $n = 4$. By varying P, data on a new initial curve is obtained and the procedure is repeated. This approximate method of constructing solutions for hyperbolic systems has some advantages over other numerical methods. In the next section, this is used to predict the future output for CBMPC design.

5.2 CBMPC Design

For hyperbolic systems discussed in this chapter, multiple characteristics determine the solution of PDE systems. In this chapter, the CBMPC is developed for systems of 2 characteristics, which include processes modelled by systems of 2 first-order PDEs and second-order scalar hyperbolic PDEs.

5.2.1 First-order Systems

Following the procedure discussed in the last section, a general semilinear system of first-order equations with two dependent variable v_1 and v_2 and two independent variables t

and x can be transformed into a "characteristic normal form":

$$\begin{aligned}
&\frac{\partial v_1}{\partial t} + a_1 \frac{\partial v_1}{\partial x} = f_1(v_1, v_2, u), \\
&\frac{\partial v_2}{\partial t} + a_2 \frac{\partial v_2}{\partial x} = f_2(v_1, v_2, u), \\
&y = h(v_1(x_{out}), v_2(x_{out})),
\end{aligned} \tag{5.9}$$

where t is time, x is spatial coordinate, v_1 and v_2 are distributed state variables, u is the manipulated variable, y is process output, a_1 and a_2 are constants or functions of x, f_1 and f_2 are continuous functions, h is an output function. If $a_1 = a_2$, the system has one single characteristic. Otherwise, the system has 2 characteristics. The characteristics for Equation (5.9) are two curves determined by:

$$\begin{aligned}
C_1 \text{ characteristic} &: \frac{dx}{dt} = a_1, \\
C_2 \text{ characteristic} &: \frac{dx}{dt} = a_2.
\end{aligned} \tag{5.10}$$

The variation of state variables v_1 and v_2 can be described by the ordinary differential equations:

$$\begin{aligned}
\frac{dv_1}{dt} &= f_1(v_1, v_2, u) \text{ along } C_1 \text{ characteristic}, \\
\frac{dv_2}{dt} &= f_2(v_1, v_2, u) \text{ along } C_2 \text{ characteristic}.
\end{aligned} \tag{5.11}$$

Thus, using the Method of Characteristics, the system of PDEs (5.9) is transformed into a system of ODEs along the characteristic curves in Equation (5.10).

If the PDEs in Equation (5.9) are homogeneous, *i.e.*, $f_1(v_1, v_2, u) = 0$ and $f_2(v_1, v_2, u) = 0$, the characteristic ODEs in Equation (5.11) are decoupled and Riemann invariants exist. Therefore, an explicit solution can be obtained for v_1, v_2 as well as y. In most applications, however, the PDE models are inhomogeneous and $f_1(v_1, v_2, u)$ and $f_2(v_1, v_2, u)$ are nonlinear functions. Thus the characteristic ODEs are coupled with respect to the characteristic curves and solution is more complex than that for the systems discussed in the last chapter. For these systems, the future state variables at one spatial point have to be obtained by simultaneously integrating both characteristic ODEs

along two nonparallel characteristic curves. Predictions of future output values can be obtained by discretizing the initial state at a finite number of spatial points, then projecting characteristic curves from each of these points and computing the values of state variables at intersection points. Figure 5.3 illustrates the calculation of the state variables at point P from the values at point Q and point R. The segment QR is the *domain of dependence* of point P, since the values of state variables at point P are completely defined by state variable values on the segment QR (Rhee *et al.*, 1986). The values of points Q and R are used in the calculation of the state variable value at point P. The spatial coordinates of point P are obtained from Equation (5.10) as:

$$\int_{x(\mathrm{Q})}^{x(\mathrm{P})} \frac{1}{a_1} dx + t(\mathrm{Q}) = \int_{x(\mathrm{R})}^{x(\mathrm{P})} \frac{1}{a_2} dx + t(\mathrm{R}), \tag{5.12}$$

and the time coordinate of P is

$$t(\mathrm{P}) = t(\mathrm{Q}) + \int_{x(\mathrm{Q})}^{x(\mathrm{P})} \frac{1}{a_1} dx. \tag{5.13}$$

In the case where a_1 and a_2 are constants, the spatial coordinate and time coordinate of P can be written as:

$$x(\mathrm{P}) = \frac{a_1 x(\mathrm{R}) - a_2 x(\mathrm{Q}) + a_1 a_2 (t(\mathrm{R}) - t(\mathrm{Q}))}{a_1 - a_2}, \tag{5.14}$$

$$t(\mathrm{P}) = \frac{a_1 t(\mathrm{Q}) - 2a_2 t(\mathrm{Q}) + a_2 t(\mathrm{R}) + x(\mathrm{R}) - x(\mathrm{Q})}{a_1 - a_2}. \tag{5.15}$$

Then, the value of the state variables v_1 and v_2 at point P can be obtained from Equation (5.11) using Euler's method as follows:

$$v_1(\mathrm{P}) = v_1(\mathrm{Q}) + f_1(\mathrm{Q}) \int_{x(\mathrm{Q})}^{x(\mathrm{P})} \frac{dx}{a_1}, \tag{5.16}$$

$$v_2(\mathrm{P}) = v_2(\mathrm{R}) + f_2(\mathrm{R}) \int_{x(\mathrm{R})}^{x(\mathrm{P})} \frac{dx}{a_1}. \tag{5.17}$$

A more accurate estimate can be obtained by replacing $f_1(\mathrm{Q})$ by $\frac{1}{2}[f_1(\mathrm{Q}) + f_1(\mathrm{P})]$ and $f_2(\mathrm{R})$ by $\frac{1}{2}[f_2(\mathrm{R}) + f_2(\mathrm{P})]$.

By varying point P and repeating the procedure, the value of state variables at different locations and different future times can be calculated. For output predictions at fixed

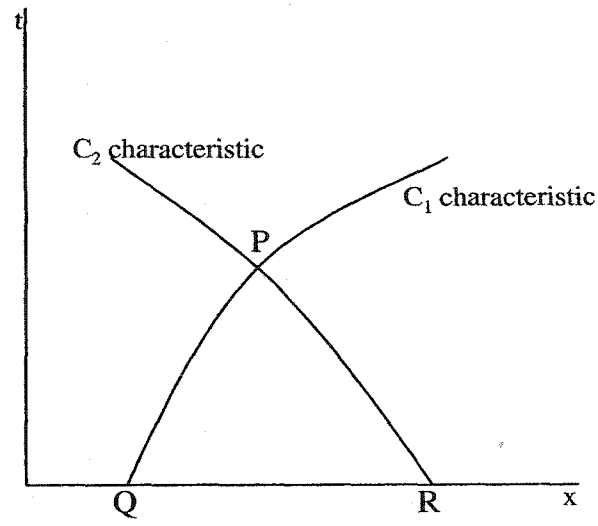

Figure 5.3: Characteristic curves of a system of PDEs with multiple characteristics

sampling time instants, the state variables at intersection points of the characteristic curves are calculated by integrating Equation (5.10) and (5.11). If the state variable v_1 at $x = 1$ is the output to be controlled, the prediction of the output can be carried out as shown in Figure 5.4. The output at the future sample times can be obtained from the value of the state variables at the intersection points.

In the above output prediction procedure, the domain of dependence determining the state variable value at one point in a future time is approximated by two points. The discretization for these systems is more complicated than the systems discussed in the last chapter. Since the discretization affects prediction accuracy, a careful discretization is needed in order to get a desired accuracy. On the other hand, the approximation of the state variable value within segment QR by that at point Q and R reflects the true solution of hyperbolic PDE systems more closely than other numerical solution methods as shown in Figure 5.3. This method can accommodate the use of larger spatial grids and time steps with a minimal loss of accuracy. The improved efficiency of this method for predicting future output is illustrated for the control of a counter-flow PFR.

Using the output prediction method described above, the value of the output for a prediction horizon time can be obtained for some specified control actions. Then, the

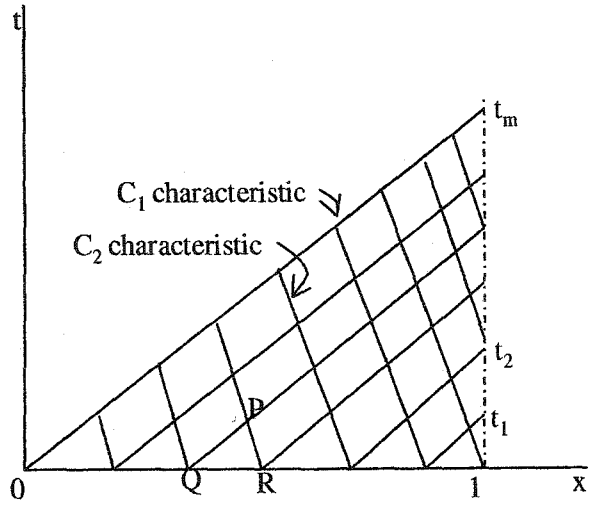

Figure 5.4: State variable prediction along characteristics

control action can be calculated in the same way as discussed in the last chapter. The predicted output is expressed in the locally linearized form:

$$\hat{\mathbf{y}} = \mathbf{y_0} + \mathbf{S}\Delta\mathbf{u}. \tag{5.18}$$

The control actions are designed to minimize the objective function:

$$\mathbf{J} = (\mathbf{y}^r - \hat{\mathbf{y}})^T\mathbf{Q}(\mathbf{y}^r - \hat{\mathbf{y}}) + \Delta\mathbf{u}^T\mathbf{R}\Delta\mathbf{u}, \tag{5.19}$$

where $\mathbf{y}^r$ are the output setpoints, $\hat{\mathbf{y}}$ are the predicted future outputs, $\mathbf{Q}$ and $\mathbf{R}$ are positive weighting matrices. The solution of the optimization problem is given by:

$$\Delta\mathbf{u} = (\mathbf{S}^T\mathbf{Q}^T\mathbf{Q}\mathbf{S} + \mathbf{R}^T\mathbf{R})^{-1}\mathbf{S}^T\mathbf{Q}^T\mathbf{Q}(\mathbf{y}^r - \hat{\mathbf{y}_0}). \tag{5.20}$$

Choosing prediction horizon time equal to the residence time and a control horizon $m_c = 1$, the calculation of control actions at every sample instant can be carried out as follows:

Step I Obtain the current state variable values at a finite number of spatial points $x_1, ..., x_m$, which may need state estimation or interpolation from measurement.

Step II In the space of (t, x), draw characteristic lines from x_1 to x_m, such that they intersect with $x = x_{out}$ and form a grid (see Figure 5.4).

Step III Assume that the current control action is the past control action u_{-1}. Calculate the values of time and spatial coordinates and state variables at the intersection points immediately connected to the initial points, and then obtain the output value at t_1. Use the obtained variable values as initial points and repeat the calculation to get the output values at t_2 until t_m. This gives $\hat{\mathbf{y}}_0$.

Step IV Assuming that the current control action is $u_{-1} + \delta$, where δ is a small disturbance, repeat Step III and calculate the output prediction y at $t_1, t_2, ..., t_m$ under $u_{-1} + \delta$.

Step V Calculate S using the following equation:

$$\mathbf{S} = \left(\frac{\partial \hat{\mathbf{y}}}{\partial \mathbf{u}}\right)_0 = \frac{\hat{\mathbf{y}}|_{\mathbf{u}_{-1}+\delta} - \hat{\mathbf{y}}|_{\mathbf{u}_{-1}}}{\delta}. \tag{5.21}$$

Step VI Substitute the obtained S and $\hat{\mathbf{y}}_0$ into Equation (5.20) to get the required control action.

These steps can be used to update the control action whenever necessary. The grid size of the discretization can be adjusted to get the desired prediction accuracy, and therefore the acceptable performance.

5.2.2 Second-order Systems

Although few chemical processes have been found that require second or higher-order hyperbolic PDE models, some fluid phenomena exhibit wave patterns that can be described by second-order hyperbolic PDEs. In this section, the Method of Characteristics is used in the design of a CBMPC for a second-order hyperbolic scalar PDE system.

Consider a general semi-linear, second-order hyperbolic equation

$$av_{tt} + 2bv_{tx} + cv_{xx} + e = 0, \tag{5.22}$$

where a, b and c are functions of t and x, e is a function of t, x, v, v_t, v_x and u. Equation (5.22) can be classified as hyperbolic, parabolic or elliptic according to the coefficient values in the second-order partial derivatives of the equation. For hyperbolic processes, restricted to a region R in (t, x) plane where

$$b^2 - ac > d > 0, \tag{5.23}$$

Equation (5.22) has two characteristics:

$$\begin{aligned} \lambda_+ &= \frac{b + \sqrt{b^2 - ac}}{a}, \\ \lambda_- &= \frac{b - \sqrt{b^2 - ac}}{a}. \end{aligned} \tag{5.24}$$

In order to use the Method of Characteristics to generate the solution manifold for a hyperbolic second-order PDE (5.22), the solution is expressed along the characteristics in the following way:

$$\begin{aligned} \frac{\partial}{\partial t}(v_t + \lambda_+ v_x) + \lambda_- \frac{\partial}{\partial x}(v_t + \lambda_+ v_x) + \frac{e}{a} - (\lambda_+)_t v_x - \lambda_-(\lambda_+)_x v_x &= 0, \\ \frac{\partial}{\partial t}(v_t + \lambda_- v_x) + \lambda_+ \frac{\partial}{\partial x}(v_t + \lambda_- v_x) + \frac{e}{a} - (\lambda_-)_t v_x - \lambda_+(\lambda_-)_x v_x &= 0. \end{aligned} \tag{5.25}$$

Since λ_+ and λ_- are the known characteristics of the PDE, the functions $(\lambda_+)_t$, $(\lambda_-)_t$, $(\lambda_+)_x$ and $(\lambda_-)_x$, which represent the partial derivatives of the known characteristics, are also known. Since it is often assumed for control purposes that the processes are time invariant, it follows that $(\lambda_+)_t = 0$ and $(\lambda_-)_t = 0$. Defining two new variables $p = \dfrac{\partial v}{\partial x}$ and $q = \dfrac{\partial v}{\partial t}$, Equation (5.25) can be written as:

$$\begin{aligned} \frac{\partial q}{\partial t} + \lambda_- \frac{\partial q}{\partial x} + \lambda_+ \left(\frac{\partial p}{\partial t} + \lambda_- \frac{\partial p}{\partial x}\right) + \frac{e}{a} - \lambda_-(\lambda_+)_x p &= 0, \\ \frac{\partial q}{\partial t} + \lambda_+ \frac{\partial q}{\partial x} + \lambda_- \left(\frac{\partial p}{\partial t} + \lambda_+ \frac{\partial p}{\partial x}\right) + \frac{e}{a} - \lambda_+(\lambda_-)_x p &= 0. \end{aligned} \tag{5.26}$$

The original second-order hyperbolic PDE (5.25) is then decomposed into two first-order hyperbolic PDEs with new variables p and q. In fact, a system of two first-order PDEs can be combined into a single second-order hyperbolic PDE. For example, a counter-flow

double pipe heat exchanger modelled by two first-order PDEs:

$$\begin{aligned} \frac{\partial T_1}{\partial t} + u_1 \frac{\partial T_1}{\partial x} + h_0(T_1 - T_2) &= 0, \\ \frac{\partial T_2}{\partial t} - u_2 \frac{\partial T_2}{\partial x} - a h_0(T_1 - T_2) &= 0, \end{aligned} \tag{5.27}$$

can be written into the single second-order hyperbolic PDE:

$$\begin{aligned} \frac{\partial^2 T_1}{\partial t^2} + (u_1 - u_2)\frac{\partial^2 T_1}{\partial t \partial x} - u_1 u_2 \frac{\partial^2 T_1}{\partial x^2} = -h_0 \frac{\partial T_1}{\partial t} \\ + h_0 u_2 \frac{\partial T_1}{\partial x} + a h_0^2 (T_1 - T_2). \end{aligned} \tag{5.28}$$

It is noted that this second-order hyperbolic PDE cannot completely determine the original system of first-order PDEs. It has to be combined with one of the first-order PDEs in order to determine the temperature of the system.

Similarly, the system of first-order PDEs (5.26) does not completely represent the original second-order PDE (5.22). It needs to be combined with a contact form existing on the solution manifold. The contact form for variables p, q and v in a second-order PDE system is:

$$w = dv - p dx + q dt, \tag{5.29}$$

where d is a differential operator. It is required that w zero on the tangent space to the solution manifold. The two first-order hyperbolic PDEs in Equation (5.26), along with the contact form (5.29), describe the original second-order hyperbolic PDE exactly. Applying a suitable transformation $(t, x) \longrightarrow (\xi, \eta)$, the two characteristic vector fields of the system can be written in (t, x) space as:

$$\begin{aligned} \frac{\partial}{\partial \xi} &= \frac{\partial}{\partial t} + \lambda_- \frac{\partial}{\partial x}, \\ \frac{\partial}{\partial \eta} &= \frac{\partial}{\partial t} + \lambda_+ \frac{\partial}{\partial x}. \end{aligned} \tag{5.30}$$

Taking ξ and η as two new independent variables, Equation (5.26) can be expressed by ξ and η in the simple form:

$$\begin{aligned} \frac{\partial q}{\partial \xi} + \lambda_+ \frac{\partial p}{\partial \xi} + \frac{e}{a} - \lambda_- (\lambda_+)_x p &= 0, \\ \frac{\partial q}{\partial \eta} + \lambda_- \frac{\partial p}{\partial \eta} + \frac{e}{a} - \lambda_+ (\lambda_-)_x p &= 0. \end{aligned} \tag{5.31}$$

Noticing that every equation only involves partial differentiation with respect to only one independent variable, one can express the equation by an ODE along the characteristic directions. This can be achieved by transferring variables p and q into new variables w_1 and w_2:

$$\begin{aligned} w_1 &= q + \lambda_+ p, \\ w_2 &= q + \lambda_- p. \end{aligned} \tag{5.32}$$

The partial differentiation of w_1 and w_2 with respect to the new independent variables ξ and η can be directly derived from Equation (5.31). The differentiation of v with respect to the variables ξ and η is:

$$\begin{aligned} \frac{\partial v}{\partial \xi} &= \lambda_- p + q, \\ \frac{\partial v}{\partial \eta} &= \lambda_+ p + q. \end{aligned} \tag{5.33}$$

These equations can then be expressed in characteristic ODE form along the two characteristic directions $\frac{dx}{dt} = \lambda_+$ and $\frac{dx}{dt} = \lambda_-$. Along the λ_+ characteristic, the ODEs are:

$$\begin{aligned} \dot{t} &= 1, \\ \dot{x} &= \lambda_+, \\ \dot{w}_2 &= -\frac{e}{a} + \lambda_+ (\lambda_-)_x p, \\ \dot{v} &= \lambda_+ p + q, \end{aligned} \tag{5.34}$$

while along the λ_- characteristic, they are:

$$\begin{aligned} \dot{t} &= 1, \\ \dot{x} &= \lambda_-, \\ \dot{w}_1 &= -\frac{e}{a} + \lambda_- (\lambda_+)_x p. \end{aligned} \tag{5.35}$$

To avoid redundancy, the contact form can only appear once in either λ_+ or λ_- characteristics.

Equations (5.34) and (5.35) are equivalent to the "characteristic normal form" of Equation (5.22), given by (Simpson, 1967):

$$\begin{aligned}
-\lambda_+\frac{\partial t}{\partial \xi}+\frac{\partial x}{\partial \xi}&=0,\\
\frac{\partial q}{\partial \xi}+\lambda_-\frac{\partial p}{\partial \xi}+\frac{e}{a}\frac{\partial t}{\partial \xi}&=0,\\
\frac{\partial u}{\partial \xi}+u\frac{\partial t}{\partial \xi}+-p\frac{\partial x}{\partial \xi}&=0,\\
-\lambda_-\frac{\partial t}{\partial \eta}+\frac{\partial x}{\partial \eta}&=0,\\
\frac{\partial q}{\partial \eta}+\lambda_-\frac{\partial p}{\partial \eta}-\frac{e}{a}\frac{\partial t}{\partial \eta}&=0.
\end{aligned} \tag{5.36}$$

This can easily be verified by substituting Equation (5.30) into Equation (5.36).

Given a control action, Equations (5.32), (5.34) and (5.35) can be used to predict the sampled future output for second-order hyperbolic PDE systems. The solution of the second-order PDEs requires the initial condition of state variable v as well as its first-order partial derivatives p and q. If variables v, p and q are known at current time, the output prediction can be carried out in a way similar to what is shown in Figure 5.4. In the $t-x$ plane, the spatial coordinate is discretized into a finite number of points at the current time and the two characteristic curves are drawn from each of these spatial points. Applying numerical integration schemes such as Euler, corrected Euler, or Runge-Kutta methods to Equation (5.34) and (5.35), the resulting equations, along with Equation (5.32), can be used to calculate the variables t, x, v, p, q, w_1 and w_2 at every intersection point of the characteristic curves. The output at the future sampling times t_1, $t_2, ..., t_m$ can thus be obtained. This output prediction method can be cast into the control calculation procedure described in the last subsection for first-order systems. The optimal control action can then be obtained through optimization. This procedure constitutes a generalization of CBMPC to systems with multiple characteristics.

The initial values for v, p and q are required for the prediction of the future values of the state variables. If the process is initially at steady state, the infinite-dimensional profile of v can be obtained by solving the ordinary differential equation obtained by setting the time derivative of the original PDE model to be zero. The variables p and q

can be estimated by $p = \frac{dv(x)}{dx}$ and $q = 0$, respectively. If the initial condition is not at steady state, the profile of state variable v can be estimated by numerical approximation from a finite set of measurements. The variable p is calculated as $p = \frac{dv(x)}{dx}$. An estimate of q is obtained by substituting the estimates of v and p into the original PDE model and by solving the resulting ODE.

5.3 Example - Counter Flow PFR

In many applications, the heating or cooling temperature of a PFR in the jacket is not spatially uniform. In such situations, the distributed state variables include both variables related to the states inside the reactor and the jacket. As a result, these systems have to be described along two different characteristics. In this section, the application of CBMPC for a non-isothermal PFR with counter-flow heating media in the jacket is considered. The reactor described in last section is used. However, it is assumed that the jacket fluid has a spatially varying temperature. The fluid velocity of the jacket rather than the temperature is manipulated to control the outlet concentration of product B. The schematic of the process is shown in Figure 5.5.

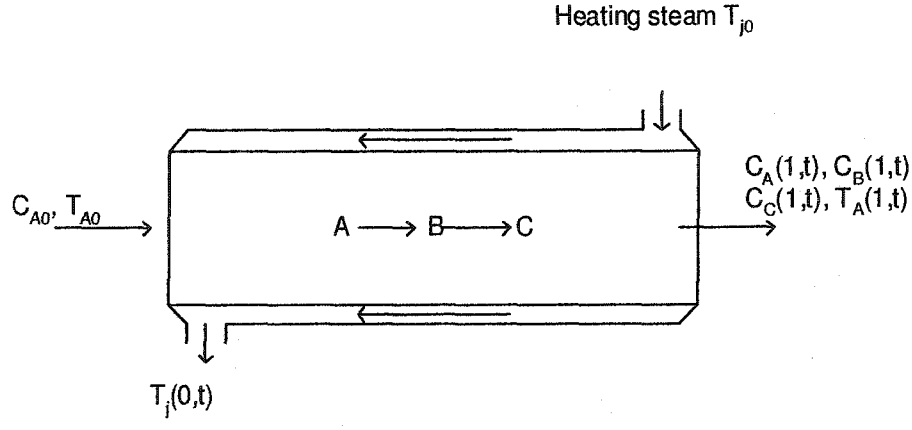

Figure 5.5: Counter flow PFR

The process model is given by:

$$\begin{aligned}
\frac{\partial C_A}{\partial t} &= -v_l \frac{\partial C_A}{\partial x} - k_{10} e^{-E_1/RT_r} C_A, \\
\frac{\partial C_B}{\partial t} &= -v_l \frac{\partial C_B}{\partial x} + k_{10} e^{-E_1/RT_r} C_A - k_{20} e^{-E_2/RT_r} C_B, \\
\frac{\partial T_r}{\partial t} &= -v_l \frac{\partial T_r}{\partial x} + \frac{(-\Delta H_{r_1})}{\rho_m c_{pm}} k_{10} e^{-E_1/RT_r} C_A \\
&\quad + \frac{(-\Delta H_{r_2})}{\rho_m c_{pm}} k_{20} e^{-E_2/RT_r} C_B + \frac{U_w}{\rho_m c_{pm} V_r} (T_j - T_r), \\
\frac{\partial T_j}{\partial t} &= u \frac{\partial T_j}{\partial x} + \frac{U_{wj}}{\rho_{mj} c_{pmj} V_j} (T_r - T_j),
\end{aligned} \tag{5.37}$$

subject to the boundary conditions:

$$C_A(0,t) = C_{A0}, \quad C_B(0,t) = 0, \quad T_r(0,t) = T_{r0}, \quad T_j(1,t) = T_{j0}, \tag{5.38}$$

where: t is time, $x \in [0,1]$ is the normalized spatial coordinate along the reactor, C_A and C_B are the concentrations of the species A and B in the reactor, T_r is the temperature of the reactor, T_j is the temperature in the jacket, ΔH_{r_1} and ΔH_{r_2} are enthalpy of the two reactions, ρ_m and c_{pm} is the density and heat capacity of the fluid in the reactor, ρ_{mj} and c_{pmj} are the density and heat capacity of the fluid in the jacket, V_r is the volume of the reactor, V_j is the volume of fluid in the jacket, U_w is the heat-transfer coefficient in the reactor, U_{wj} is the heat-transfer coefficient in the jacket, C_{A0} and T_{A0} are concentration and temperature of the inlet stream in the reactor, u is the velocity of fluid in the jacket.

In comparison with the PDE model for the plug flow reactor with uniform heating discussed in Chapter 4, Equation (5.37) includes one additional PDE to model the variation of the jacket temperature. The first three equations are the same as for uniform heating and can be described by a system of ODEs along the characteristic vector field:

$$\xi_1 = \frac{\partial}{\partial t} + v_l \frac{\partial}{\partial x}. \tag{5.39}$$

Since the heating fluid in the jacket flows in a different direction and at a different rate than the reactants in the reactor, the PDE representing the jacket temperature has to be described by a different vector field:

$$\xi_2 = \frac{\partial}{\partial t} - u \frac{\partial}{\partial x}. \tag{5.40}$$

Since this process has slow and complex dynamics, it is desirable to design a controller that takes into account the long-term effect of the control action. The design of an MPC requires a scheme for the prediction of the output. In this case, the output prediction is performed using the Method of Characteristics described in the last section, which predicts the behavior of the system along the characteristic vector fields ξ_1 and ξ_2. Along ξ_1, the solution of Equation (5.37) is described by the set of ODEs:

$$\begin{aligned}
\dot{t} &= 1, \\
\dot{x} &= v_l, \\
\dot{C}_A &= -k_{10}e^{-E_1/RT_r}C_A, \\
\dot{C}_B &= k_{10}e^{-E_1/RT_r}C_A - k_{20}e^{-E_2/RT_r}C_B, \\
\dot{T}_r &= \frac{(-\Delta H_{r_1})}{\rho_m c_{pm}}k_{10}e^{-E_1/RT_r}C_A + \\
&\quad \frac{(-\Delta H_{r_2})}{\rho_m c_{pm}}k_{20}e^{-E_2/RT_r}C_B + \frac{U_w}{\rho_m c_{pm}V_r}(T_j - T_r).
\end{aligned} \tag{5.41}$$

Along the vector field ξ_2, it is given by:

$$\begin{aligned}
\dot{t} &= 1, \\
\dot{x} &= -u, \\
\dot{T}_j &= \frac{U_w}{\rho_{mj} c_{pmj} V_j}(T_r - T_j).
\end{aligned} \tag{5.42}$$

The future output is predicted by numerically integrating Equation (5.41) and (5.42). The integration of Equations (5.41) and (5.42) is carried out for a finite number of discrete spatial points to generate the output prediction at future sampling times. Unlike traditional methods of discretization, the discretization here does not involve approximation. It provides the initial spatial points for integration. Assume that, at the current time t, the dependent variables in the reactor and in the jacket are given at m discrete spatial locations x_i, $i = 1, ..., m$, along the reactor. From each of these m points, two characteristic lines can be drawn in the (t, x) space corresponding to the two characteristic vector fields ξ_1 and ξ_2 for a fixed value of the control u. The characteristic lines from $x_1, x_2, ..., x_m$ form

a grid in (t, x) space. By indicating the time and spatial coordinates of the intersection points at the i^{th} sampling time and j^{th} spatial position as t_{ij} and x_{ij}, $j = 1, 2, ..., m$, $i = 1, 2, ..., \infty$, the time and spatial coordinates of the intersection points in the grid can be calculated from the initial discretization points using the integration of vector fields ξ_1 and ξ_2:

$$t_{i+1,j} = -\frac{x_{ij} - ut_{i,j-1} - v_l t_{ij} - x_{i,j-1}}{u + v_l}, \tag{5.43}$$

$$x_{i+1,j} = \frac{ux_{ij} + v_l ut_{i,j-1} + v_l x_{i,j-1} - v_l ut_{ij}}{u + v_l}. \tag{5.44}$$

The value of the state variables at the intersection points is computed by integrating Equation (5.41) and (5.42) along vector fields ξ_1 and ξ_2, respectively, from the current time to next sample time. A variety of numerical schemes for integration are available. In this example, a corrected Euler method was used to compute the prediction of the state variables at the intersection points. Assuming that the output is C_B at $x_{out} = 1$, the output at the discrete future time can be estimated as in Figure 5.4. The sample instants, at which the outlet concentration can be predicted, are $t_0 + \Delta t_j$, where

$$\Delta t_j = \frac{1 - x_{1j}}{v_l}, \qquad j = 1, 2, ..., m. \tag{5.45}$$

The output is predicted from the above prediction procedure. The sampling time can be modified by adjusting the discretization at the initial time.

The controller is designed to minimize an objective function:

$$J = \sum_{i=1}^{m} (y^r - y_i)^2 + \lambda(\Delta u)^2, \tag{5.46}$$

where: y^r is the setpoint of outlet concentration C_B. The optimal input trajectory subject to the linearized output function is computed following the nonlinear quadratic DMC algorithms (Mutha *et al.*, 1997). The model parameters used for simulation are listed in Table 3.1. In addition, the jacket properties are given as $C_{pmj} = 0.8$ kcal/(kg $\circ$ K), $V_j = 8$ lt, $\rho_{mj} = 0.10$ kg/lt, $T_{j0} = 375$ K. The simulation is performed by discretizing the PDE model along the space into 60 points and solving the resulting system of ODEs. The number of discretization points for the control calculation is taken to be $m = 10$. The

parameters of the nonlinear quadratic DMC algorithm used are $p = m = 10$, $m_c = 1$, and $\lambda = 0.0004$ as tuning parameters. The initial condition is assumed to be steady state for a flow rate of 0.5 m/min. The initial steady state variable profiles are shown in Figure 5.6.

Figure 5.7 shows a process response for a setpoint change of $C_B(x = 1)$ from 0.83 mol/lt to 1 mol/lt. The proposed CBMPC yields a smooth output setpoint tracking response. The process output converges to the setpoint quickly without large overshoot and oscillations.

In the CBMPC calculation, a spatial discretization grid is used to get the future output prediction at the appropriate discrete sample times. In control of the PFR with uniform heating discussed in the last chapter, discretization did not affect the prediction accuracy and the control performance. In this chapter, the effect of discretization was examined for the counter-flow PFR, to investigate its effect on CBMPC performance for systems with multiple characteristics. Figure 5.8 shows the performance of the CBMPC using different discretizations. It can be seen that an insufficient number of discretization points ($m = 2$ or 3) do not yield good prediction accuracy and poor tracking performance is observed. A reasonably fine discretization ($m \geq 6$ in this example) is required to obtain good prediction accuracy and the desired control performance.

The performance of the CBMPC in comparison with that of a MPC based on a finite difference method was also investigated. Figure 5.9 gives the performance comparison of the two MPC methods. For the proposed CBMPC, satisfactory performance can be obtained using discretization $m = 10$. On the other hand, finer discretization is required in finite-difference based MPC in order to get the good performance. Using 20 discretization points ($m = 20$) in the finite difference approximation, the MPC yields a closed-loop performance comparable to that of the proposed MPC ($m = 10$) except a slightly larger offset in the finite difference-based MPC. Obviously, finite difference based MPC can reach the performance of CBMPC when enough discretization is made. It is the computational efficiency that makes the CBMPC more favorable than finite-difference based MPC. The computational efficiency of the proposed CBMPC with different discretization points and that of the finite difference based MPC are compared

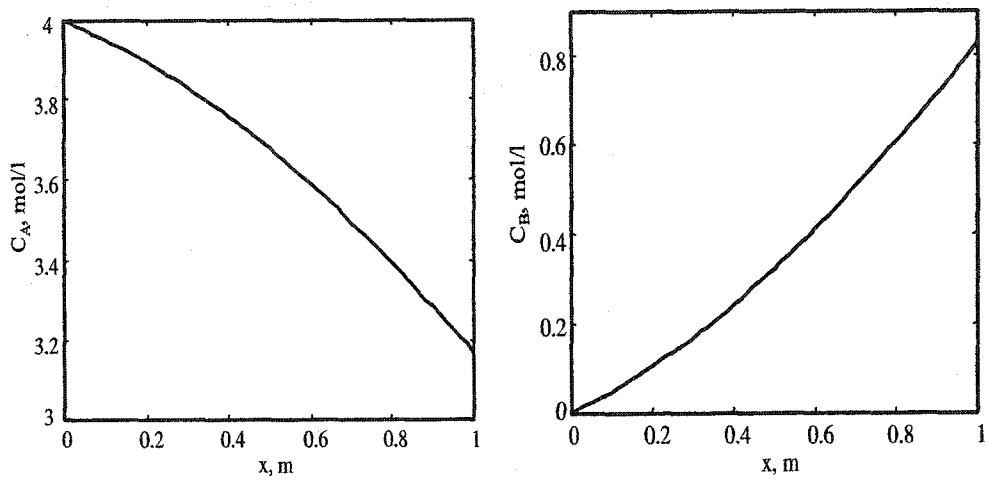

(a) C_A (b) C_B

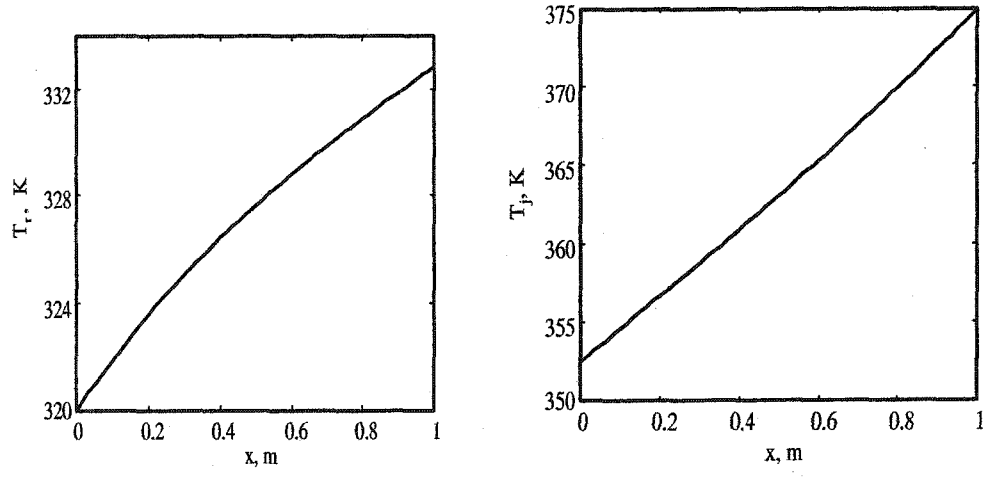

(c) T_r (d) T_j

Figure 5.6: Initial state variable profiles in the counter-flow PFR

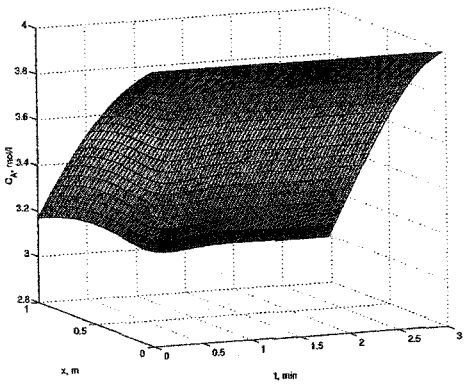

(a) C_A

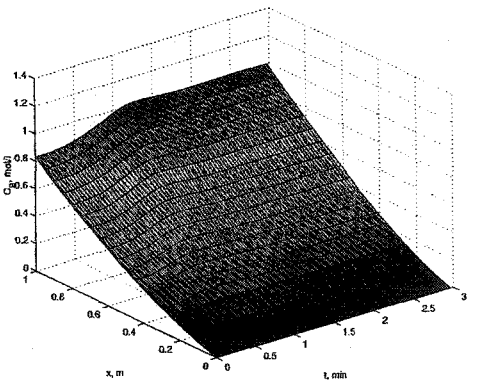

(b) C_B

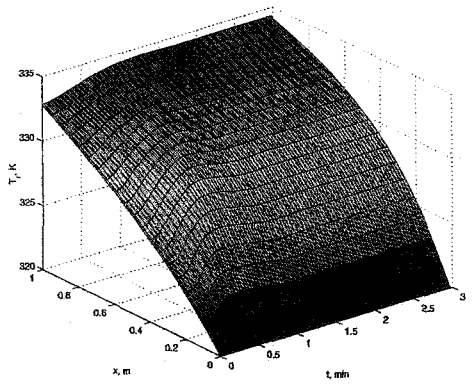

(c) T_r

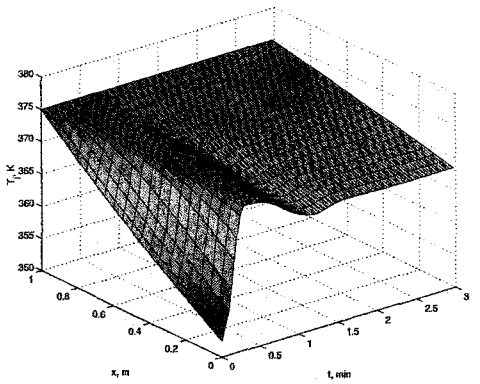

(d) T_j

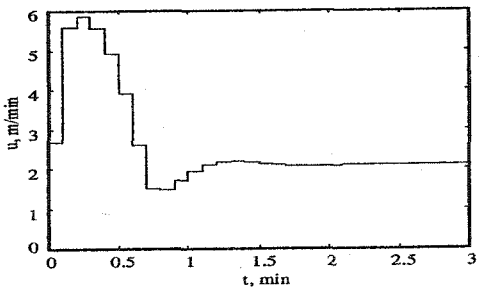

(e) u

Figure 5.7: Evolution of the state variable profiles under CBMPC in the counter-flow PFR

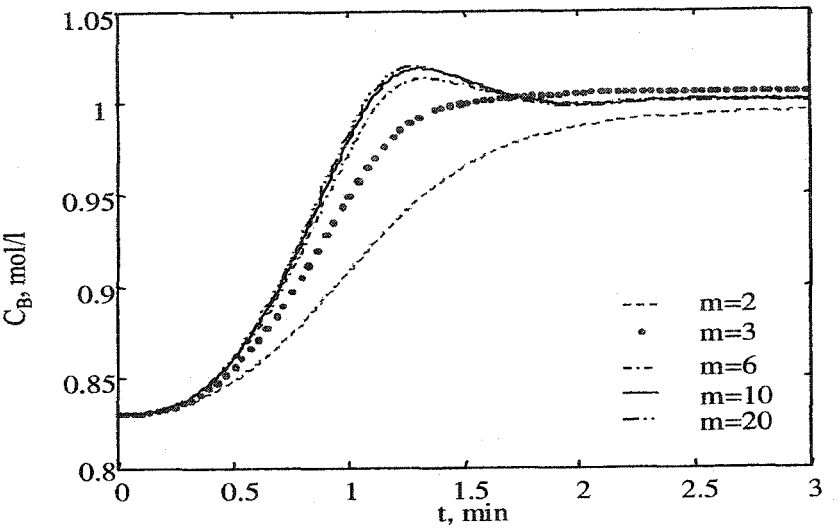

(a) C_B at outlet

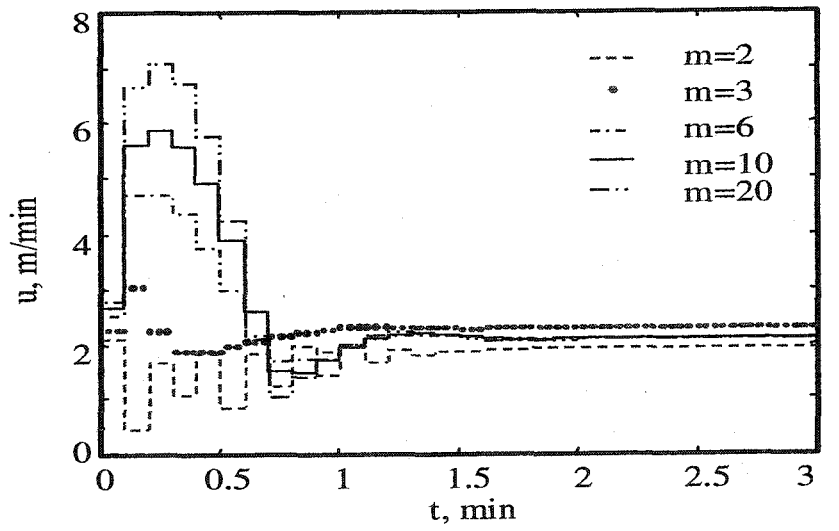

(b) manipulated variable

Figure 5.8: Output response of CBMPC for different discretizations in the counter-flow PFR

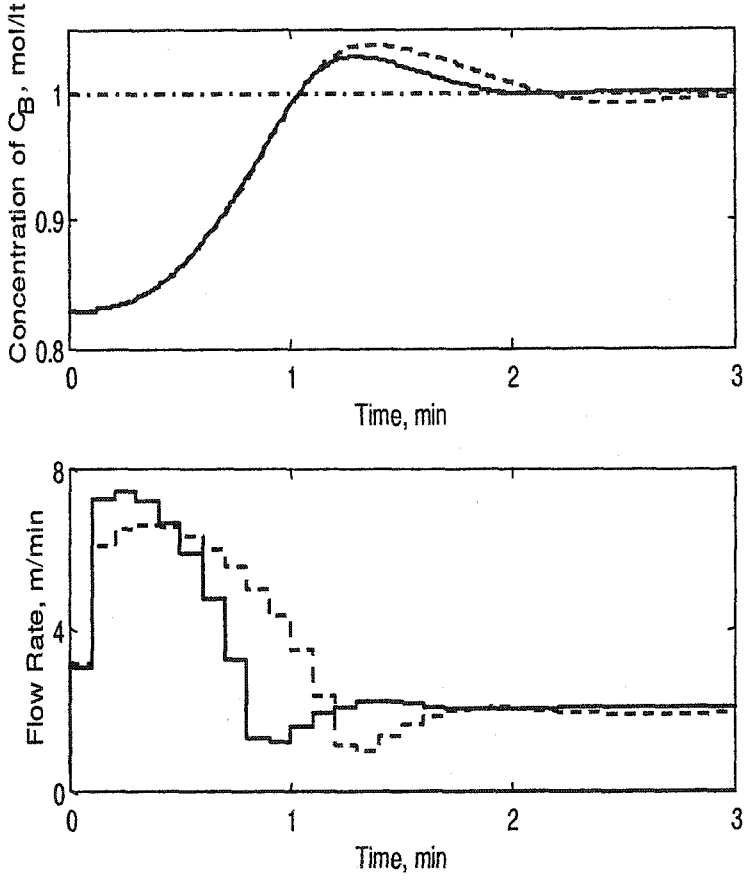

Figure 5.9: Performance comparison of CBMPC *vs.* finite difference-based MPC in the counter-flow PFR

Table 5.1: Computations of CBMPC *vs.* conventional MPC in counter-flow PFR

Control Method	flops
CBMPC ($m = 2$)	1.714×10^3
CBMPC ($m = 3$)	3.584×10^3
CBMPC ($m = 6$)	1.3298×10^4
CBMPC ($m = 10$)	3.5826×10^4
CBMPC ($m = 20$)	1.4003×10^5
finite difference-based MPC ($m = 10$)	6.31×10^6
finite difference-based MPC ($m = 20$)	1.40×10^7

in Table 5.1. For the proposed CBMPC for systems with multiple characteristics, the computational demand increases with the number of discretization points in control calculation. The computation required in the CBMPC is much more efficient than that in the finite difference-based MPC. The improved computational efficiency makes the proposed CBMPC advantageous in implementation to industrial processes.

5.4 Summary

In this chapter, a CBMPC method is developed for generalized PDE systems with multiple characteristics. In particular, the focus has been on systems in which two characteristic lines pass through every point of the solution surface. For these systems, two or more state variables are coupled in the non-parallel characteristic ODEs. The resulting Method of Characteristics is more complex, but is manageable. Discretizing the current state variable at a finite number of spatial points and combining the numerical integration schemes into

the Method of Characteristics, the output at future times can be predicted from current state variable profiles. The CBMPC exploits this prediction procedure to compute an optimal control action. Since the numerical Method of Characteristics closely reflects the true solution of the PDE systems, the proposed CBMPC can produce the desirable closed-loop performance due to high prediction accuracy that does not require demanding on-line computation. This control approach uses the efficient numerical scheme in the control development, and therefore overcomes the difficulties existing in the standard feedback control for these systems, as discussed in chapter 3.

The proposed CBMPC was evaluated, via simulation, on a counter flow PFR. The controlled process output has a desirable closed-loop response to setpoint changes. In contrast to the case for single characteristics, the discretization was shown to have an impact on the closed-loop performance. Satisfactory performance could be recovered by refining the discretization. The CBMPC was also shown to outperform the conventional MPC approach based on finite difference method.

In the last two chapters, the CBMPC has been developed for systems that are deterministic, strictly hyperbolic and have no model-plant mismatch. Although these represent ideal cases for a range of important industrial processes, many industrial processes do not strictly belong to this class of systems, but can be considered close. Among such systems are convection-dominated parabolic systems. Extending the proposed CBMPC to these system is important, due to their wide existence, and is discussed in the next chapter.

Chapter 6

CBMPC for Convection-Dominated Parabolic Systems

A common form of parabolic DPS encountered in chemical engineering and other industries is diffusion-convection-reaction processes, which arise very frequently in various reactors and other applications (*e.g.*, compression processes, dendritic growth, thermal aging of plastic material, batch sedimentation, absorption process, pollutant propagation, *etc*). The dynamics of such processes can usually be modelled by second-order parabolic partial differential equations. This chapter focuses on the design of PDE-based MPC for convection-dominated diffusion problems.

When convection mechanism is dominant, a second-order parabolic system contains obvious hyperbolic features. It is then reasonable to consider the extension of the CBMPC technique to these systems. Two approaches are used, in this chapter, to extend the CBMPC and develop the control methods for convection-dominated parabolic systems. First approach considers the diffusion term in a second-order parabolic model as a bounded uncertainty. A robust control approach is developed that combines a model-plant mismatch compensation scheme into the CBMPC for hyperbolic systems. In a

second approach, a finite difference approximation of the diffusion term is used. The CBMPC for hyperbolic systems is then applied to the resulting approximate models. In fact, the technique of combining the Method of Characteristics with the finite element or finite difference methods has been considered in the mathematical field (Douglas and Russell, 1982; Marion and Mollard, 2000). These studies demonstrate the advantage of this approach over other numerical techniques. To best of our knowledge, the use of this method for the control of parabolic PDE systems is new.

This chapter is structured as follows. Section 6.1 presents some properties and solution methods for convection-dominated parabolic systems. Section 6.2 describes two CBMPC approaches developed for these systems. In Section 6.3, the control methods are applied for control of a bleaching reactor. A summary is provided in Section 6.4.

6.1 Convection-Dominated Systems

Convection-dominated parabolic systems occur in convection-diffusion problems, in which both diffusive and convective mass transfer are involved. When convection dominates, such systems are referred to as convection-dominated parabolic systems. A general convection-diffusion problem is described by

$$\frac{\partial v}{\partial t} + a(x)\frac{\partial v}{\partial x} - b(x)\frac{\partial^2 v}{\partial x^2} = f(x, v), \tag{6.1}$$

where the coefficient $a(x)$ reflects the fluid velocity and $b(x)$ is the diffusivity. In this description, the convection dominance can be indicated by the relative ratio of the coefficients $b(x)/a(x)$, or the inverse of Pèclet Number. The Pèclet Number is a dimensionless number and is defined as $Pe = \frac{la}{b}$.

Solution methods for convection-dominated parabolic systems are usually the same as those for other parabolic systems. Although the vast literature exists for parabolic problems, spanning a wide variety of mathematical techniques, the most commonly used methods are probably eigenfunction expansions and the finite difference method (Ockendon *et al.*, 1999).

Eigenfunction expansions are used to generate finite dimensional approximations of parabolic PDEs. This technique can often result in a low order approximation. For convection-dominated systems, this property can be lost because of their nearly hyperbolic nature. Since all eigenmodes of hyperbolic systems contain almost the same amount of energy, an infinite number of eigenmodes are required to represent these systems. The large dimension of eigenfunction expansions renders this method unusable for the control of convection-dominated systems.

The finite difference method has been used extensively for simulation and control of PDE systems. In spite of their wide acceptance and popularity, both explicit and implicit finite difference methods involve significant computational requirement for approximation accuracy. Thus, use of finite difference approaches for MPC of convection-dominated systems can lead to prohibitively demanding techniques and as such, is an unattractive approach.

To overcome these limitations for convection-dominated parabolic problems, it is natural to seek numerical methods that reflect their almost hyperbolic nature. As discussed in previous chapters, the Method of Characteristics provides a computationally efficiently solution method for hyperbolic systems. It may be appropriate for constructing solutions to convection-dominated parabolic problems as well. For parabolic systems, a small diffusion term can be easily identified and approximated with a large spatial grid without impacting the overall accuracy. It is shown in this chapter that the combination of the Method of Characteristics with the finite difference schemes produces a computationally efficient solution method for convection-dominated parabolic systems.

Denoting the characteristic direction associated with the operator $v_t + av_x$ in Equation (6.1) by $\tau = \tau(x)$, and

$$\frac{\partial}{\partial \tau(x)} = \frac{\partial}{\partial t} + a(x)\frac{\partial}{\partial x}, \tag{6.2}$$

Equation (6.1) can be written as:

$$\frac{\partial v}{\partial \tau(x)} - b(x)\frac{\partial^2 v}{\partial x^2} = f(x, v). \tag{6.3}$$

Applying the finite difference scheme to Equation (6.3), the solution at times $t_i = i\Delta t$

can be approximated for a time step $\Delta t > 0$. Let

$$\bar{x} = x - a(x)\Delta t, \tag{6.4}$$

and note that

$$\begin{aligned} \frac{\partial v}{\partial \tau(x)} &= \frac{v(x,t_i) - v(\bar{x},t_{i-1})}{\Delta \tau} \\ &= \frac{v(x,t_i) - v(\bar{x},t_{i-1})}{[(x-\bar{x})^2 + (\Delta t)^2]^{1/2}}. \end{aligned} \tag{6.5}$$

These procedures can yield an improvement in approximation accuracy. Approximation of $\partial v/\partial t$ by standard backward difference leads to the error of the form $K \left\| \partial^2 v/\partial t^2 \right\| \Delta t$ in suitable norms, while the above method yields $K \left\| \partial^2 v/\partial \tau^2 \right\| \Delta t$. In problems with significant convection, the solution changes much less rapidly in the characteristic τ direction than in the t direction (Douglas and Russell, 1982). Thus, this scheme will permit the use of larger time steps, with corresponding improvements in efficiency, at no cost in accuracy. There is no stability limitation on the size of Δt.

When convection is distinctively more important than diffusion (*i.e.*, for large Peclet numbers), the diffusion term $b(x)\dfrac{\partial^2 v}{\partial x^2}$ can be replaced by centered, second difference approximation with minimal impact on overall accuracy. Therefore, Combination of the Method of Characteristics with Finite Difference approximation (CMCFD) permits convection-dominated parabolic problems to be solved with high accuracy and comparatively small computational load. In this chapter, the CMCFD approach is used to develop MPC for convection-dominated parabolic systems.

6.2 Mismatch Compensation

Consider a convection-dominated parabolic process modelled by

$$\begin{aligned} &\frac{\partial v}{\partial t} + a(x)\frac{\partial v}{\partial x} - b(x)\frac{\partial^2 v}{\partial x^2} = f(x,v,u), \\ &y = v(x_{out}). \end{aligned} \tag{6.6}$$

When the diffusion term $b(x)\frac{\partial^2 v}{\partial x^2}$ is negligible, it may be possible to approximate the PDE in Equation (6.6) by a hyperbolic PDE:

$$\frac{\partial v}{\partial t} + a(x)\frac{\partial v}{\partial x} = f(x, v, u), \tag{6.7}$$

which can be described along the characteristic direction in the ODE form:

$$\begin{aligned} \dot{t} &= 1, \\ \dot{x} &= a(x), \\ \dot{v} &= f(x, u, v), \\ y &= v(x_{out}). \end{aligned} \tag{6.8}$$

Then, the future output can be predicted by numerically integrating Equation (6.8). The CBMPC for the system in Equation (6.6) can be developed using the strategy for hyperbolic systems discussed in Chapter 4. The locally linearized output prediction equation is modified by adding a mismatch compensation term:

$$\hat{\mathbf{y}} = \hat{\mathbf{y}}_\mathbf{0} + \mathbf{S}\Delta\mathbf{u} + \mathbf{e}, \tag{6.9}$$

where $\mathbf{e}$ is a mismatch term and includes the contribution of the diffusion term on the output. In Equation (6.9), $\hat{\mathbf{y}}_\mathbf{0}$ and $\mathbf{S}$ are calculated in the same way as that for a hyperbolic system based on Equation (6.7), the components of $\mathbf{e}$ are calculated using the similar strategy that is used for disturbance effects in DMC. It is taken to be zero initially and is updated iteratively at every sample time instant using the formula:

$$\begin{aligned} e_k^{new} &= e_k^{old} + L(y_k^m - \hat{y}_k), \\ e_{k+1} &= e_{k+2} = \ldots = e_k, \end{aligned} \tag{6.10}$$

where y_k^m is the measured output at k sample time instant, $\hat{y}_k$ is the predicted output at the k^{th} sample time instant, L is an updating factor and is often taken to be 1. As shown in Figure 6.1, the measured output is compared with the predicted output and an updated prediction is obtained and used in the MPC development.

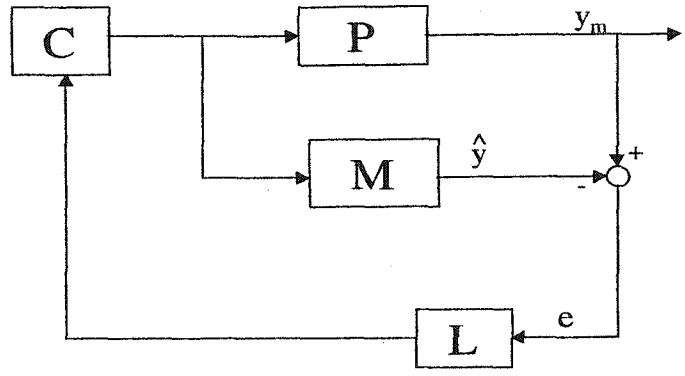

Figure 6.1: Structure of model-plant mismatch compensation in CBMPC

The control action that minimizes the objection function

$$\mathbf{J} = (\mathbf{y}^r - \hat{\mathbf{y}})^T \mathbf{Q} (\mathbf{y}^r - \hat{\mathbf{y}}) + \Delta \mathbf{u}^T \mathbf{R} \Delta \mathbf{u}, \tag{6.11}$$

is:

$$\Delta \mathbf{u} = (\mathbf{S}^T \mathbf{Q}^T \mathbf{Q} \mathbf{S} + \mathbf{R}^T \mathbf{R})^{-1} \mathbf{S}^T \mathbf{Q}^T \mathbf{Q} (\mathbf{y}^r - \hat{\mathbf{y}}_\mathbf{0} - \mathbf{e}). \tag{6.12}$$

By neglecting the effect of diffusion, the current control action can influence the output only until the residence time. Thus it is reasonable to choose a prediction horizon time to be equal to the residence time. The CBMPC for the system in Equation (6.6) can be developed using the following procedure:

Step I At time t_0, assume $e_k = 0$.

Step II Calculate $\hat{\mathbf{y}}_\mathbf{0}$ and S based on Equation (6.8), by using the same technique as that described in chapter 4. Calculate the control action $\Delta \mathbf{u}$ using Equation (6.12).

Step III Implement the first element of $\Delta \mathbf{u}$. Get the output measurement y^m at time t_1. Update e using Equation (6.10).

Step IV Repeat Steps II and III.

This compensation scheme can be used to correct the output prediction obtained from the approximate hyperbolic PDE models. It can also be used in other cases of model-plant

mismatch to improve the robustness of the CBMPC proposed in chapters 4 and 5. Using this scheme in CBMPC development yields an approach that applies to the systems where the effect of diffusion is small. As the contribution of the diffusion term increases, control performance of the CBMPC is expected to degrade.

6.3 Finite Difference Approximation

Adding boundary conditions to the PDE (6.6) yields:

$$\begin{aligned} &\frac{\partial v}{\partial t} + a(x)\frac{\partial v}{\partial x} - b(x)\frac{\partial^2 v}{\partial x^2} = f(x, v, u), \\ &\frac{\partial v}{\partial x}(x = 0) = \alpha(v_{x=0} - v_{in}), \\ &\frac{\partial v}{\partial x}(x = 1) = \beta(v_{x=1} - v_{out}) = 0, \\ &y = v(x_{out}). \end{aligned} \tag{6.13}$$

As discussed in the previous section, ignoring the diffusion term yields the characteristic vector field:

$$\frac{\partial}{\partial \xi} = \frac{\partial}{\partial t} + a(x)\frac{\partial}{\partial x}. \tag{6.14}$$

Along this characteristic direction, the parabolic PDE in Equation (6.13) can be described as:

$$\begin{aligned} \dot{t} &= 1, \\ \dot{x} &= a(x), \\ \dot{v} &= b(x)\frac{\partial^2 v}{\partial x^2} + f(x, v, u). \end{aligned} \tag{6.15}$$

This is an exact expression of the original PDE, but presence of a second-order spatial derivative makes it more complicated than that for a hyperbolic system.

The solution method using Equation (6.15) requires replacing the second-order derivative by some numerical approximation. Here, the approximation using centered finite difference is adopted (see Figure 6.2):

$$\frac{\partial^2 v}{\partial x^2} = \frac{v(x_{i+1}) - 2v(x_i) + v(x_{i-1})}{h_x^2}, \qquad \text{for } x = x_2, ..., x_{m-1}, \tag{6.16}$$

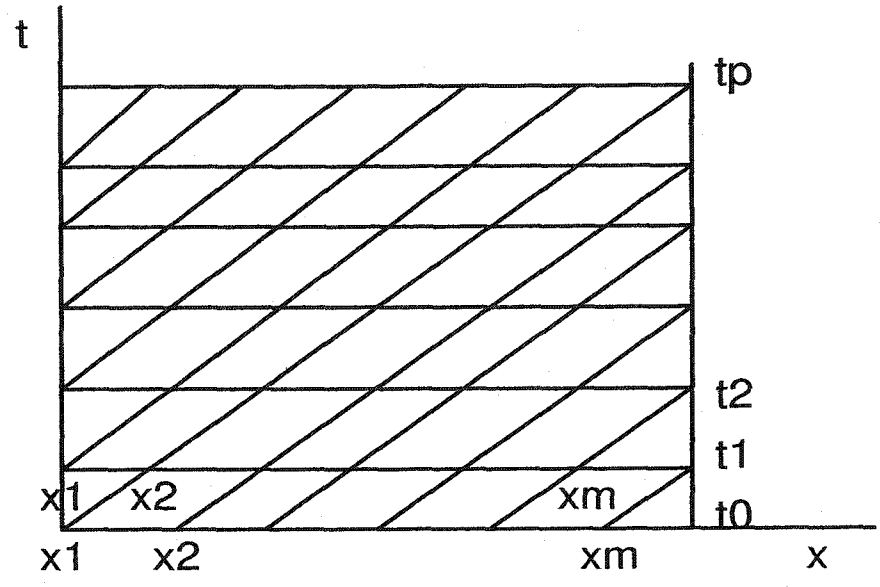

Figure 6.2: Output prediction using CMCFD

where h_x is a spatial step. The approximation of the second-order derivative of v at boundaries can be developed based on the boundary conditions:

$$\begin{aligned} \frac{\partial^2 v}{\partial x^2} &= \frac{1}{h_x}\left(\frac{v(x_2)-v(x_1)}{h_x} - \alpha(v_{x=0}-v_{in})\right), \qquad \text{for } x = x_1, \\ \frac{\partial^2 v}{\partial x^2} &= \frac{1}{h_x}\left(0 - \frac{v(x_m)-v(x_{m-1})}{h_x}\right), \qquad \text{for } x = x_m. \end{aligned} \tag{6.17}$$

Substituting the finite difference approximation of the second-order derivative in Equations (6.16) and (6.17) into Equation (6.15), the parabolic PDE model in Equation (6.13) can be described by a system of ODEs:

$$\begin{aligned} \dot{t} &= 1, \\ \dot{x} &= b(x), \\ \dot{v}_{x_1} &= a(x)\frac{1}{h_x}\left(\frac{v_2-v_1}{h_x} - \alpha(v_{x=0}-v_{in})\right) + f(x,v_1,u), \\ \dot{v}_{x_i} &= a(x)\frac{v_{i+1}-2v_i+v_{i-1}}{h_x^2} + f(x,v_i,u), \qquad i = 2,...m-1, \\ \dot{v}_{x_m} &= a(x)\frac{1}{h_x}\left(0 - \frac{v_m - v_{m-1}}{h_x}\right) + f(x,v_m,u). \end{aligned} \tag{6.18}$$

Integrating this system of equations, from the current state variable values at $x_1, x_2, ..., x_m$, leads to output prediction at future sample instants. For output prediction, the value of v at $x = 0$ is needed and can be calculated by combining the boundary condition with the finite difference approximation of the first-order spatial derivative:

$$\begin{aligned} \frac{\partial v}{\partial x} &= \alpha(v_{x=0} - v_{in}) \\ &= \frac{(v_{x_2} - v_{x_1})}{h_x}. \end{aligned} \tag{6.19}$$

Then, the value of v at $x = 0$ can be approximated by:

$$v_{x_1} = \frac{\alpha h_x v_{in} + v_{x_2}}{\alpha h_x + 1}. \tag{6.20}$$

Various numerical integration schemes can be used to integrate Equation (6.18) along the characteristic direction. The integral time step can be taken as $\Delta t = \frac{1 - x_m}{a(x)}$, or less.

Based on the prediction obtained by integrating Equation (6.18), the CBMPC for convection-dominated systems can be developed using the same approach as that for hyperbolic systems. By expressing the output-input relation in a locally linearized form:

$$\hat{\mathbf{y}} = \hat{\mathbf{y}}_\mathbf{0} + \mathbf{S}\Delta\mathbf{u}, \tag{6.21}$$

the control action minimizing the same objective function as that in Equation (6.11) is:

$$\Delta\mathbf{u} = (\mathbf{S}^T\mathbf{Q}^T\mathbf{Q}\mathbf{S} + \mathbf{R}^T\mathbf{R})^{-1}\mathbf{S}^T\mathbf{Q}^T\mathbf{Q}(\mathbf{y}^r - \hat{\mathbf{y}}_\mathbf{0}). \tag{6.22}$$

The calculation of $\mathbf{S}$ and $\hat{\mathbf{y}}_\mathbf{0}$ at every sample instant constitutes the main part of the CBMPC on-line computation. $\mathbf{S}$ and $\hat{\mathbf{y}}_\mathbf{0}$ are obtained based on the integration of Equation (6.18) for the control action u_0 and $u_0 + \delta$.

Due to the diffusion mechanism, the current control action affects the output for a period longer than the residence time. Therefore, the CBMPC for convection-dominated systems using finite-difference approximation requires a prediction horizon time larger than the residence time in order to get a stable and smooth operation.

6.4 Example - Bleaching Reactor

The bleaching process is one of the last steps in pulp production. Its purpose is to improve the brightness of the pulp to a specified level that fulfills customers needs. The control objective for a bleaching reactor is then to obtain the desired brightness with a minimum output brightness variance at the lowest possible chemical cost. In this section, the two proposed CBMPC methods are evaluated, via simulation, on a bleaching reactor modelled by a system of parabolic PDEs.

6.4.1 Using Mismatch Compensation

The CBMPC using model-plant mismatch compensation technique is applied to bleaching reactors in this subsection. Both SISO and MIMO control cases are considered.

Bleaching Reactors-SISO

A PDE model for the bleaching reactor can be obtained by mass balance on lignin and ClO_2 in the reactor and the model varies for different kinetic structures. Assuming a nonlinear kinetic structure, the model takes the form (Renou *et al.*, n.d.):

$$\begin{aligned}
\frac{\partial L}{\partial t} &= -u\frac{\partial L}{\partial x} + D\frac{\partial^2 L}{\partial x^2} - k_L C^2 L^2, \\
\frac{\partial C}{\partial t} &= -u\frac{\partial C}{\partial x} + D\frac{\partial^2 C}{\partial x^2} - k_C C^2 L^2, \\
\frac{\partial L}{\partial z}|_{z=0} &= \frac{u}{D}(L(0,t) - L_{in}(t)), \\
\frac{\partial C}{\partial z}|_{z=0} &= \frac{u}{D}(C(0,t) - C_{in}(t)), \\
\frac{\partial L}{\partial z}|_{z=1} &= \frac{\partial L_{out}}{\partial x} = 0, \\
\frac{\partial C}{\partial z}|_{z=1} &= \frac{\partial C_{out}}{\partial x} = 0,
\end{aligned} \tag{6.23}$$

where: t is time, $x \in [0,1]$ is a normalized spatial coordinate and L is the concentration of Lignin, C is the concentration of ClO_2, u is superficial velocity and D is dispersion

coefficient. The concentration of the reactant L at the outlet is the variable to be controlled, for which a setpoint is specified. The concentration of the reactant C is used as the control variable at the inlet. The process parameters are: $k_L = 0.0065$, $k_C = 0.0010$, $v = 1/30$ and $D = 0.001$.

The CBMPC proposed in Section 6.2 was applied to the system, taking the inlet concentration of Lignin as $L_{in} = 9$ Kappa, with the reactor initially at steady state. The output responses are shown in Figure 6.3 for a setpoint change from 5 Kappa to 6 Kappa. Note the transport delay of approximately 30 min observed in the process output. From Figure 6.3, it is observed that the proposed CBMPC with mismatch compensation generates a satisfactory output response.

In the bleaching reactor, the concentration of the reactant L at the inlet, L_{in}, is determined by the previous processes and may vary due to operation variations. Simulation was performed to investigate the process response of the proposed CBMPC for measured and unmeasured disturbances in L_{in}. Figure 6.4 shows the process output response and the control action for measured disturbances in L_{in}. The proposed CBMPC can reject measured disturbances in L_{in} and ensures the process output back to the desired setpoint. The capability of the CBMPC with the mismatch compensation in rejecting the unmeasured disturbances in L_{in} is illustrated in Figure 6.5. It appears that unmeasured disturbances perturb the process more than measured disturbances and the process output deviates farther from the setpoint, but the CBMPC can reject the unmeasured disturbances and drive the process output back to setpoint. The capability of the proposed CBMPC to reject the unmeasured disturbances results from the mismatch compensation scheme used.

Renou and Perrier (Renou and Perrier, 2000) used global differences as an approximation for the spatial partial derivatives and developed a nonlinear controller for the bleaching process with the form:

$$\begin{aligned} C_{\text{in}}(t) = \frac{1}{v+D}(vC_{\text{out}}(t) + DC_{\text{out}}(t) + \frac{C_{\text{out}}(t) - C_{\text{out}}(t-1)}{\Delta t} \\ + \frac{k_{C_1}}{k_{L_1}}[u - v(L_{\text{out}}(t) - L_{\text{in}}(t)) + D(L_{\text{in}} - L_{\text{out}}), \\ u = \lambda[(L_{\text{sp}} - L_{\text{out}}(t)) + \gamma \textstyle\int_0^t (L_{\text{sp}} - L_{\text{out}}(\tau))d\tau], \end{aligned} \tag{6.24}$$

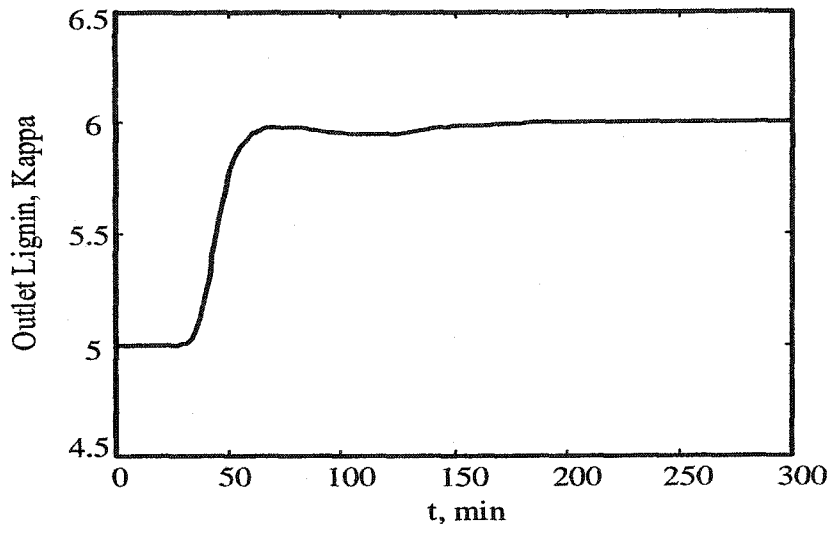

(a) output

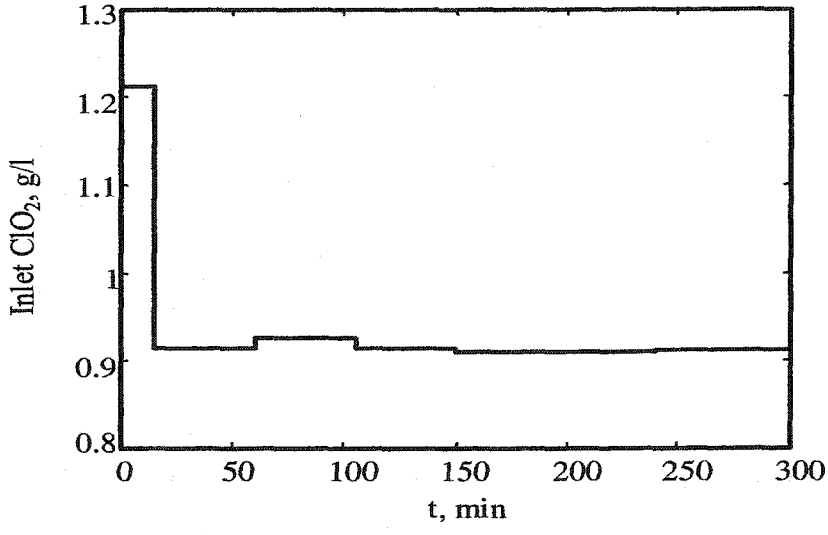

(b) manipulated variable

Figure 6.3: Output response of the CBMPC with mismatch compensation in the bleaching reactor

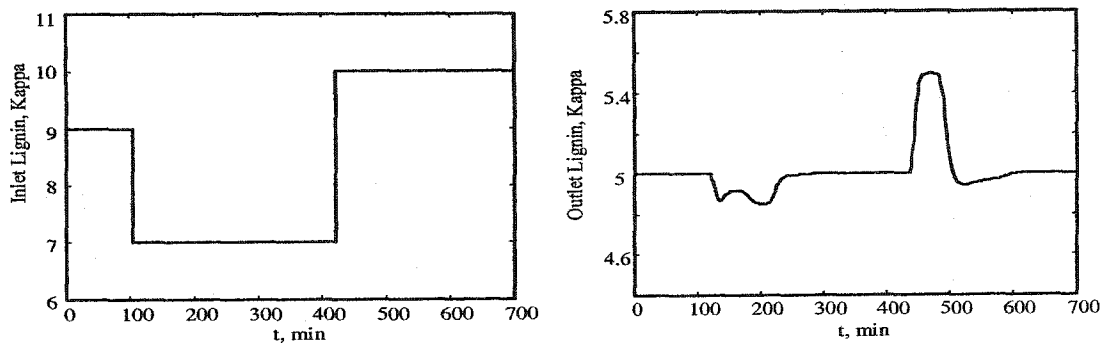

(a) measured disturbance (b) output

Figure 6.4: Output response to measured disturbances using CBMPC with mismatch compensation in the bleaching reactor

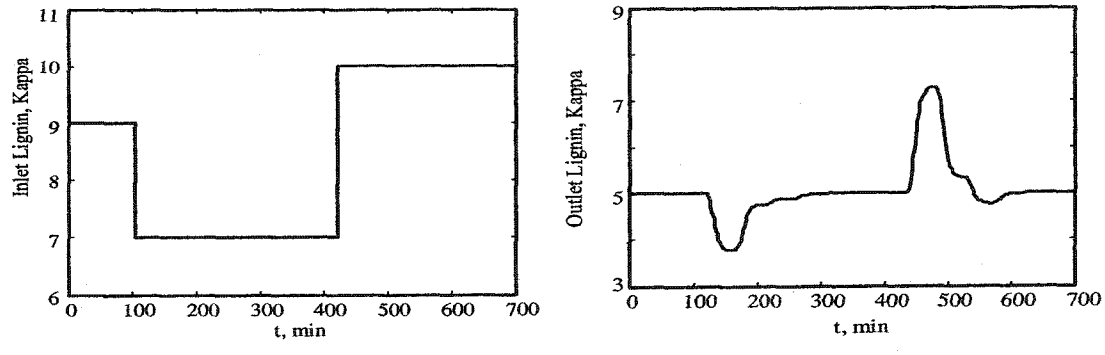

(a) unmeasured disturbance (b) output

Figure 6.5: Output response to unmeasured disturbances using CBMPC with mismatch compensation in the bleaching reactor

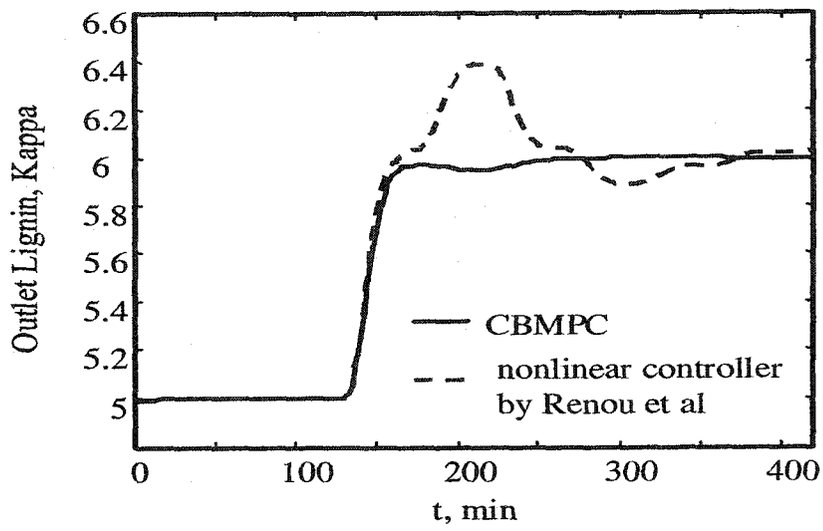

(a) output

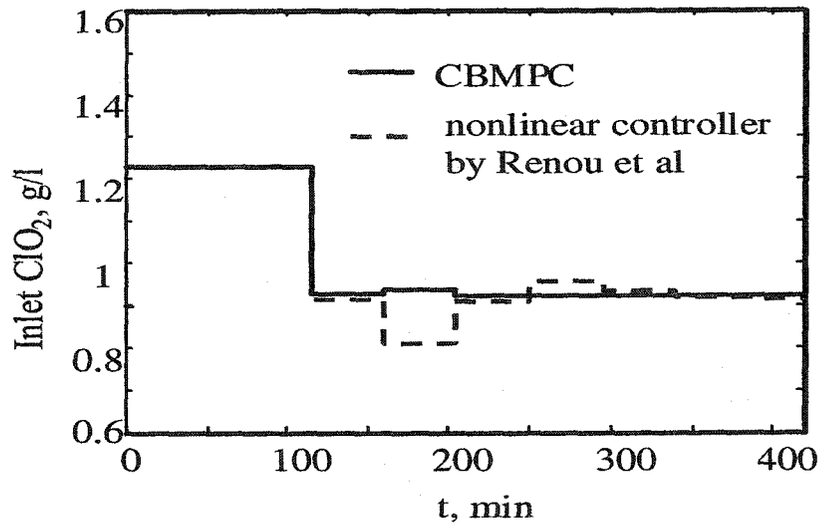

(b) manipulated variable

Figure 6.6: Performance comparison of CBMPC with mismatch compensation *vs.* nonlinear feedback control in the bleaching reactor

where λ and γ were PI tuning parameters, for which $\lambda = -0.05$ and $\gamma = 0.02$ were used in the simulation. The setpoint tracking behavior of the proposed CBMPC scheme and the nonlinear controller in Equation (6.24) are compared in Figure 6.6. For this simulation study, the proposed CBMPC approach exhibits better performance than the nonlinear controller of Equation (6.24) in terms of output response, with less aggressive control action.

Bleaching Reactor-MIMO

In this section, the applicability of the CBMPC with the mismatch compensation to multi-input multi-output control is examined on a bleaching reactor. Assuming a linear kinetic structure, the reactor is modelled by:

$$\begin{aligned}
\frac{\partial L}{\partial t} &= -u\frac{\partial L}{\partial x} + D\frac{\partial^2 L}{\partial x^2} - k_1 C - k_2 L, \\
\frac{\partial C}{\partial t} &= -u\frac{\partial C}{\partial x} + D\frac{\partial^2 C}{\partial x^2} - k_3 C - k_4 L, \\
\frac{\partial L}{\partial z}|_{z=0} &= \frac{u}{D}(L(0,t) - L_{in}(t)), \\
\frac{\partial C}{\partial z}|_{z=0} &= \frac{u}{D}(C(0,t) - C_{in}(t)), \\
\frac{\partial L}{\partial z}|_{z=1} &= \frac{\partial L_{out}}{\partial x} = 0, \\
\frac{\partial C}{\partial z}|_{z=1} &= \frac{\partial C_{out}}{\partial x} = 0.
\end{aligned} \tag{6.25}$$

The two outputs are the outlet concentrations of Lignin and ClO_2, L_{out} and C_{out}, and the two inputs are the inlet concentrations of Lignin and ClO_2, L_{in} and C_{in}.

Similar to the SISO case, the controller for this system is developed based on the approximate model obtained by ignoring the diffusion term in Equation (6.25). According to the Method of Characteristics, the current control variables L_{in} and C_{in} only affect the process output L_{out} and C_{out} in the future at the residence time $\Delta t = 1/u$. Therefore, the CBMPC with a prediction horizon of $1/u$ is used.

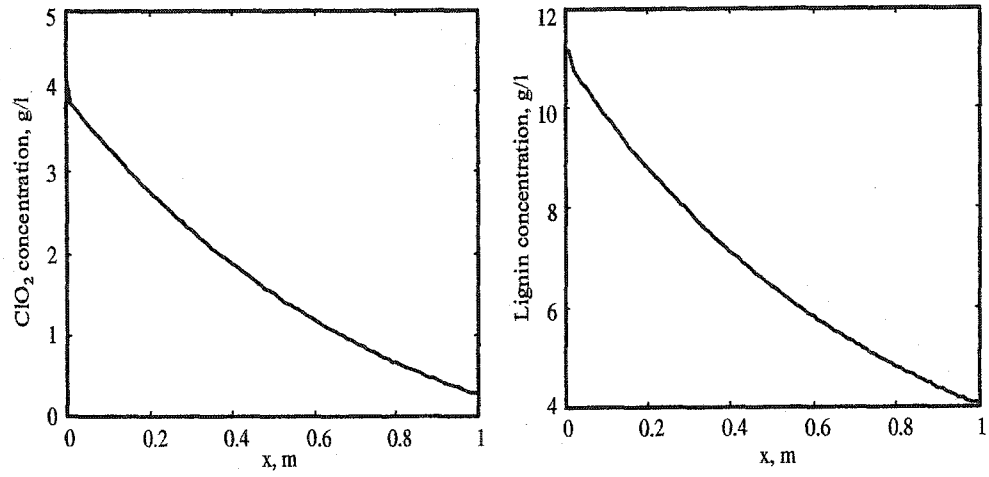

(a) ClO_2 (b) lignin

Figure 6.7: Initial profiles of the state variables in the MIMO bleaching reactor

Set

$$K = -\begin{bmatrix} k_1 & k_2 \\ k_3 & k_4 \end{bmatrix} . \tag{6.26}$$

Since the reactions are linear, the analytical expression of the future outputs from the approximate model can be expressed explicitly using the Method of Characteristics:

$$\begin{bmatrix} C_{out} \\ L_{out} \end{bmatrix} (t + \Delta t) = \exp(K\Delta t) \begin{bmatrix} C_{in} \\ L_{in} \end{bmatrix} (t) + \begin{bmatrix} e_C \\ e_L \end{bmatrix} . \tag{6.27}$$

In the above expression, e_C and e_L are obtained iteratively as described in the last section. The control variables L_{in} and C_{in} are formulated such that the process outputs converge to their setpoint.

The simulation was performed by discretizing the PDE model along the space into 100 points and applying the finite difference method to Equation (6.25). The model parameters were taken as: $v = 0.05$ m/s, $D = 0.0005\ m^2/s$, $k_1 = 0.03$ 1/s, $k_2 = 0.02$ 1/s, $k_3 = 0.05$ 1/s, $k_4 = 0.04$ 1/s. For the initial state variable profiles as shown in Figure

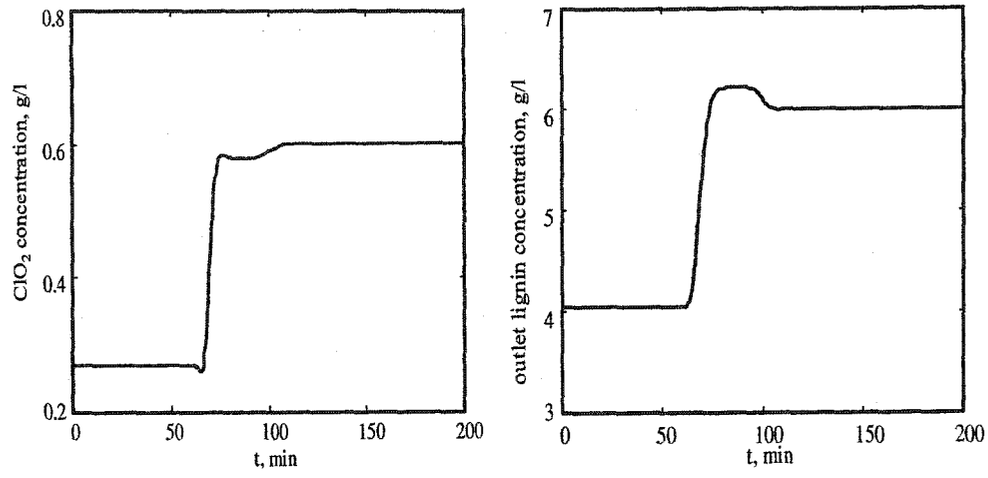

(a) controlled variable C_{out} (b) controlled variable L_{out}

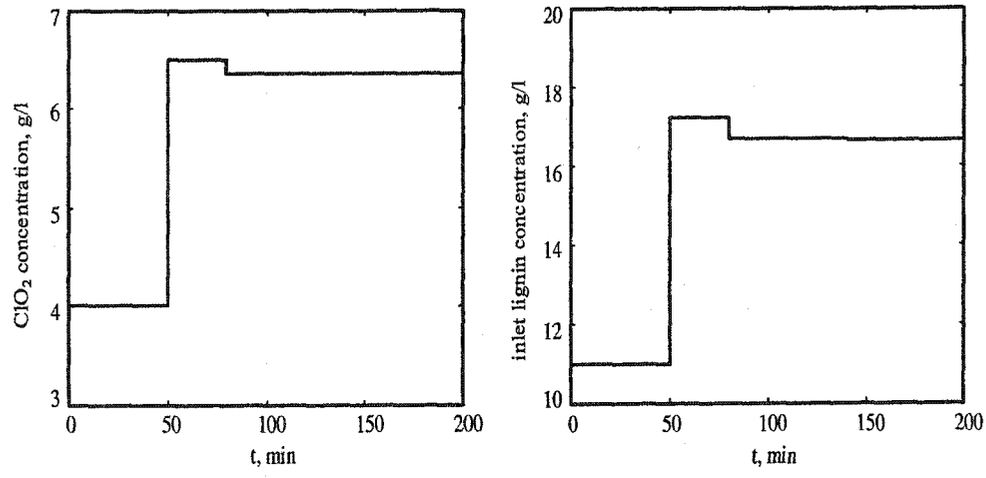

(c) manipulated variable C_{in} (d) manipulated variable L_{in}

Figure 6.8: Process response to setpoint changes under CBMPC with mismatch compensation in the MIMO bleaching reactor

6.7, the process response for the setpoint change was examined when the setpoint of C changes to 0.6 g/l and the setpoint of L changes to 6 g/l. From Figure 6.8, it can be seen that the CBMPC using the mismatch compensation scheme is able to drive the process outputs to their setpoints. In spite of the inherent process transport delay, the process has quick response to the setpoint changes under the CBMPC.

The performance of the controller to disturbances were investigated. Figure 6.9 shows the process response for the measured disturbances in u. It is observed that the CBMPC rejects the measured disturbances well and the process returns to the setpoint quickly. Figure 6.10 shows the output response if the disturbances in u are unmeasured. Even though the process displays larger deviation from the setpoint for the unmeasured disturbance than that for the measured disturbance, the process outputs return to the setpoint in a reasonably short period of time and the CBMPC using mismatch compensation has the capability of rejecting the unmeasured disturbances.

6.4.2 Using Finite Difference Approximation

The bleaching reactor discussed in the last subsection can also be used to illustrate the CBMPC with the finite difference approximation in this section. As in model (6.23), the inlet concentration C_{in} is manipulated to control the outlet concentration L_{out}.

The process output is predicted using the CBMPC scheme based on CMCFD, which requires the approximation of the diffusion term using the finite difference method. For the finite difference approximation of the diffusion term, the process is discretized into m grids. The prediction sampling time is set to be $\frac{1}{mu}$, where u is defined as in Equation (6.23). The finite difference approximation of the diffusion term is obtained at the beginning of every sample instant and assumed to keep constant until the next sample instant. By this approximation, output prediction can be performed by integrating the low-dimensional ODEs. The accuracy of the output prediction using CMCFD requires the convection term to be dominant over the diffusion term (*i.e.*, large Peclet number).

For the purpose of simulation, the process was represented by discretizing the PDE

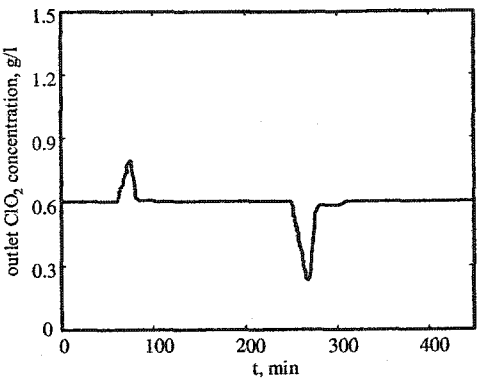

(a) controlled variable C_{out}

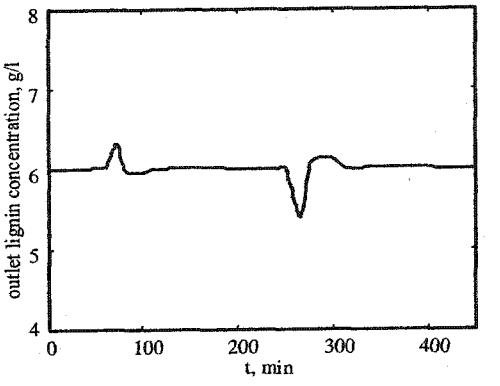

(b) controlled variable L_{out}

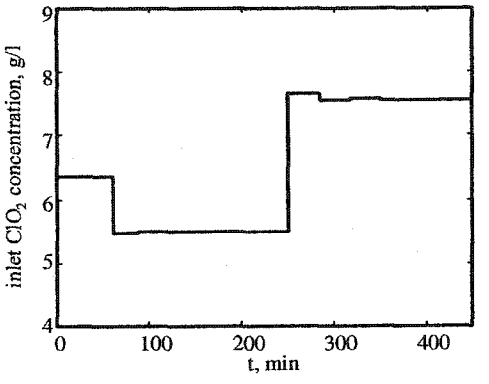

(c) manipulated variable C_{in}

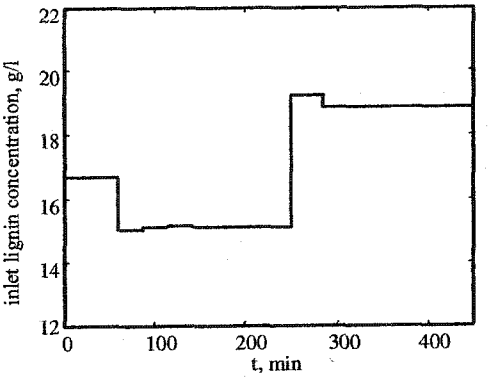

(d) manipulated variable L_{in}

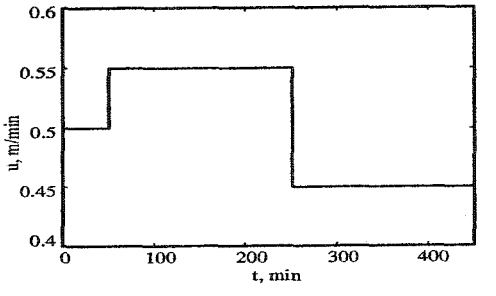

(e) measured disturbances in u

Figure 6.9: Process response to measured disturbances in u under CBMPC in the bleaching reactor

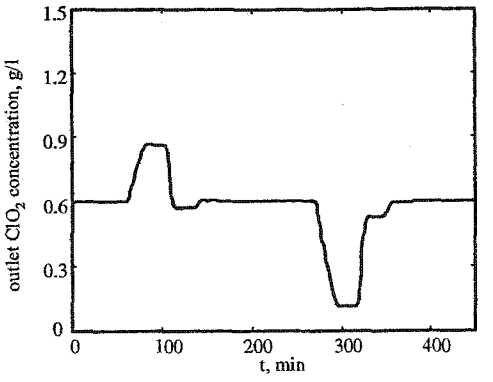

(a) controlled variable C_{out}

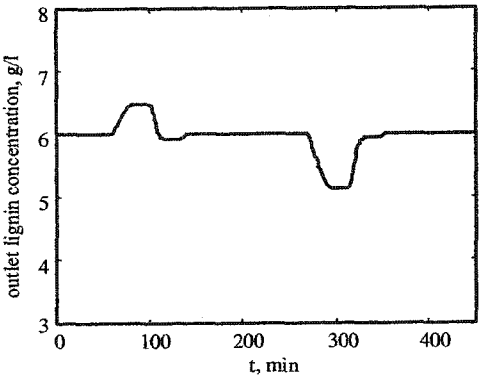

(b) controlled variable L_{out}

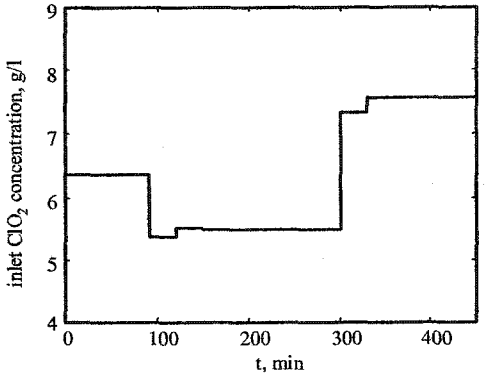

(c) manipulated variable C_{in}

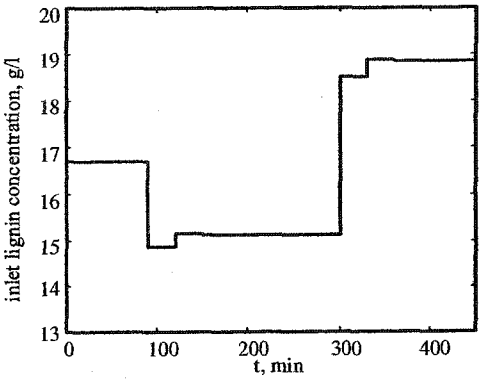

(d) manipulated variable L_{in}

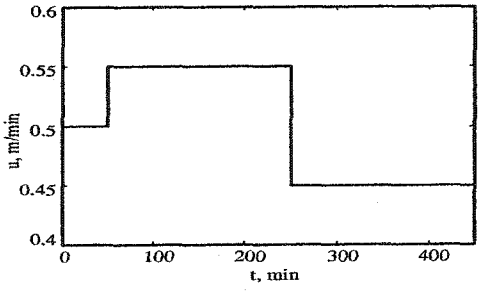

(e) unmeasured disturbances in u

Figure 6.10: Process response to unmeasured disturbances in u under CBMPC in the bleaching reactor

model into a large number of ODEs (more than 200 discretization points). The initial condition used was the steady state with $C_{in} = 1.3$ g/l and $L_{in} = 9$ Kappa. For a change in manipulated variable C_{in} from 1.3 g/l to 2 g/l, the process output prediction using CMCFD ($m = 10$) was compared with the 'real' process output obtained via fine discretization for different values of $1/Pe$. Figure 6.11 shows the comparison of output prediction using different schemes, where solid line indicates the 'true' process output, dashed line indicates the predicted output using CMCFD, and dash-doted line indicates the predicted output obtained by ignoring the effect of diffusion and using the Method of Characteristics. When $D = 0$, the diffusion term vanishes and CMCFD technique becomes the Method of Characteristics and provides an accurate description of the process. For small values of 1/Pe, CMCFD generates better prediction than the pure Method of Characteristics at a slightly higher computation expense. As 1/Pe increases, the predicted output using CMCFD displays oscillation and the solution becomes unstable. This is because the large discretization spatial steps for approximating the diffusion term can lead to solution instability when diffusion becomes important.

The absolute values of the error for the predicted steady state output using both CMCFD and the pure Method of Characteristics are shown in Table 6.1 and Figure 6.12. It can be seen that the absolute error of the steady state output prediction using CMCFD is much smaller than that using the Method of Characteristics when diffusion exists but is not dominant. When 1/Pe increases to 0.06, the absolute error using CMCFD increases considerably and appears to increase exponentially beyond this point.

Using the operating conditions and the parameter values given in the last section, performance of the CMCFD-based MPC was examined for a setpoint change. Choosing $m = 5$ and the prediction horizon as $p = 15$, the MPC based on CMCFD technique yields a output response for a setpoint change to 6 kappa, as shown in Figure 6.13. It is observed that the process output converges to the setpoint quickly and smoothly without frequent control moves. In the case of no model plant mismatch, the process produces offset-free response.

The advantages of the proposed CMCFD-based CBMPC for convection-dominated

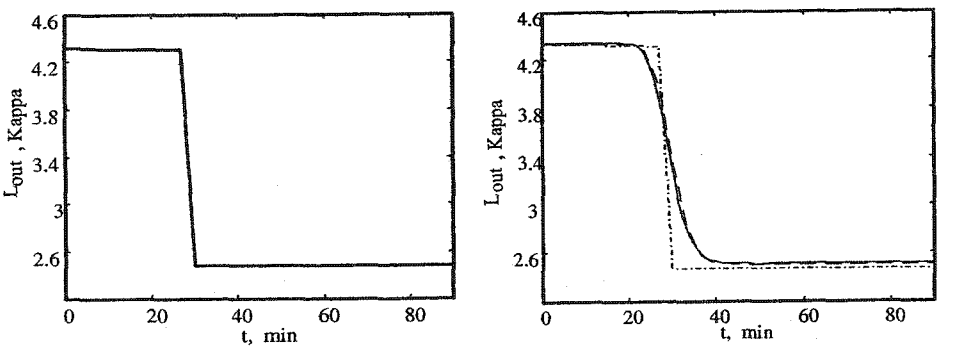

(a) $\frac{1}{Pe} = 0$ (b) $\frac{1}{Pe} = 0.006$

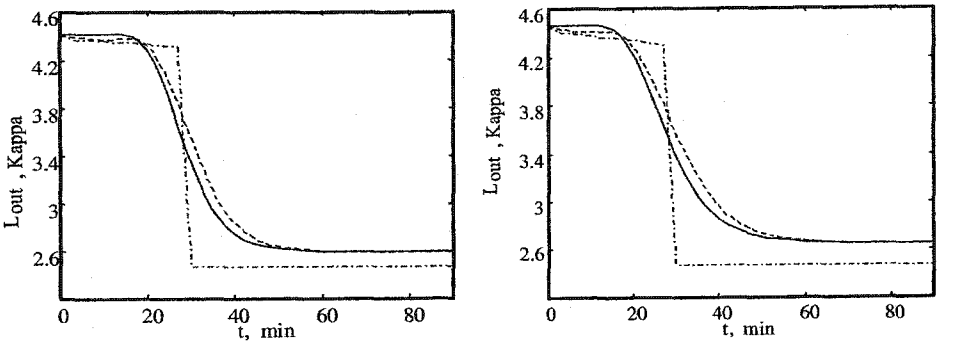

(c) $\frac{1}{Pe} = 0.03$ (d) $\frac{1}{Pe} = 0.045$

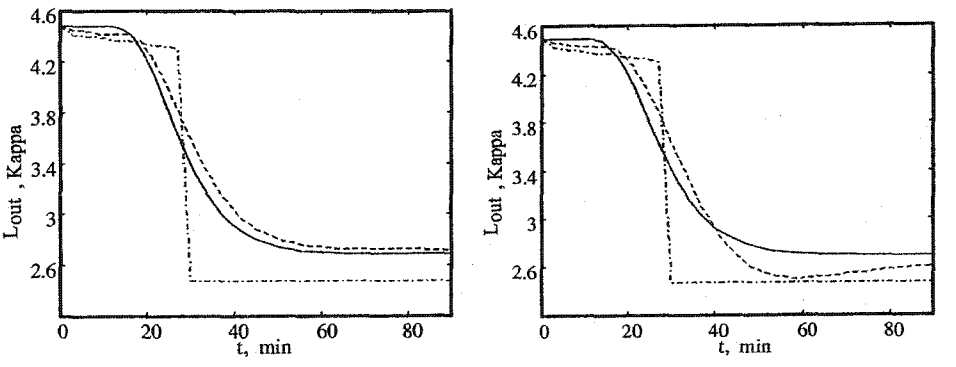

(e) $\frac{1}{Pe} = 0.054$ (f) $\frac{1}{Pe} = 0.06$

Figure 6.11: Output prediction of CMCFD for different 1/Pe in the bleaching reactor (C_{in} changes from 1.3 g/l to 2 g/l)

Table 6.1: Steady state output prediction error

1/Pe	Method of Characteristics	CMCFD
0	0	0
0.003	0.0194	0.0035
0.006	0.0344	0.0036
0.015	0.0716	0.0005
0.03	0.126	0.0013
0.045	0.0895	0.008
0.054	0.2122	0.0401
0.06	0.2209	0.0895

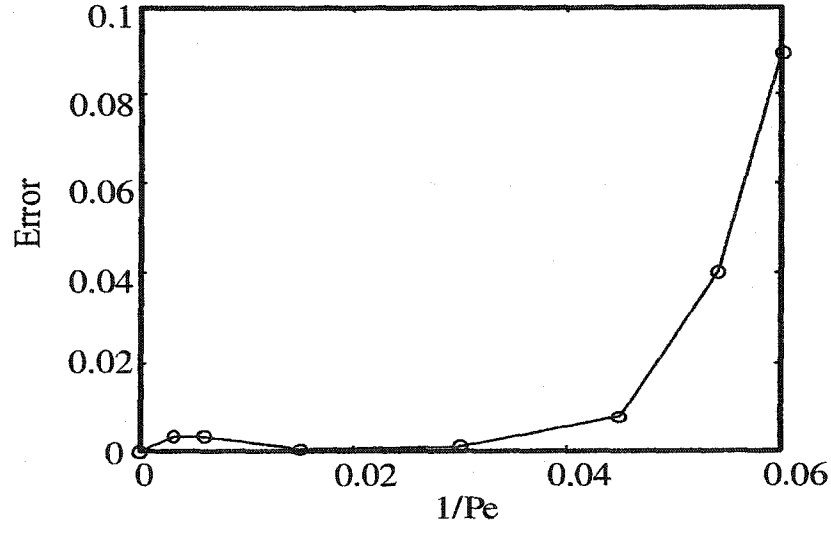

Figure 6.12: Output prediction error of CMCFD in the bleaching reactor

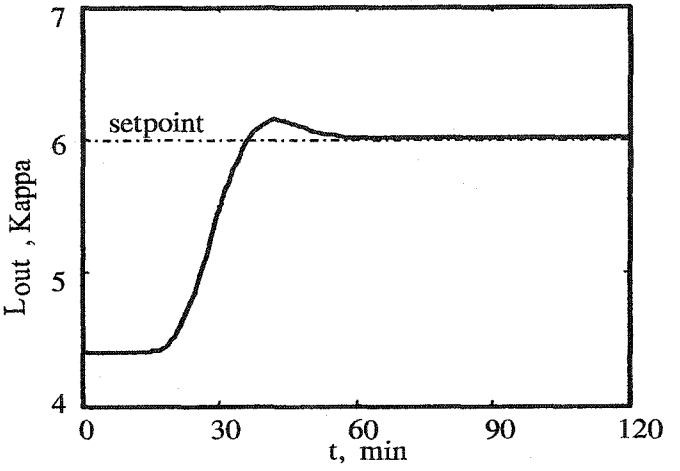

(a) output

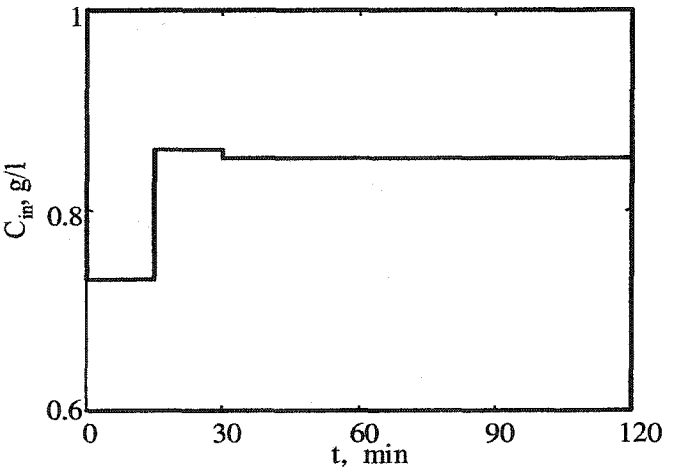

(b) manipulated variable

Figure 6.13: Output response of the CBMPC with CMCFD in the bleaching reactor

Table 6.2: Computations for CBMPC *vs.* conventional MPC in the bleaching reactor

Control Method	flops (in Matlab ©)
MPC using CMCFD (m=5)	4.756×10^5
MPC using finite difference (m=10)	4.207×10^6

parabolic systems can be shown by comparing the performance and computational efficiency of the MPC using the CMCFD with that using the finite difference method. The output response for a setpoint change using the CMCFD-based MPC and the finite difference based MPC is compared in Figure 6.14. For the outlet lignin concentration setpoint of 6 kappa, CMCFD-based MPC with 5 discretization points generates similar response to that of the finite difference based MPC with 10 discretization points, except that the finite difference based MPC generates larger offset and overshoot. The computational requirements of these two MPC methods are compared in Table 6.2, using "flops", the number of floating operations in Matlab. It is noted that the proposed CMCFD-based MPC requires only one tenth of the computation flops of the finite-difference based MPC, with smaller offset and smoother response. From an analysis of the two computation methods, the computational demand of the CMCFD-based MPC increases linearly with the number of discretization points while the finite difference based MPC increases nearly exponentially with the number of discretization points. Therefore, the proposed CBMPC using CMCFD has the advantage of combining prediction accuracy with computational efficiency, and yields a high performance control that is easy to implement.

The CMCFD-based CBMPC was compared with the CBMPC using mismatch compensation. The CBMPC using mismatch compensation for the bleaching reactor is developed by ignoring the diffusion term and applying the Method of Characteristics. The model-plant mismatch resulting from ignoring the diffusion term is compensated

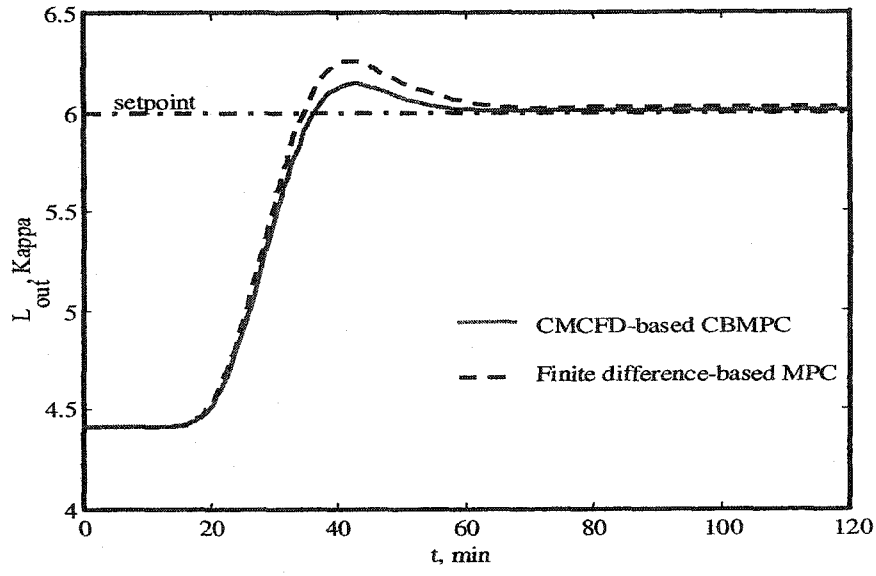

Figure 6.14: Comparison of CMCFD-based CBMPC *vs.* finite difference-based MPC

by adding the model-plant mismatch compensation term to the MPC. Since there is a remarkable time lag for the output to be affected by the input and the input can be adjusted by the error compensation term only after the effect of input is observed in the output, the CBMPC with mismatch compensation is expected to result in sluggish response in comparison to the CMCFD-based CBMPC. From Figure 6.15, the CMCFD-based CBMPC yields much quicker convergence to the setpoint.

In CMCFD, the impact of the prediction horizon on control performance is different from the CBMPC using the pure Method of Characteristics. The performance of proposed CBMPC based on CMCFD was examined for different prediction horizons. With a spatial discretization $m = 5$, the sampling time being $1/5u$. Figure 6.16 shows the output response for a setpoint change with prediction horizon being 3 residence times, 2 residence times and 1.5 residence times, respectively. It is observed that the prediction horizon of 1.5m or less results in oscillatory or even unstable process response. When the prediction horizon is 2m, the process output displays quick and smooth response with little overshoot. The overshoot decreases as the prediction horizon increases. Therefore, in contrast to hyperbolic systems, the parabolic system requires a prediction horizon larger

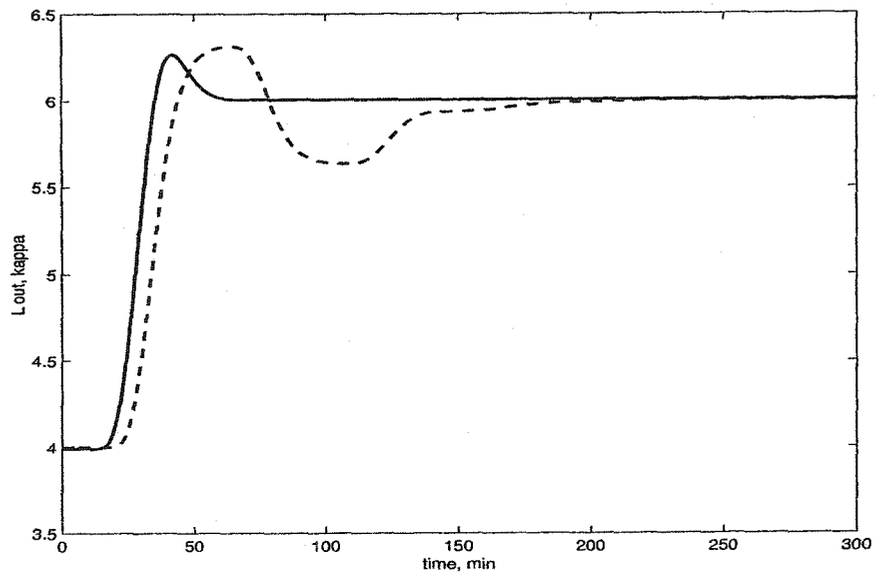

Figure 6.15: Comparison of CMCFD-based CBMPC *vs.* CBMPC with mismatch compensation

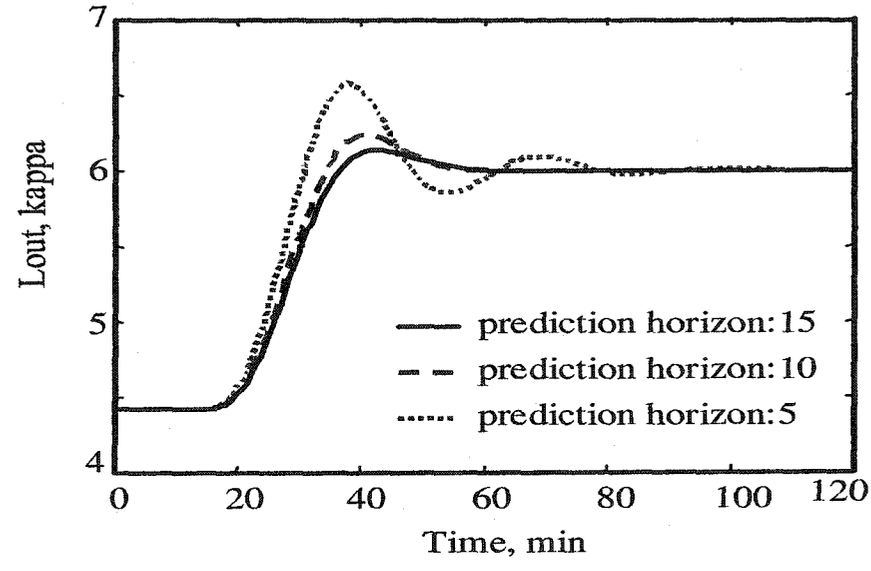

Figure 6.16: Output response of the CMCFD-based CBMPC for different prediction horizons

than the residence time, which leads to some increases in computational requirements.

6.5 Summary

Convection-dominated systems display hyperbolic nature, which can be exploited to develop a characteristic-based MPC for these systems. In this chapter, two approximation approaches are used to deal with the effect of diffusion and are combined into the CBMPC proposed for hyperbolic systems in the last two chapters.

The CBMPC with mismatch compensation takes the diffusion term as model-plant mismatch and adds a mismatch compensation term to the output prediction equation obtained from the approximate hyperbolic models. Simulation study of a bleaching reactor shows that this control scheme performs well, is computationally efficient, and is capable of dealing with both measured and unmeasured disturbances. The mismatch compensation used in this chapter also provides an effective way of dealing with model-plant mismatch for any of the problems within the scope of this thesis.

The CBMPC with CMCFD approximates the diffusion term by finite difference and then applies the Method of Characteristics to the resulting approximate model. When the diffusion term is relatively small, convection-dominated parabolic problems can be solved with the CMCFD approach using small dimensionality and satisfactory accuracy. Simulation on the bleaching reactor shows that this method applies to diffusion problems within a range of Pèclet numbers. In the bleaching reactor discussed in this chapter, the CMCFD provides an output prediction with high accuracy when the 1/Pe is in the range of $0 - 0.06$. This range increases with the finer discretization; however, a finer discretization increases the computational demand. Therefore, it is advantageous to apply the CMCFD for the output prediction when 1/Pe is small.

Overall, the computational demands of the CMCFD-based MPC are larger than those of the CBMPC with mismatch compensation due to the larger dimension of the approximate characteristic ODEs and longer prediction horizon requirement. In fact, the computation requirement of the CMCFD-based MPC is between the CBMPC and

the finite-difference based MPC. However, the CMCFD-based CBMPC produces better performance than the CBMPC with the mismatch compensation, resulting from the higher prediction accuracy. It can effectively overcome the sluggishness of output response, resulting from the time lag between input and output, and yields quick output convergence to setpoint for convection-dominated parabolic systems.

Chapter 7

Conclusions and Recommendations

Many industrial processes are distributed parameter systems and can be modelled by first-order hyperbolic PDEs or second-order parabolic PDEs with high hyperbolicity. Geometric understanding of these PDE models leads to a powerful solution method, the Method of Characteristics, for these systems. Control development based on this method shows the promise of improving the control performance and generating a control design that is advantageous for implementation in industrial operations. This thesis has been devoted to the development of high performance control for DPS by exploring the characteristic properties of the PDE models.

7.1 Conclusions

Although the Method of Characteristics has been well recognized as an elegant solution method for PDE systems, limited results have been reported on the control development for PDE systems using this method. This thesis provides the design of standard feedback control and model predictive control for PDE systems using the Method of Characteristics. Initial work focussed on designing a standard feedback control for systems modelled by first-order scalar PDEs using a nonlinear feedback control strategy

based on the characteristic ODEs of the underlying PDE model. The resulting feedback control scheme has a relatively simple formulation in comparison to available feedback controller in the literature and good performance in comparison to conventional PI control.

The development of the standard feedback control for first-order scalar PDE systems was discussed in Chapter 3. Based on the Method of Characteristics, a state feedback control scheme was formulated using nonlinear feedback control technique with an additional integral term. The resulting state feedback controllers possess the simple form of PI control plus a feedforward term. In comparison to the available feedback control methods for PDE systems, the proposed feedback control approach does not require demanding computation and can produce satisfactory performance to setpoint changes and various disturbances. Asymptotic stability of the state feedback control was proved based on the technique of a time transformation along the characteristics. The implementation of the state feedback control requires estimation of the infinite-dimensional state variables, which has been a challenging subject in DPS control. In this thesis, design of an infinite-dimensional state observer was discussed based on the semigroup theory, and a sufficient condition for the estimated state to converge to the true state was proposed. The simulation study illustrated an example of designing an infinite-dimensional state observer. General design methods remain to be developed.

In spite of the good performance of the proposed feedback control approach, several limitations of this method became evident: the proposed controller performance is limited by the "speed" of the process dynamics and will be sluggish for DPS with slow dynamics; the control scheme is only applicable to a narrow class of hyperbolic systems; and extension of the method to more complex system is not promising. Recognition of these limitations of standard feedback control for DPS motivated research on the characteristic-based MPC.

Due to the observation that in DPS the effect of control action on output is usually not immediate and control without explicitly including the prediction horizon can lead to sluggish or oscillatory process response, research was directed towards model predictive

control. The Method of Characteristics permits one to predict the future output from the current state variable profile with high accuracy and efficient computation. The resulting CBMPC fully exploits the information from the Method of Characteristics and yields a control approach that combines an accurate continuous PDE model with a digital MPC formulation. The application of the Method of Characteristics in model predictive control is a new approach, as there has been no previous work reported in the literature. The research in this thesis indicates that such an approach provides an efficient use of geometric tools in advanced control of complex systems and is a worthwhile subject.

Extensive efforts were made to develop the characteristic-based MPC for various hyperbolic PDE systems, and examples were used to illustrate different cases. The MPC technique for hyperbolic systems was also extended to an important group of second-order parabolic PDE systems using a combination of the finite-differences and the Method of Characteristics, a technique that has garnered the interest of mathematicians, but has been neglected by control researchers. In the MPC approach of this thesis, a particular focus has been on output control (mostly single output) at the boundary.

Chapter 4 presented the CBMPC development for processes with a relatively simple characteristic nature. In MPC, prediction of future process behavior has a great influence on the resulting control performance and the required on-line computations. Use of the Method of Characteristics for future output prediction was one of the focuss in Chapter 4. The characteristic-based output prediction method was presented for hyperbolic systems with single characteristics. Such systems can be exactly described by a system of ODEs, and the decoupled nature of these characteristic ODEs makes the output prediction in the proposed CBMPC accurate and computationally efficient. For linear, scalar PDE systems, this method led to an offline control law. Otherwise, a nonlinear quadratic MPC algorithm was used to calculate the control action. The CBMPC for linear systems discussed in this chapter was proved to have guaranteed stability. A terminal constraint was added to the proposed CBMPC approach to ensure stability of the method for quasilinear systems. Simulation studies using a heat-exchanger and a PFR with uniform heating were presented to illustrate the CBMPC development for linear and quasilinear systems.

The CBMPC for hyperbolic systems with a single characteristic is a straightforward application of the characteristics inherent in the PDE models.

The CBMPC for hyperbolic systems with multiple characteristics was discussed in chapter 5. The focus was on systems of two first-order PDEs and second-order scalar PDEs. Applying the Method of Characteristics to these more complicated systems led to multiple sets of characteristic ODEs. The coupled nature of the ODEs affects the prediction accuracy and computational efficiency of the CBMPC for such systems. In spite of the increased computational load, the resulting CBMPC is capable of yielding reasonable performance due to high prediction accuracy. The corresponding on-line computation is less than the MPC using the finite difference method. Complexity of the CBMPC for systems with multiple characteristics increases significantly in comparison to that for single characteristics. The CBMPC design for systems with more than two characteristics does not involve new ideas, and was not considered in the thesis. However, it is expected that, as dimension and/or complexity of the characteristics increase, the CBMPC may not be an effective approach in comparison with other MPC schemes.

Chapter 6 presented an extension of the CBMPC to convection-dominated second-order parabolic systems. Many industrial processes characterized by diffusion and convection often possess important hyperbolic nature due to the relative dominance of convection. Two control strategies were proposed using the different ways of approximating the diffusion terms. CBMPC with mismatch compensation generates acceptable control performance with efficient computation. Moreover, the proposed mismatch compensation technique provides a way of improving the robustness for all CBMPC in this thesis. Approximating the diffusion term via finite differences leads to a new approach, the combination of the finite-difference and the Method of Characteristics, which makes an efficient and relatively accurate numerical scheme to predict the future process states and outputs for these processes. Use of this technique in controller development is innovative and no previous work has been reported.

The characteristic-based control methods proposed in this thesis are shown to be promising approaches in the control of DPS due to improved performance and relatively

low computational requirements. The application of these approaches may require some preliminary geometric analysis of the systems and their PDE model. The advantages of such methods diminish as the characteristics of the PDE models become complicated or the hyperbolicity of the systems decreases. The applicability of the proposed control approaches is limited by the characteristic nature of the systems.

7.2 Recommendations

This thesis was devoted to the control developments for DPS using geometric techniques and significant progress was made in developing characteristic-based control approach. It is recognized from the thesis that the PDE-based control using geometric tools is a fascinating subject and the research of this thesis is by no means exhaustive.

Design of an infinite dimensional state observer is important but challenging in control of DPS. The thesis proposed a state observer design structure based on Semigroup theory. However, the abstract formulation does not provide guidelines for selection of design parameters and/or operators. Further development of infinite dimensional state observers will include justification of the observer structures, specific guidelines of design procedures as well as the parameter selection.

The proposed state feedback control was proved to have closed-loop stability. The output feedback control laws were obtained by combining the state feedback controllers and the state observers. The thesis did not imply that stability of the resulting output feedback controllers were ensured by separate stability of the state feedback controllers and the state observers. Therefore, it is important to investigate stability of the proposed output feedback controllers.

In this thesis, it was assumed that there were no model plant mismatch. Since this can be a significant issue in industrial practice, further work is required. Similarly, only deterministic processes were considered here, yet most industrial processes exhibit some stochastic behavior. Consideration of the stochastic dynamics would widen the applicability of the proposed techniques.

To implement the proposed CBMPC, it requires the information of current state variables at some discrete spatial points. The state observer for CBMPC and the requirement of number and location of measuring sensors for observer design will be in the future work.

The characteristic-based MPC in this thesis did not consider constraints. Convenience of handling constraints is one of the reasons that MPC has gained wide popularity. The proposed CBMPC should extend easily to handle constraints in a similar fashion to other MPC schemes. Further work may be required to build a constrained CBMPC scheme.

Due to the finite horizon nature, general MPC schemes do not have guaranteed stability. In recognizing the importance of stability for the control laws, the stability of the CBMPC for systems with single characteristics was discussed. It was found that the CBMPC for linear systems had guaranteed stability. Further research is needed to address stability of the CBMPC for more complicated processes.

Much of the work in this thesis was mainly concerned with the systems having single characteristics or double characteristics of the opposite directions. In practical situations, the characteristics patterns in between exist and are not addressed by the thesis. The relative patterns of double characteristics definitely affect the discretization, sampling time and other elements of the control design. A complete study on the effect of the characteristics patterns on control design has a theoretical and practical significance.

Characteristics are the main geometric property of a PDE system concerned by the thesis; however, it is only a special case of isovectors in a general PDE system within the context of exterior differential equations. The limitation of characteristics affects the applicability of the proposed control methods. Using more generalized geometric properties such as isovectors in high performance control would be a great breakthrough from both mathematical and control point of view.

Control of DPS is a challenging but valuable subject. Many areas are unexplored in this field and opportunities exist for explorative researchers to develop advanced control theories for DPS.

Bibliography

Alvarez-Ramirez, J. (2001). Linear boundary control for a class of nonlinear pde processes. *Systems and Control Letters* **44**, 395–403.

Aris, R. (1969). *Elementary Chemical Reactor Analysis*. Prentice Hall Inc.. Englewood Cliff, N.J.

Arnold, V.I. (1988). *Geometric Methods in the Theory of Ordinary Differential Equations*. Springer-Verlag. New York.

Badgewell, T.A. (1997). Robust stability conditions for siso model predictive control algorithms. *Automatica* **33**(7), 1357–1361.

Bhattacharyya, S., A. Pal and G. Nath (1996). Unsteady flow and heat transfer between rotating coaxial disks. *Numerical Heat Transfer, Part A* **30**(5), 519–532.

Braatz, Richard D., Matthew L. Tyler and Manfred Morari (1992). Identification and cross-directional control of coating processes. *AIChE Journal* **38**(9), 1329–1339.

Brosilow, C. and B. Joseph (2002). *Techniques of Model-Based Control*. Prentice Hall. Upper Saddke River, NJ.

Brown, J. (2001). Modal decomposition of convection-reaction-diffusion systems. Master's thesis. University of Alberta. Edmonton, Canada.

Bryant, R.L., S.S. Chern, R.B. Gardner, H.L. Goldschmidt and P.A. Griffiths (1991). *Exterior Differential Systems*. Springer-Verlag. New York.

Butkowskii, A.G. (1969). *Distributed Parameter Systems*. American Elsevier.

Campbell, John C. and James B. Rawlings (1998). Predictive control of sheet- and film-forming processes. *AIChE Journal* **44**(8), 1713–1723.

Chakravarti, Shrikar and W. Harmon Ray (1999). Boundary identification and control of distributed parameter systems using singular functions. *Chemical Engineering Science* (54), 1181–1204.

Chen, H. and F. Allgower (1998). A quasi-infinite horizon nonlinear model predictive control scheme with guaranteed stability. *Automatica* **34**(10), 1205–1217.

Christofides, P.D. and P. Daoutidis (1996). Feedback control of hyperbolic pde systems. *AIChE Journal* **42**(11), 3063–3086.

Christofides, P.D. and P. Daoutidis (1998). Robust control of hyperbolic pde systems. *Chemical Engineering Science* **53**(1), 85–105.

Clarke, D.M., C. Mohtadi and P.S. Tuffs (1987*a*). Generalized predictive control–part i: the basic algorithm. *Automatica* **23**, 137–148.

Clarke, D.M., C. Mohtadi and P.S. Tuffs (1987*b*). Generalized predictive control–part ii: extension and interpretation. *Automatica* **23**, 149–160.

Cochran, J.A. (1972). *The Analysis of Linear Integral Equations*. McGraw-Hill.

Culter, C.R. and B.L. Ramaker (1979). Dynamic matrix control: a computer control algorithm. *86th National Meeting AIChE, Houston, TX*.

Curtain, R.F. and H.J. Zwart (1995). *An introduction to Infinite-dimensional Linear Systems Theory*. Springer-Verlag. New York.

Denn, M. M. (1987). *Process Modeling*. Longman Scientific & Technical. New York.

Doolin, Brian F. (1990). *Introduction to Differential Geometry for Engineers*. Marcel Dekker. New York.

Douglas, JR Jim and Thomas F. Russell (1982). Numerical methods for convection-dominated diffusion problems based on combining the method of characteristics with finite element or finite difference procedures. *SIAM Journal on Numerical Analysis* **19**(5), 871–885.

Duchateau, P. and D. Zachmann (1989). *Applied Partial Differential Equations*. Harper & Row Publisher. New York.

Eaton, J. and J.B. Rawlings (1992). Model-predictive control of chemical processes. *Chemical Engineering Science* **47**(4), 705–720.

Garcia, C.E. (1984). Quadratic dynamic matrix control of nonlinear processes: an application to a batch reaction process. *AIChE Annual Meeting, San Francisco, CA*.

Garcia, C.E. and M. Morari (1982). Internal model control 1. a unifying review and some new result. *Ind. Eng. Chem.Process Des. Dev.* **21**(2), 308–323.

Garcia, C.E. and Morshedi (1986). Quadratic programming solution of dynamic matrix control (qdmc). *Chem. Engng Commun.* **46**, 73–87.

Gay, D.H. and W.H. Ray (1995). Identification and control of distributed parameter systems by means of the singular value decomposition. *Chemical Engineering Science* **50**(10), 1519–1539.

Godasi, S., A. Karakas and A. Palazoglu (1999). A study on the control of nonlieanr distributed parameter systems. *Proceedings of the American Control Conference, San Diego, California*.

Hanczyc, E.M. and A. Palazoglu (1995). Sliding mode control of nonlinear distributed parameter chemical processes. *Industrial Engineering & Chemistry Research* **34**, 557–566.

Henson, M.A. (1998). Nonlinear model predictive control: Current status and future directions. *Computers and Chemical Engineering* **23**, 187–202.

Hernández, E. and Y. Arkun (1992). Design of pole placement controllers for systems described by two-dimensional models. *Chemical Engineering Science* **47**(2), 297–310.

Isidori, A. (1995). *Nonlinear Control Systems*. Springer-Verlag.

Jury, E.I. (1964). *Theory and Application of the Z-transform Method*. Huntington. New York.

Laroche, Béatrice, Philippe Martin and Pierre Rouchon (1998). Motion planning for a class of partial differential equations with boundary control. *Proceedings of the 37th IEEE Conference on Design & Control.*

Maner, B.R., F.J. Doyle III, B.A. Ogunnaike and R. Pearson (1996). Nonlinear model predictive control of a simulated multivariable polymerization reactor using second-order volterra models. *Automatica* **32**(9), 1285–1301.

Marion, M. and A. Mollard (2000). A multilevel characteristics method for periodic convection-dominated problems. *Numerical Methods for Partial Differential Equations* **16**(1), 107–132.

Mayne, D.Q., J.B. Rawlings, C.V. Rao and P.O. Scokaert (2000). Constrained model predictive control: stability and optimality. *Automatica* **36**, 789–814.

McOwen, R. (1996). *Partial Differential Equations*. Prentice-Hall Inc.

Mutha, R.K., W.R. Cluett and A. Penlidis (1997). Nonlinear model-based predictive control of control nonaffine systems. *Automatica* **33**(5), 907–913.

Norquay, S.J., A. Palazoglu and J.A. Romagnoli (1998). Model predictive control based on wiener models. *Chemical Engineering Science* **53**(1), 75–84.

Ockendon, J., S. Howison, A. Lacey and A. Movchan (1999). *Applied Parial Differential Equations*. Oxford.

Park, H.M. and D.H. Cho (1996). The use of the karhunen-loeve decomposition for the modeling of distributed parameter systems. *Chemical Engineering Science* **51**(1), 81–98.

Patwardhan, A.A., G.T. Wright and T.F. Edgar (1992). Nonlinear model-predictive control of distributed-parameter systems. *Chemical Engineering Science* **47**(4), 721–735.

Rani, K.Y. and H. Unbehauen (1997). Study of predictive controller tuning method. *Automatica* **33**(12), 2243–2248.

Rao, C.V. and J.B. Rawlings (2000). Linear programming and model predictive control. *Journal of Process Control* **10**, 283–289.

Rawlings, J.B. (2000). Tutorial overview of model predictive control. *IEEE Control Systems Magazine* **20**(3), 38–52.

Ray, W.H. (1978). Some recent applications of distributed parameter systems theory–a survey. *Automatica* **14**, 281–287.

Ray, W.H. (1981). *Advanced Process Control*. McGraw-Hill.

Renou, S. and M. Perrier (2000). Nonlinear control design for pulp bleaching. *Control System 2000, Victoria, BC,*.

Renou, S., M. Perrier and D. Dochain (n.d.). Direct adaptive control of a parabolic system.

Rhee, H.K., R. Aris and N.R. Amundson (1986). *First-order Partial Differential Equations: Theorey and Application of Hyperbolic Systems of Quasilinear Equations*. Vol. II. Prentice Hall. New Jersey.

Richalet, J., A. Rault, L. Testud and J. Papon (1976). Algorithmic control of industrial process. *Proceedings of the Fourth IFAC Symposium on Identification and System Estimation* pp. 1119–1167.

Richalet, J., A. Rault, L. Testud and J. Papon (1994). Model predictive control of chemical processes. *Industrial Engineering & Chemistry Research* **33**, 2140.

Sadek, I.S. and M.A. Bokhari (1998). Optimal control of a parabolic distributed parameter system via orthogonal polynomials. *Optim. Control Appl. Meth* **19**, 205–213.

Scokaert, P.O.M., D.Q. Mayne and J.B. Rawlings (1999). Suboptimal model predictive control (feasibility implies stability). *IEEE Transactions on Automatic Control* **44**(3), 648–654.

Sen, A.K. (1974). Variable gain-phase method for feedback stabilization of multimode plasma instabilities. *Plasma Phys.* **16**, 509.

Shang, H., J.F. Forbes and M. Guay (2000). Output feedback control of first-order pde systems. *ADCHEM, Italy*.

Shirvani, M., M. Inagaki and T. Shimizu (1995). Simplification study on dynamic models of distributed parameter systems. *AIChE Journal* **41**(12), 2658–2660.

Shvartsman, S.Y. and I.G. Kevrekidis (1998). Nonlinear model reduction for control of distributed parameter systems: a computer-assisted study. *AIChE Journal* **44**(7), 1579–1594.

Simpson, D. (1967). A numerical method of characteristics for solving hyperbolic partial differential equations. PhD thesis. Iowa State University. Ames, Iowa.

Sira-Ramirez, H. (1989). Distributed sliding mode control in systems described by quasilinear partial differential equations. *Systems and Control Letters* **13**, 117–181.

Sistu, P.B. and B.W. Bequette (1996). Nonlinear model-predictive control: closed-loop stability analysis. *AIChE Journal* **42**(12), 3388–3402.

Smith, Carlos A. and Armando B. Corripio (1985). *Principles and Practice of Automatic Process Control*. John Wiley & Sons.

VanAntwerp, J.G. and R.D. Braatz (2000). Fast model predictive control of sheet and film processes. *IEEE Transactions on Control Systems Technology* **8**(3), 408–417.

Winkin, Joseph J., Denis Dochain and Philippe Ligarius (2000). Dynamic analysis of distributed parameter tubular reactors. *Automatica* **36**, 349–361.